Year : 2011

FORMATION OF A SPATIAL MEMORY TRACE: A BEHAVIORAL, CELLULAR AND MOLECULAR STUDY

PARAFITA Julia

UNIL | Université de Lausanne
Faculté de biologie et de médecine

Centre de Neurosciences Psychiatriques

FORMATION OF A SPATIAL MEMORY TRACE: A BEHAVIORAL, CELLULAR AND MOLECULAR STUDY

Thèse de doctorat en Neurosciences

présentée à la

Faculté de Biologie et de Médecine
de l'Université de Lausanne

par

Julia PARAFITA

Biologiste diplômée de l'Université de Santiago de Compostela, Espagne

Jury

Prof. Jean-Pierre Hornung, Président
Prof. Pierre J. Magistretti, Directeur
Dr. Sylvain Lengacher, Superviseur
Prof. Carmen Sandi, Expert
Prof. Serge Laroche, Expert

Thèse n° 62
Lausanne 2011

Programme doctoral interuniversitaire en Neurosciences des Universités de Lausanne et Genève

UNIL | Université de Lausanne

UNIVERSITÉ DE GENÈVE

UNIL | Université de Lausanne
Faculté de biologie et de médecine

LEMANIC NEURO SCIENCE DOCTORAL SCHOOL

Programme doctoral interuniversitaire en Neurosciences des Universités de Lausanne et Genève

Imprimatur

Vu le rapport présenté par le jury d'examen, composé de

Président	Monsieur Prof. Jean-Pierre **Hornung**
Directeur de thèse	Monsieur Prof. Pierre **Magistretti**
Co-directeur de thèse	
Experts	Madame Prof. Carmen **Sandi**
	Monsieur Prof. Serge **Laroche**
	Monsieur Dr Sylvain **Lengacher**

le Conseil de Faculté autorise l'impression de la thèse de

Madame Julia Parafita

Licence en biologie Uni de Compostelle

intitulée

**FORMATION OF A SPATIAL MEMORY TRACE:
A BEHAVIORAL, CELLULAR AND MOLECULAR STUDY**

Lausanne, le 10 mai 2011

pour Le Doyen
de la Faculté de Biologie et de Médecine

Prof. Jean-Pierre Hornung

ACKNOWLEDGEMENTS

This work was supported by FNRS grant 3100AO-108336/1 and /2 to PJM. I would like to thank all people who contributed to the experimental work and discussions during this thesis. Special thanks to my thesis director, Pierre Magistretti, for believing in my capacities and for giving me the opportunity of doing my thesis in his research laboratory. Also special thanks to Fulvio Magara and Sylvain Lengacher for excellent supervision, for sharing his expertise in behavior-2DG and molecular biology, respectively, and for all the time spent with me in discussions. I wish to thank Elsy Dunand for her help with cryostat sectioning and MCID images acquisition, Maude Marti Favre for her help with laser microdissection, Monika Saxena for her help with MCID analysis, Delphine Ribes and Jean-Philippe Thiran for the JULIDE collaboration.

Very warm thanks to:

All LNDC members (formers and presents): Aurélie, Benjamin, Cendrine, Corinne, Daniel, Egi, Emilie, Evelyne, Gabi, Igor, Jean-Marie, Jiangyan, Joël, Manuel, Maxime, Mireille, Monika, Nicolas, Pascal, Pierre (Marquet), Renaud, Sophie, Sylvain, Zhizhong, for all scientific and non-scientific discussions.

Luc Pellerin and Jacqueline Ros, for helping me at the beginning of my thesis.

The “nanas-lab club”: Annabelle, Camille, Carole, Elsy, Hélène, Ingrid, Julie, Karin, Lucie, Mathilde and Maude for all extra-professional activities. Let’s keep our blog alive!

People in Cery: especially Nadia and Raffaella for being flexible on lunchtime during my behavioral experiments.

Carlos, por este soño (cousa de meigas!) feito realidade, and Ainhoa because she is the best thing that has ever happened in my life.

All my family and friends in Spain, for supporting me through all my decisions.

My family-in-law here in Switzerland: Dolores, Antonio, Lucía, Inés, José-Antonio, Mari (prima), Mari (cuñada), Jesús and Antón.

My very close Swiss friends: Espe, Erika, Christophe, Alexis, Isabel, Thierry, Nadia, Noémie, Nathalie, Sylvain, Valentin, Lucas, Astrid, Yves, Elly, Arthur, Bea, Miguel, Kilian and Estela.

My parents, to whom I owe the person I am today.

To the memory of my mother.

THESIS ABSTRACT

This thesis project was aimed at studying the molecular mechanisms underlying learning and memory formation, in particular as they relate to the metabolic coupling between astrocytes and neurons. For that, changes in the metabolic activity of different mice brain regions after 1 or 9 days of training in an eight-arm radial maze were assessed by (^{14}C) 2-deoxyglucose (2DG) autoradiography. Significant differences in the areas engaged during the behavioral task at day 1 (when animals are confronted for the first time to the learning task) and at day 9 (when animals are highly performing) have been identified. These areas include the hippocampus, the fornix, the parietal cortex, the laterodorsal thalamic nucleus and the mammillary bodies at day 1; and the anterior cingulate, the retrosplenial cortex and the dorsal striatum at day 9. Two of these cerebral regions (those presenting the greatest changes at day 1 and day 9: the hippocampus and the retrosplenial cortex, respectively) were microdissected by laser capture microscopy and selected genes related to neuron-glia metabolic coupling, glucose metabolism and synaptic plasticity were analyzed by RT-PCR. 2DG and gene expression analysis were performed at three different times: 1) immediately after the end of the behavioral paradigm, 2) 45 minutes and 3) 6 hours after training. The main goal of this study was the identification of the metabolic adaptations following the learning task. Gene expression results demonstrate that the learning task profoundly modulates the pattern of gene expression in time, meaning that these two cerebral regions with high 2DG signal (hippocampus and retrosplenial cortex) have adapted their metabolic molecular machinery in consequence. Almost all studied genes show a higher expression in the hippocampus at day 1 compared to day 9, while an increased expression was found in the retrosplenial cortex at day 9. We can observe these molecular adaptations with a short delay of 45 minutes after the end of the task. However, 6 hours after training a high gene expression was found at day 9 (compared to day 1) in both regions, suggesting that only one day of training is not sufficient to detect transcriptional modifications several hours after the task. Thus, gene expression data match 2DG results indicating a transfer of information in time (from day 1 to day 9) and in space (from the hippocampus to the retrosplenial cortex), and this at a cellular and a molecular level. Moreover, learning seems to modify the neuron-glia metabolic coupling, since several genes involved in this coupling are induced. These results also suggest a role of glia in neuronal plasticity.

RESUME DU TRAVAIL DE THESE

Ce projet de thèse a eu pour but l'étude des mécanismes moléculaires qui sont impliqués dans l'apprentissage et la mémoire et, en particulier, à les mettre en rapport avec le couplage métabolique existant entre les astrocytes et les neurones. Pour cela, des changements de l'activité métabolique dans différentes régions du cerveau des souris après 1 ou 9 jours d'entraînement dans un labyrinthe radial à huit-bras ont été évalués par autoradiographie au 2-désoxyglucose (2DG). Des différences significatives dans les régions engagées pendant la tâche comportementale au jour 1 (quand les animaux sont confrontés pour la première fois à la tâche) et au jour 9 (quand les animaux ont déjà appris) ont été identifiés. Ces régions incluent, au jour 1, l'hippocampe, le fornix, le cortex pariétal, le noyau thalamic laterodorsal et les corps mamillaires; et, au jour 9, le cingulaire antérieur, le cortex retrosplenial et le striatum dorsal. Deux de ces régions cérébrales (celles présentant les plus grands changements à jour 1 et à jour 9: l'hippocampe et le cortex retrosplenial, respectivement) ont été découpées par microdissection au laser et quelques gènes liés au couplage métabolique neurone-glie, au métabolisme du glucose et à la plasticité synaptique ont été analysées par RT-PCR. L'étude 2DG et l'analyse de l'expression de gènes ont été exécutés à trois temps différents: 1) juste après entraînement, 2) 45 minutes et 3) 6 heures après la fin de la tâche. L'objectif principal de cette étude était l'identification des adaptations métaboliques suivant la tâche d'apprentissage. Les résultats de l'expression de gènes démontrent que la tâche d'apprentissage module profondément le profile d'expression des gènes dans le temps, signifiant que ces deux régions cérébrales avec un signal 2DG élevé (l'hippocampe et le cortex retrosplenial) ont adapté leurs « machines moléculaires » en conséquence. Presque tous les gènes étudiés montrent une expression plus élevée dans l'hippocampe au jour 1 comparé au jour 9, alors qu'une expression accrue a été trouvée dans le cortex retrosplenial au jour 9. Nous pouvons observer ces adaptations moléculaires avec un retard court de 45 minutes après la fin de la tâche. Cependant, 6 heures après l'entraînement, une expression de gènes élevée a été trouvée au jour 9 (comparé à jour 1) dans les deux régions, suggérant que seulement un jour d'entraînement ne suffit pas pour détecter des modifications transcriptionelles plusieurs heures après la tâche. Ainsi, les données d'expression de gènes corroborent les résultats 2DG indiquant un transfert d'information dans le temps (de jour 1 à jour 9) et dans l'espace (de l'hippocampe au cortex retrosplenial), et ceci à un niveau cellulaire et moléculaire. D'ailleurs, la tâche d'apprentissage semble modifier le couplage métabolique neurone-glie, puisque de nombreux gènes impliqués dans ce couplage sont induits. Ces observations suggèrent un rôle important de la glie dans les mécanismes de plasticité du système nerveux.

LIST OF ABBREVIATIONS

2DG: ^{14}C-2-deoxyglucose

AC: active control

ACC: anterior cingulate cortex

ADP: adenosine diphosphate

Aldo: aldolase

AMP: adenosine monophosphate

AMPA receptor: amino-3-hydroxy-5-methyl-4-isoxazolpropionic acid receptor

ANLSH: astrocyte–neuron lactate shuttle hypothesis

ANOVA: analysis of variance

Arc: Activity regulated cytoskeletal-associated protein

ATP1a2: Na^+/K^+-ATPase alpha 2 subunit

ATP: adenosine triphosphate

BDNF: brain-derived neurotrophic factor

BOLD: blood oxygenation level dependent effect

^{14}C-DG-6-P: ^{14}C-2-deoxyglucose-6-phosphate

CA: CornuAmmonis

CaMKII: Ca^{2+}/calmodulin-dependent protein kinase II

cDNA: complementary deoxyribonucleic acid

C/EBP: CCAAT-enhancer binding protein

CMRGlu: cerebral metabolic rate for glucose

CNS: central nervous system

CREB: cAMP-response element binding

DG: dentate gyrus

DNA: deoxyribonucleic acid

Egr1: early growth response 1 (= Zif268)

eIF: eukaryotic initiation factor

Eno: enolase

F6P: fructose-6-phosphate

$FADH_2$: flavin adenine dinucleotide, reduced

fMRI: functional magnetic resonance imaging

fx: fornix

G6pdh: glucose-6-phosphate dehydrogenase

GABA: gamma aminobutyric acid

Gap43: growth associated protein 43

GAP: glyceraldehydes-3-phosphate

Gapdh: glyceraldehydes-3-phosphate dehydrogenase

GLUTs: glucose transporters

GSH: glutathione

GTFs: general transcription factors

GTP: guanosine triphosphate

Gyg: glycogenin

Gys: glycogen synthase

Hk: hexokinase

HP: hippocampus

IHC: immunohistochemistry

IRES: internal ribosomal entry sites

ISH: in situ hybridization

ITK: national library of medicine insight segmentation and registration toolkit

LCM: laser capture microdissection

LD: laterodorsal nucleus of the thalamus

LDA: low density array

Ldh: lactate dehydrogenase

LMPC: laser microdissection and pressure catapulting

LTP: long-term potentiation

MAPK: mitogen-activated protein kinase

MB: mammillary bodies

MCTs: monocarboxylate transporters

mRNA: messenger ribonucleic acid

NA: noradrenaline

NADH: nicotinamide adenine dinucleotide, reduced

NADPH: nicotinamide adenine dinucleotide phosphate, reduced

NMDA receptor: N-methyl-D-aspartate receptor

OD: optical density

OLP: on-line processing

PCR: polymerase chain reaction

Pcx: pyruvate carboxylase

Pdk: pyruvate dehydrogenase kinase

PET: positron emission tomography

Pfk: phosphofructokinase

Pk: pyruvate kinase

PKA: protein kinase A

PKC: protein kinase C

PP1: phosphatase protein 1

PP: post-processing

PPd: post-processing delayed

PSD95: post synaptic density 95 (= Dlg4)

PTG: protein targeting to glycogen

PTLp: posterior parietal cortex

Pygb: glycogen phosphorylase, brain

QC: quiet control

RAM: eight-arm radial maze

rCBF: regional cerebral blood flow

RNA: ribonucleic acid

rRNA: ribosomal ribonucleic acid

ROI: regions of interest

RS: retrosplenial cortex

RT-PCR: real time-polymerase chain reaction

s.e.m: standard error of the mean

Taldo :transaldolase

TCA cycle: tricarboxylic acid cycle

TE buffer: Tris-EDTA buffer

Tkt: transketolase

tRNA: transfer ribonucleic acid

VIP: vasoactive intestinal peptide

TABLE OF CONTENTS

LIST OF FIGURES

LIST OF TABLES

I

INTRODUCTION

1 INTRODUCTION

The study of the learning and memory processes has occupied a large part of the neuroscientific community during the last decades. Rodents are maybe the favorite laboratory animals for behavioural studies due to the low cost, easy handling and similar genome to the one of human being, allowing researchers to study the neurobiological mechanisms of learning and memory from a cellular, metabolic and genetic point of view. A large battery of tests has been developed to assess different aspects and kinds of learning in rodents.

1.1 BEHAVIORAL PARADIGMS FOR SPATIAL LEARNING

A high variety of behavioural paradigms (as radial arm maze, water maze, T-maze, Y-maze and Barnes maze) have been used to study spatial cognition and exploration in rodents. From all of them, I will focus on the radial arm maze (RAM). The RAM was introduced by David Olton and Robert Samuelson in 1976 (Olton and Samuelson, 1976). The original apparatus was designed with eight radial arms and was thought to study spatial learning in rats. Later, the same device but adapted for mice was developed (Pick and Yanai, 1983). The number of arms can differ enormously from one study to another, researchers using maze paradigms ranging from 3 to 48 arms. Cole and Chappell-Stephenson tried to establish the limits of spatial performance in rats, starting from an eight-arm radial maze and adding sets of eight arms to get 16, 24, 32, 40 and finally 48 arms(Cole and Chappell-Stephenson, 2003). They concluded that the limit of spatial learning in their multiple behavioural paradigms was between 16 and 24 food locations, even though they said that the arrangement of arms, meaning the separation between adjacent arms, was more important for rat performance than the number of arms.

RAM has been used to study a broad range of issues as natural behaviour, short- and long-term memory, spatial and non spatial memory, working and reference memory, strain and species differences in spatial competence, drug effects on behaviour and ageing effects, among others (Foreman and Ermakova, 1998). Indeed, mouse strain differences exist for behavioural traits being the C57 inbred strains of mice (including C57BL/6, C57BL/10, C57BR, and C57L) one of the best strains for behavioral tasks as open field locomotion, Morris water maze, contextual fear conditioning and eight-arm radial maze (Crawley et al., 1997). Animal behavior studies can be correlated with human performance results, at least at

the level of the hippocampal formation which is one of the most important brain regions implicated in spatial learning and memory formation (Kesner and Hopkins, 2006).

Now, only a few words to briefly describe the other devices used to assess spatial learning and memory:

Morris water maze

The Morris water maze was developed by Richard G. Morris in 1981(Morris, 1981). The original paradigm consists in a circular pool containing warm and opaque water. The pool was divided in four equal quadrants. In one of them, the target quadrant, an escape platform is hidden under the water level, being invisible for animals. What is measured in this type of maze is the "latency", the time the animal needs to reach the escape platform after has been immersed in the water (Morris, 1984; Paul et al., 2009).

T maze

This device consists in a maze in the form of "T". Animals are placed at the base of the T and allowed to explore the maze and to choose one of the arms. This behavioral paradigm shows that rodents prefer the arm that they have not visited before, so they remember which was the last arm visited (Deacon and Rawlins, 2006; Paul et al., 2009).

Y maze

The Y maze could be considered as a variant of the T maze. Three identical arms are disposed as a "Y". The animal starts in one of the arms and can explore the rest of the maze. Novelty vs familiarity choices were assessed (Paul et al., 2009).

Barnes maze

It consists in an elevated, open and circular platform containing 18-20 holes around the platform. The animal is placed in the center of the device and an aversive stimulus, as a loud noise or an intense light, is turned on. The animal must find the escape hole and the experimenter measures the latency and the number of errors (Paul et al., 2009).

1.2 SPATIAL LEARNING, MEMORY AND BRAIN ANATOMY

It is known that the hippocampal formation is essential for spatial learning, but this process involves a large number of regions. Spatial learning and memory depends probably upon the coordinated action of different brain structures constituting a functionally integrated neural network. Interconnection of different brain regions may form memory systems that

operate independently but, at the same time, in association with other memory systems. Thus, the various brain memory systems operate in parallel to support behaviour (Squire, 2004).

1.2.1 SPATIAL LEARNING AND THE HIPPOCAMPUS

The medial temporal lobe, especially the hippocampus, is required for declarative episodic learning and memory (Eichenbaum, 2000; Squire, 2004; Squire et al., 2004), see figure 1-1 for the different memory systems. Furthermore, a bidirectional dialogue between the hippocampus and the cortex is at the basis of memory formation and consolidation (Eichenbaum, 2000; Remondes and Schuman, 2004; Frankland and Bontempi, 2005).

The hippocampal formation or hippocampal system includes the hippocampus and some other adjacent regions. However, there is no consensus about how many and which regions form this hippocampal formation. Amaral and Lavenex define the hippocampal formation as the following 6 regions: dentate gyrus, hippocampus proper, subiculum, presubiculum, parasubiculum and entorhinal cortex, being the hippocampus formed by only the Cornu Ammonis (CA) subregions: CA1, CA2 and CA3 (Amaral and Lavenex, 2006). Other authors consider the hippocampus as a large region including the CA subregions, the dentate gyrus and the subicular complex, then the entorhinal, perirhinal and postrhinal cortices complete the hippocampal system (Zola-Morgan and Squire, 1993; Squire et al., 2004).

The principal cell type of the dentate gyrus (DG) is the granule cell. DG is formed by 3 layers: 1) the polymorphic layer, containing the initial segments of the axons; 2) the granule layer, containing the cell bodies of granule cells and 3) the molecular layer formed by the dendrites. The major type cell of CA is the pyramidal neuron. CA regions present also different layers: 1) the alveus, containing the axons of pyramidal cells; 2) the stratum oriens formed by basal dendrites; 3) the stratum pyramidale which contains the cell bodies; 4) the stratum radiatum formed by the proximal segments of apical dendrites and 5) the stratum lacunosum/moleculare containing the distal segments of apical dendrites (O'Keefe and Nadel, 1978).

Spatial information processing in the hippocampus occurs through different stages as pattern separation, pattern association and pattern completion. Pattern separation is the ability to encode and separate events in space and time. Pattern association is to form associations

between events and items. And pattern completion is the capacity of retrieve well-established information based of partial or incomplete inputs (Kesner and Hopkins, 2006).

1.2.2 MEMORY CLASSIFICATION

Memory is the brain capacity to classify, encode, retain and recall a wide diversity of information and experiences throughout the life (Dunning and During, 2003). Memory can be classified, according to the duration, in short-term (from seconds to hours) and long-term memory (from hours to years) (McGaugh, 2000); and according to the kind of information to be process, in declarative and non-declarative memory (figure 1-1). Declarative memory is an explicit and conscious form of memory, whereas non-declarative memory is an implicit and unconscious one. Two types of declarative memory are well-established: episodic and semantic memory. Episodic memory refers to autobiographical events that occur in a particular spatial and temporal context and semantic memory to general knowledge (Squire et al., 1993; Squire, 2004).

In the context of a spatial learning paradigm, we can talk about two more types of memory: working and reference memory. Working memory is defined as the information that must be retained during a single trial, and reference memory as the information that must be maintained from trial to trial, and day to day, allowing performance to improve across the training days (Foreman and Ermakova, 1998). For example, in the learning paradigm used in this study (RAM with 3 arms baited with food) the reference memory is used to remember which are the three baited arms from day to day, the working memory is used to remember which arms have already been visited on the current trial. Some authors consider working memory and short-term memory as synonymous.

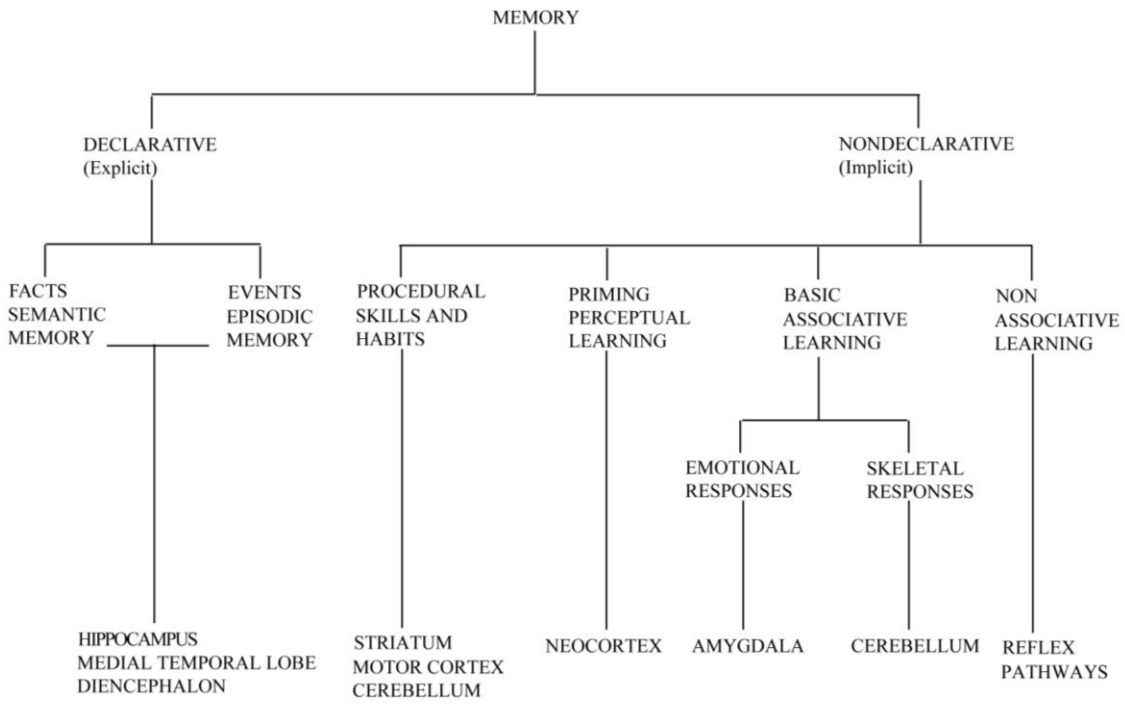

Figure 1-1: Memory systems and the corresponding brain regions

Modified from Squire, 2004.

1.2.3 LEARNING AND MEMORY-RELATED BRAIN REGIONS

The processes of learning and memory involve several brain regions and circuits (D'Hooge and De Deyn, 2001; van Groen et al., 2002; Maguire et al., 2003; Maviel et al., 2004; Sommer et al., 2005; Conejo et al., 2007; Lopez et al., 2009), and even distinct subregion activations within the same brain region during the different phases of memory namely, encoding, consolidation and retrieval (Lepage et al., 1998; Moser and Moser, 1998a; Greicius et al., 2003; Pothuizen et al., 2004; Ros et al., 2006). The medial temporal lobe, formed by the hippocampal region in the broad sense (CA, DG, subiculum, perirhinal, entorhinal and parahippocampal cortices) and the medial diencephalon, formed by the thalamus and hypothalamus, are the major brain systems related to anterograde amnesia (Aggleton and Saunders, 1997; Squire, 2004; Squire et al., 2004).

The hippocampus projects to the anterior thalamic nuclei (formed by the anterodorsal, the anteromedial and the anteroventral nucleus) and the mammillary bodies through the fornix, thus if this region is cut and anterograde tracers are placed in the subiculum no label is found neither in the mammillary bodies nor in the anterior thalamic nucleus (Aggleton et al., 1986). Subicular projections are also found in the laterodorsal nucleus of the thalamus (LD), but in

this case not all afferents pass through the fornix but rather use another parallel temporal route via the pulvinar (Aggleton and Saunders, 1997). Mammillary bodies project to the anterior thalamic nuclei via the mammillothalamic tract (Aggleton et al., 2010). In turn, the anterior thalamic nuclei establish connections with the neocortex in such a way that the anteromedial nucleus projects to deep layers of the anterior cingulated and retrosplenial cortex, whereas the anterodorsal and anteroventral nuclei mainly project to superficial layers of the retrosplenial cortex (Shibata, 1993).

The striatum is the major input station to the basal ganglia. Basal ganglia include the caudate nucleus, the putamen, the nucleus accumbens, the globus pallidus, the substantia nigra, the ventral tegmental area and the subthalamic nucleus. Anatomically, the so-called (dorsal) striatum corresponds to the caudate nucleus and the putamen. Major afferent projections to the striatum come from different regions of the cortex and the thalamus; Then, caudate and putamen send most of their outputs to the globus pallidus and subtantia nigra which, in turn, project to the thalamus sending them back to the cortex, forming a "cortico-basal ganglia-thalamic" loop (Haber, 2003; Haber and Calzavara, 2009).

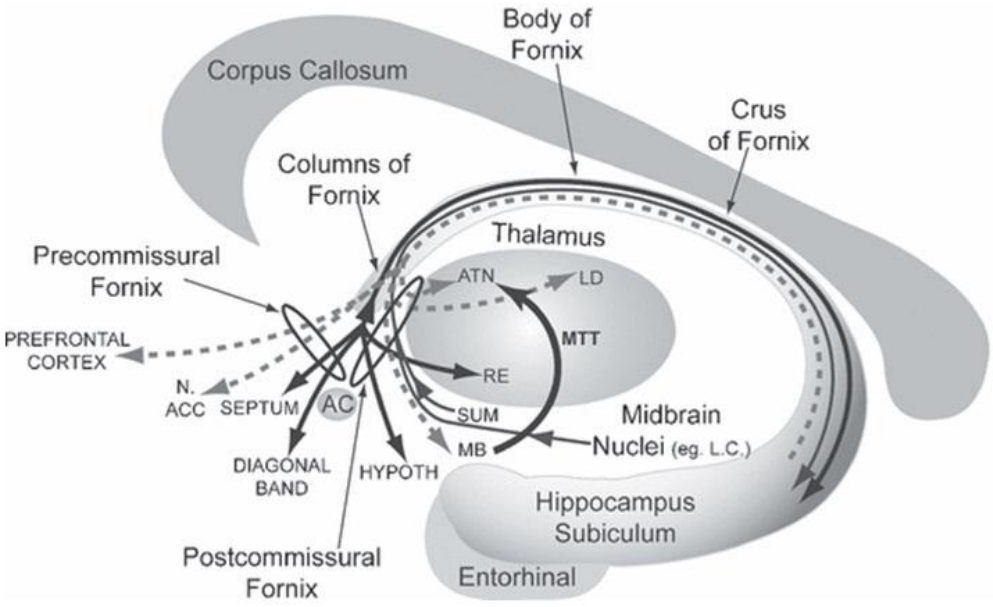

Figure 1-2: Schematic representation of some learning-related brain regions

Representation of some of the learning and memory-related brain regions described above and their interconnections. AC: anterior commisure; ATN: anterior thalamic nuclei; HYPOTH: hypothalamus; LC: locus coeruleus; LD: laterodorsal nucleus of the thalamus; MB: mammillary bodies; MTT: mammillothalamic tract; RE: nucleus reuniens; SUM: supramammillary nucleus. Taken from Aggleton et al., 2010.

1.3 ^{14}C-2-DEOXYGLUCOSE TECHNIQUE (2DG)

The use of oxygen and glucose by the brain allow us to estimate the level of functional activity in different cerebral regions during normal state, during activity (for example, learning) or even during pathological conditions. In other words, establishing the brain energy metabolism, by measuring the oxygen and/or glucose consumption, give us an idea about functional activity in the brain as a whole or in a part of the brain. That leads to the development of several techniques based on the utilization of radioactive tracers to determine cerebral blood flow and metabolism, as described by Kety in the 60's (Kety, 1967). These first "autoradiographic" techniques had some inconvenient as the radioisotopes for oxygen and glucose were too rapidly metabolized to carbon dioxide and cleared from tissues, making the energetic metabolism measurement complicated. This was solved when Sokoloff developed the ^{14}C-2-deoxyglucose (2DG) technique (Sokoloff et al., 1977).

2DG is a ^{14}C-labelled molecule which is transported in the same way as glucose to the brain. Its degradation is stopped after the first step of the glycolysis, the conversion in ^{14}C-2-deoxyglucose-6-phosphate (^{14}C-2-DG-6-P), because of a chemical difference on the second carbon atom of the molecule. This molecule (^{14}C-2-DG-6-P) remains in tissues time enough to measure and quantify radioactivity in the regions where glucose is being consumed (figure 1-3).

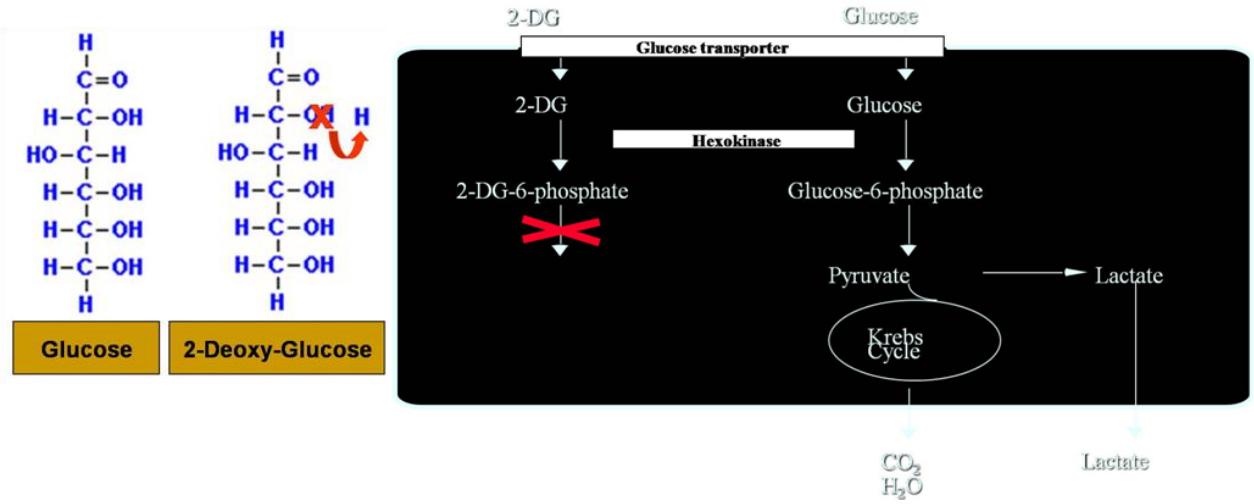

Figure 1-3: 2DG molecule structure and metabolism

2DG molecule is characterized by the replacement of the hydroxyl group on the second carbon atom by a hydrogen atom. 2DG and glucose are transported between blood and brain tissues by the same saturable carrier and, in tissues they compete for the enzyme hexokinase, which phosphorylates both substrates to their respective hexose-6-phosphate. 2-deoxyglucose-6-phosphate cannot be isomerized to fructose-6-phosphate (because of the lack of OH); so its metabolism ceases at this point of the metabolic pathway.

The 2DG technique is a well-established and very appropriate method to map brain glucose utilization in small animals; it has been used in several studies aimed at mapping the brain regions engaged in learning and memory (Bontempi et al., 1996; Bontempi et al., 1999; Ros et al., 2006), or activated by administration of specific drugs (Li et al., 1998; Brett et al., 2001) as well as in pathological conditions (Mori et al., 1995; Dodart et al., 1999) among others. Moreover, the spatial resolution of autoradiography is higher than the more recent developed microPET (Positron Emission Tomography) technology (Rice et al., 2006; Sokoloff, 2008).

The same basic principle of the 2DG technique is shared by the PET and fMRI (functional magnetic resonance imaging) techniques (Poeppel and Krause, 2008). Neuronal activity leads to an increase in oxygen and glucose consumption. The local physiological response is an increase in blood flow to cerebral regions with high neural activity. Changes in regional cerebral blood flow (rCBF) leads to changes in the relative concentrations of oxyhaemoglobin and deoxyhaemoglobin as well as to changes in the regional cerebral blood volume. The fMRI technique measures changes in blood oxygenation taking in consideration the different magnetic properties of oxygenated and deoxygenated blood that alter the MR signal. It is based on the BOLD (blood oxygenation level dependent) effect. The PET technique measures directly rCBF and also distribution of neurotransmitters and neuroreceptors thanks to certain radioactive-labeled substances. For instance, ^{15}O-water and ^{18}F-deoxyglucose are being used to study blood flow and glucose metabolism respectively (Kennedy et al., 2001), ^{18}F-dopa for dopamine metabolism (Elkashef et al., 2000; Otonkoski et al., 2006), ^{11}C-raclopride for the study of the distribution and quantities of D2 dopamine receptors (Brooks, 2003; Thobois et al., 2003; Steeves et al., 2009) and ^{11}C-flumazenil for benzodiazepines and GABA receptors (Galldiks et al., 2008; Salmi et al., 2008). All radioisotopes for PET technology have a short half-life: 2 minutes for ^{15}O, 20 minutes for ^{11}C and 2 hours for ^{18}F(Miller et al., 2008), compared to classical 2DG (5700 years for ^{14}C). Thus, 2DG autoradiography is an appropriate method for long research projects and studies in small laboratory animals.

1.4 BRAIN ENERGY METABOLISM

The brain has very high energetic demands: it represents only 2% of the body weight but it consumes about 20% of the energy produced by the organism (Magistretti, 2006, 2008). At least 80% of these energy demands are related to neuronal electrochemical signaling

processes, in particular those mediated by glutamate (Magistretti, 2009). Neurons are the only nerve cells that transmit nerve impulses; they communicate by synapses that can occur between neurons or between a neuron and a muscular cell or a gland. The majority of synapses in the nervous system are excitatory (about 85%), they cause a depolarization on the postsynaptic neuronal membrane, and the major neurotransmitter released is glutamate (see figure 1-4). There are also inhibitory synapses which represent a more little percentage and cause a postsynaptic membrane hyperpolarization. The more important inhibitory neurotransmitter is the gamma aminobutyric acid (GABA).

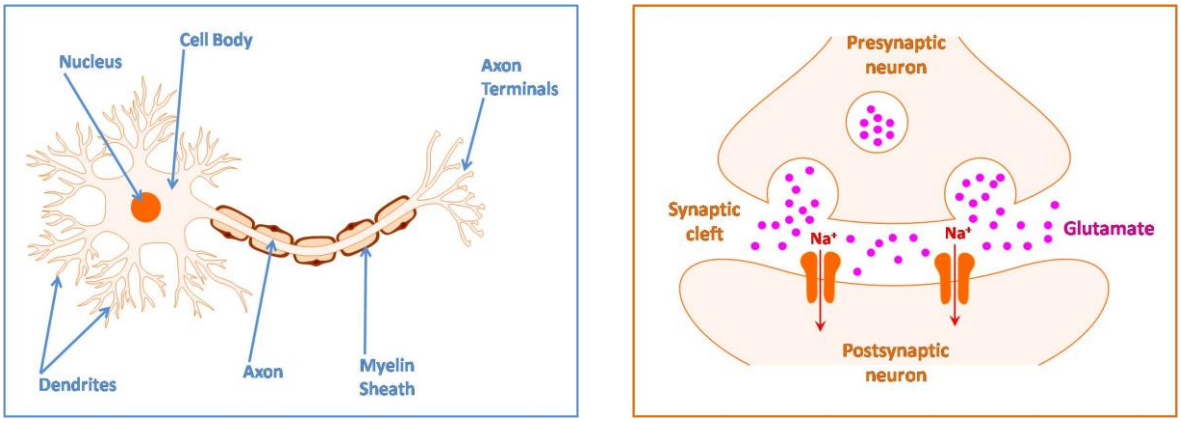

Figure 1-4: Scheme representing a neuron and an excitatory chemical synapse

Although there are many types of neurons, a typical one is formed by a cell body or soma containing the nucleus (with DNA), and by different types of prolongations. Many shorts ramifications take and bring information to the cell body: the dendrites. A long prolongation is responsible for transmission of nerve signals: the axon. This part of the neuron is coated by myelin which makes synaptic transmission faster. During synapses, neurotransmitters, as glutamate, contained in vesicles localized on the presynaptic terminal are released on the synaptic cleft and taken by specific receptors localized on the membrane of the postsynaptic neuron.

When some kind of information must be transmitted throughout the nervous system, an action potential is generated due to a transient alteration in the permeability to ions of the axonal membrane. The arrival of the action potential to the presynaptic termination increases the intracellular concentration of Ca^{2+}, making possible the fusion between the synaptic vesicles (containing neurotransmitters) and the membrane. In this way, neurotransmitters are released to the synaptic cleft where they remain for a little time until be taken by specific receptors localized on the membrane of the postsynaptic cell. Rapid clearance of neurotransmitters from the synaptic cleft is important to permit the transmission of another

action potential. All these processes (generation of action potentials as well as release, recapture and recycling of neurotransmitters) have a considerable energy cost.

Major energy substrates are oxygen and glucose, both arriving to the brain by blood vessels. Glucose oxidation in carbon dioxide (CO_2) and water produces a high quantity of ATP (adenosine triphosphate), a very rich energy molecule. Complete glucose degradation, implicating glycolysis, Krebs cycle and electron transport chain, can generate about 38 ATP molecules for each molecule of glucose. Some metabolic pathways related to glucose metabolism will be described in more detail below.

1.4.1 GLYCOLYSIS

Glucose degradation is the major pathway for the generation of energy (ATP), and glycolytic intermediates also serve as precursors for biosynthesis of other cellular constituents, highlighting the importance of this metabolic pathway. Glycolysis consists in 10 metabolic reactions taking place in the cytosol and during which one molecule of glucose produce two molecules of pyruvate. All reactions for this pathway are summarized in the figure 1-5. The overall reaction produces 2 molecules of pyruvate, 2 nicotinamide adenine dinucleotide (NADH) and 2 ATP.

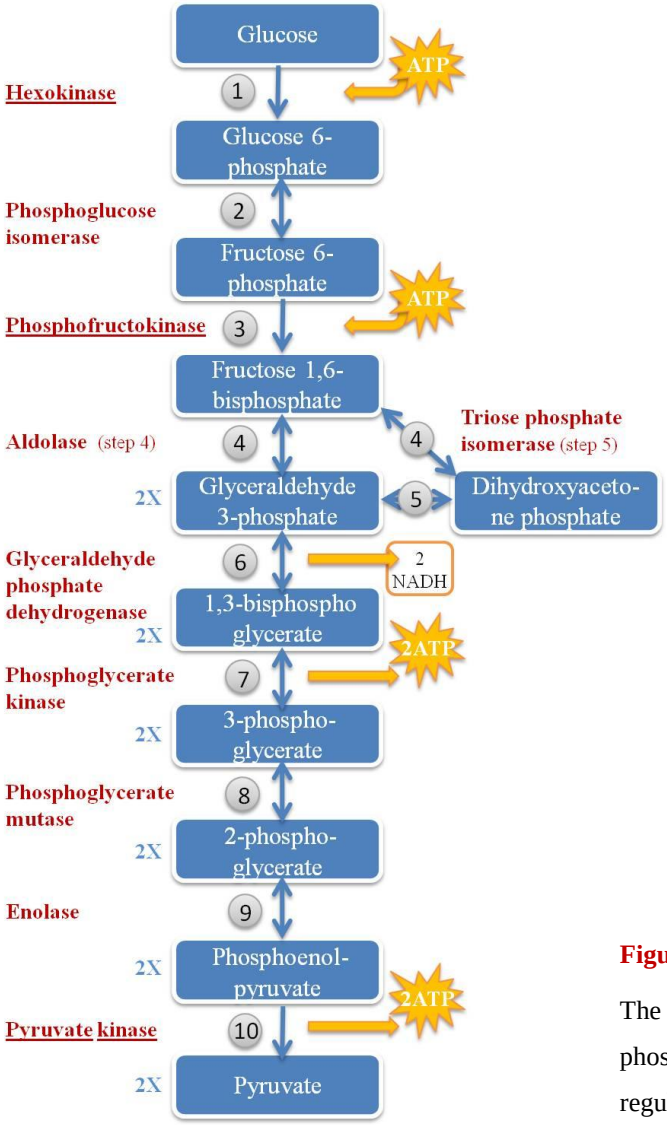

Figure 1-5: Glycolysis

The three underlined enzymes (hexokinase, phosphofructokinase and pyruvate kinase) are the regulation key steps of this pathway.

The reactions 1, 3 and 10, catalyzed by hexokinase, phosphofructokinase and pyruvate kinase respectively, are the key steps for the regulation of this pathway. Hexokinase (Hk) catalyzes the phosphorylation of hexoses, being the most common glucose but it can phosphorylates also 2-deoxyglucose (as shown in figure 1-3) and others (as fructose, sorbitol and glucosamine) (Michal, 1999) to hexoses-6-phosphate. Four different isoforms have been identified: Type I, Type II, Type III and Type IV, the last one also called glucokinase (Wilson, 2003) presenting some differences in term of affinity for glucose and of sensitivity to inhibition by the product, glucose-6-phosphate. Phosphofructokinase (Pfk) is the more important regulating enzyme and catalyzes the conversion of fructose-6-phosphate to fructose-1,6-bisphosphate. During this step, a new phosphate coming from ATP is added to the fructose-6-phosphate molecule. Phosphofructokinase (Pfk) is modulated by the energy

status of the cell. Thus it is activated by AMP, ADP and inorganic phosphate and inhibited by ATP, citrate and fatty acids. High ATP levels decrease Pfk activity as they signal sufficient energy availability. There are 3 different isoforms of phosphofructokinase: pfkl (liver), pfkm (muscle) and Pfkp (platelet). Pyruvate kinase (Pk) catalyzes the last step of glycolysis. It is responsible for the transfer of a phosphate group, coming from phosphoenolpyruvate, to an ADP molecule. End products of this reaction are pyruvate and ATP. Pk is activated by its substrate (phosphoenolpyruvate) and also by fructose-1,6-bisphosphate, and inhibited by ATP, as did Pfk.

1.4.2 PYRUVATE METABOLISM

The final product of the glycolysis, pyruvate, has different fates, one of them being the conversion to Acetyl-CoA which enters the Krebs cycle. This conversion is catalyzed by the pyruvate dehydrogenase complex and takes place in the mithocondria. The pyruvate dehydrogenase kinase (Pdk) inhibits the pyruvate dehydrogenase complex by phosphorylating it. This is reversed by the pyruvate dehydrogenase phosphatase that removes the phosphate from the pyruvate dehydrogenase, a process that renders it active.

Pyruvate can also be converted in oxaloacetate. This is done by the pyruvate carboxylase (Pcx), an enzyme that it is considered astrocytic-specific (Shank et al., 1985; Shank et al., 1993; Jitrapakdee et al., 2008; Teixeira et al., 2008). The function of this metabolic reaction is to replenish the Krebs cycle in carbons, in a process known as the anaplerotic (meaning replenishing) cycle. The overall stoichiometry of the Krebs cycle, also called citric acid cycle or tricarboxylic acid cycle (TCA cycle) is 3 NADH, 1 GTP and 1 $FADH_2$. Krebs cycle is always followed by the electron transport chain during which the protons and electrons obtained from these cofactor molecules create an electrochemical gradient that activate the ATP synthase, producing ATP molecules in the following way:

Electron transport system	
Cofactors	**ATP moleculesyield**
1 NADH	**3 ATP**
1 GTP	**1 ATP**

1 $FADH_2$	**2 ATP**

Table 1: ATP production from glucose oxydation

Molecules of ATP obtained during the electron transport chain from cofactors generated during glycolysis and Krebs cycle.

When oxygen is absent or in a short supply (for example, during exercise), pyruvate is converted in lactate by the lactate dehydrogenase (LDH) consuming an NADH molecule. This reaction presents a feedback regulation since high concentrations of the product, lactate, inhibit the activity of the enzyme. There is an isoform of this enzyme specific for astrocytes (LDH5, formed by 4 LDHA molecules) and other isozyme specific for neurons (LDH1, formed by 4 LDHB molecules) (Laughton et al., 2000; Pellerin and Magistretti, 2004). Lactate dehydrogenase takes part of the astrocyte-neuron lactate shuttle that will be described below.

1.4.3 PENTOSE PHOSPHATE PATHWAY

The pentose phosphate pathway is divided in two phases: oxidative and non-oxidative. The oxidative phase leads to the production of NADPH (nicotinamide adenine dinucleotide phosphate, reduced) and pentoses. The importance of NADPH production comes from the fact that it is required for biosynthetic processes (as fatty acids, cholesterol, neurotransmitters and nucleotides biosynthesis) and to control the redox potential, by regenerating glutathione (GSH) pool, necessary to protect cells and tissues against oxidative stress (Kirsch and De Groot, 2001; Biagiotti et al., 2003). The key enzyme of this first part of the pathway is the glucose-6-phosphate dehydrogenase (G6pdh), which catalyze the conversion of glucose-6-phosphate to 6-phosphoglucono-δ-lactone.

During the non-oxidative phase, several reactions implicating the transfer of carbon units between molecules lead to the formation of fructose-6-phosphate (F6P) and glyceraldehyde-3-phosphate (GAP) from the pentose molecules generated during the oxidative part. These interconversions are catalyzed by transketolase (Tkt), which is responsible for the transfer of 2 carbon atoms, and transaldolase (Taldo), which is responsible for the transfer of 3 carbon atoms. These two enzymes represent the link between the pentose phosphate pathway and the

glycolysis, since both products (F6P and GAP) are intermediate metabolites of the glycolytic pathway.

1.4.4 GLYCOGEN REGULATION

Brain glycogen is localized almost exclusively in astrocytes and constitutes the major energy reserve of the brain. Glycogen utilization increases during stimulation, while decreased neuronal activity (for example, during hibernation or anesthesia conditions) is accompanied by an increase in brain glycogen content, indicating a link between neuronal activity and glial glycogen metabolism (Swanson, 1992). Glycogen metabolism is under complex regulation involving various allosteric factors as well as covalent modifications and compartmentalization of key enzymes (Bollen et al., 1998). Phosphorylation is the key covalent mechanism in the regulation of synthesis and degradation of glycogen. This regulation is done in a reciprocal way: while phosphorylation activates glycogen phosphorylase (the enzyme responsible for glycogen degradation), it inactivates glycogen synthase (formation of glycogen). By contrast, dephosphorylation leads to inactivation of glycogen phosphorylase and activation of glycogen synthase. Protein kinase A (PKA) is the main kinase responsible for phosphorylation. Protein phosphatase-1 (PP-1) is the enzyme responsible for dephosphorylation (Bollen et al., 1998; Allaman et al., 2000).

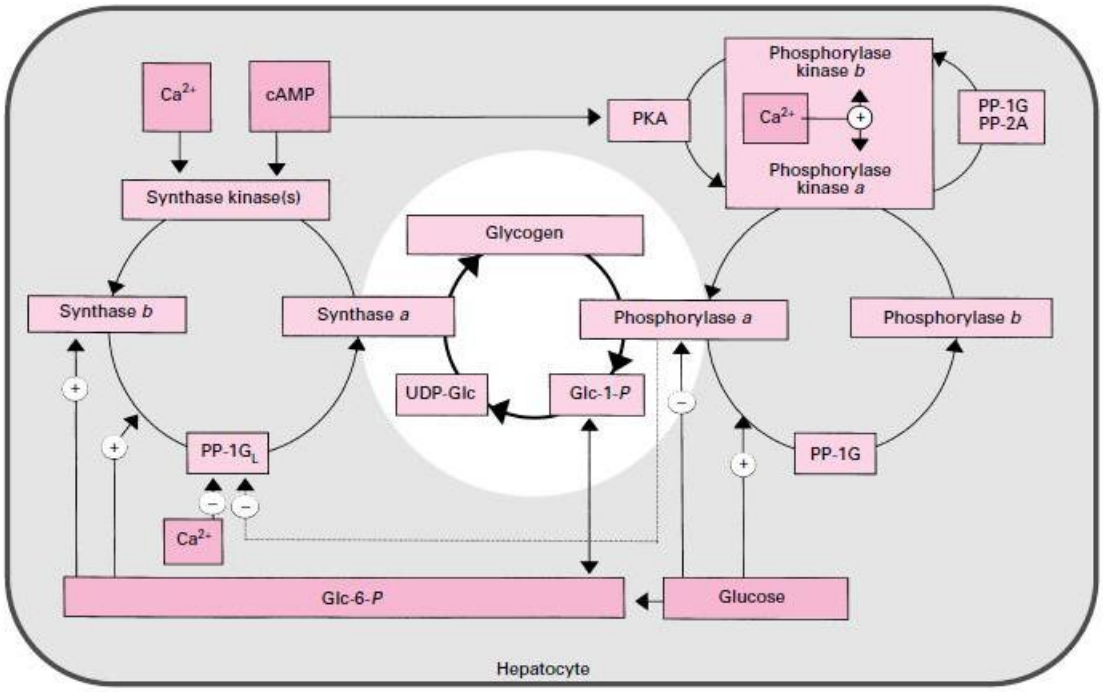

Figure 1-6: Glycogen (hepatic) regulation by enzyme phosphorylation and metabolites

Taken from Bollen et al, 1998.

Glycogen phosphorylase is allosterically activated by AMP and inhibited by glucose-6-phosphate. Glycogen synthase is allosterically activated by glucose-6-phosphate. cAMP activates PKA which phosphorylates and thereby activates phosphorylase kinase, which in turn phosphorylates and activates glycogen phosphorylase, breaking down a molecule of glycogen. cAMP also phosphorylates glycogen synthase acting in the contrary way, since the phosphorylated form of glycogen synthase is inactive. So, cAMP increase glycogenolysis and decrease glycogenesis (Alberts et al., 1994; Bollen et al., 1998; Allaman et al., 2000; Lodish et al., 2004). Some hormones and neurotransmitters were also shown to be implicated in the regulation of glycogen metabolism is astrocytes. In this way, insulin is responsible for increasing glycogen levels in this type of cells, while noradrenaline (NA) and vasoactive intestinal peptide (VIP) promotes glycogenolysis by stimulating formation of cAMP (Sorg and Magistretti, 1991; Allaman et al., 2000). Interestingly, both neurotransmitters (NA and VIP) were found to induce re-synthesis of glycogen several hours after their initial glycogenolytic effect (Sorg and Magistretti, 1992), revealing a double function of these chemicals in long-term glycogen regulation.

1.4.5 ASTROCYTE-NEURON LACTATE SHUTTLE

In page 27, a chemical synapse between a presynaptic and a postsynaptic neuron was described. Another nerve cell has been identified to play a key role in the brain energetic metabolism: the astrocyte. This glial type cell can be added to figure 1-4 to have a more complete scheme about the coupling between synaptic activity and glucose utilization, as shown is figure 1-7. Indeed, astrocytic processes (terminations) contact, in one hand, neurons at the synapse level and, in other hand, endothelial cells from capillaries. In this way, astrocytes are particularly well situated to transfer energy substrates from the circulation to "activated" neuronal cells. This glial-neuronal operational model was described in 1994 (Pellerin and Magistretti, 1994) and called some years later astrocyte-neuron lactate shuttle hypothesis (ANLSH).

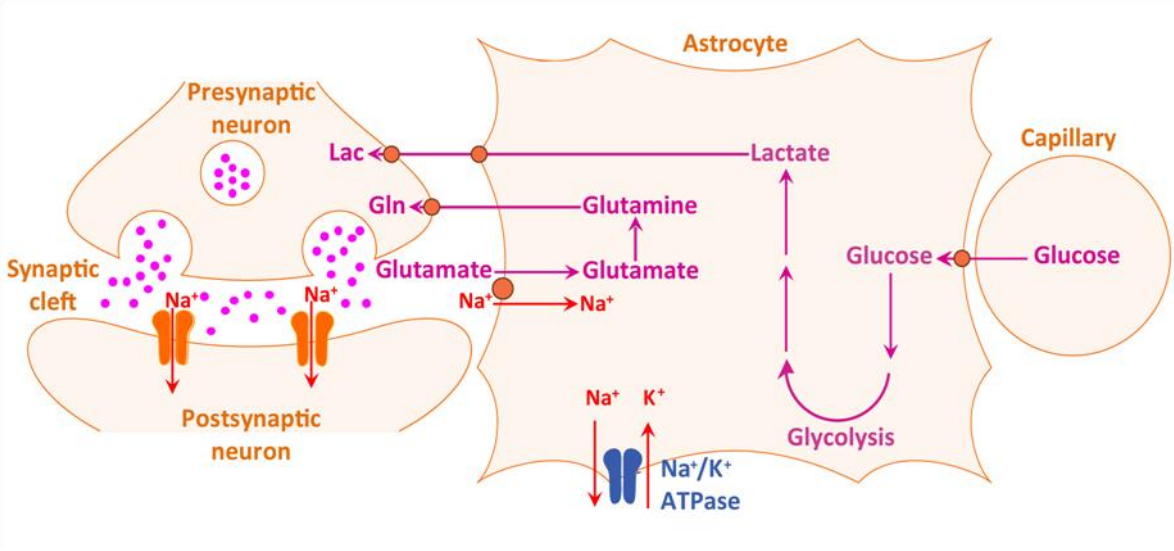

Figure 1-7: astrocyte-neuron lactate shuttle

(modified from Magistretti and Pellerin, 1999)

As described above in the same chapter and illustrated in figure 1-4, most of synapses in the brain are glutamatergic. Glutamate released during the synaptic transmission is taken by both post-synaptic neurons and astrocytes from the synaptic cleft. Glutamate entry in astrocytes is accompanied by 3 Na^+ ions, increasing its intracellular concentration. This Na^+ entry activates the Na^+/K^+-ATPase alpha2 subunit (ATP1a2), which consumes ATP. The increase of activity of this astrocytic-specific enzyme triggers glucose uptake and glycolysis in this type of glial cell. Na^+/K^+-ATPase pumps three Na^+ ions out of the cell whereas two K^+ ions are transported inside, reestablishing the intracellular ionic concentrations altered by the glutamate entry.

1.5 GENE EXPRESSION

All genetic information of a cell/organism is contained in the DNA (Deoxyribonucleic acid), even though the DNA molecule has no proper biological functions. DNA is a double strand formed by the association of "single units": nucleotides. Each nucleotide is formed by a sugar (deoxyribose), a phosphate group and a nitrogenous base. Four different nitrogenous bases can be found on a DNA molecule: adenine (A), cytosine (C), guanine (G) and thymine (T). The stability of the double strand is due to the hydrogen bonds between complementary bases: adenine forms a base pair with thymine by 2 hydrogen bonds, and cytosine forms a base pair with guanine by 3 hydrogen bonds.

1.5.1 TRANSCRIPTION: from DNA to mRNA

Most of biological activities and functions are carried out by proteins, and the accurate synthesis of proteins is crucial to the proper functioning of cells and organisms (Lodish et al., 2004). Even if all the information for an appropriate protein synthesis is contained in the DNA molecule, proteins cannot be synthesized directly from DNA: an intermediate molecule is necessary, the mRNA (messenger ribonucleic acid). The process by which DNA is converted into mRNA is called transcription (figure 1-8). During this process, not only mRNA is generated but also other RNA molecules as ribosomal RNA (rRNA) and transfer RNA (tRNA), both necessary for translation. Transcription is made by three different RNA polymerases in eukaryotes: RNA polymerase I, responsible for the synthesis of rRNA; RNA polymerase II, which produces mRNA, and RNA polymerase III which makes tRNA and others non-coding RNAs.

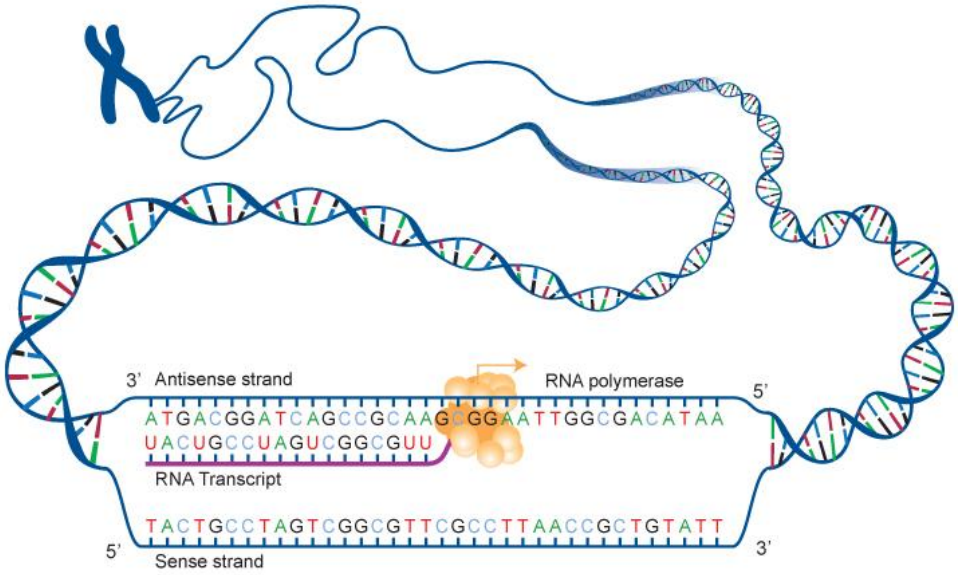

Figure 1-8: Transcription

The double DNA strand is being unwinded by the RNA polymerase and the template (antisense strand 3'→5') is being copied to a single RNA strand (5'→3'). The sense DNA strand is consider the coding strand because it corresponds to the same sequence of RNA with the only exception that thymine (T) is replaced by uracil (U) in the RNA molecule. Taken from the National Human Genome Research Institute (www.genome.gov).

Transcription can be divided into three steps: initiation, elongation and termination. The key enzyme involved in the initiation and elongation processes in eukaryotic cells is the RNA polymerase II. This enzyme can initiate transcription of DNA into RNA by binding to a specific start site (the promoter) and unwinding the double strand of DNA (Lee and Young, 2000; Shilatifard et al., 2003). As the enzyme moves along the DNA it unwinds sequential segments of the DNA molecule and adds nucleotides to the growing RNA strand. During this process, RNA polymerase II is helped by a large number of proteins called general transcription factors (GTFs), being the most common TFIIA, TFIIB, TFIID, TFIIE, TFIIF and TFIIH (from Lee and Young, 2000, table 4). Transcription terminates at short DNA sequences recognized as termination signals.

Primary transcripts are modified at both 5' and 3' ends. 5' end is capped with a methylated guanosine triphosphate and a poly(A) tail is added to the 3' end. These modifications are essential for processing, transport, translation and stability (Lee and Young, 2000). Moreover, many of the transcripts also undergo splicing, i.e. removal of the introns (non-coding sequences) and joining of the exons (coding sequences).

1.5.2 TRANSLATION: from mRNA to protein

The mRNA formed during the transcription process is transported from the nucleus to the cytoplasm and there, the information contained in this mRNA molecule is "translated" into a specific sequence of amino acids that constitute proteins (see figure 1-9).

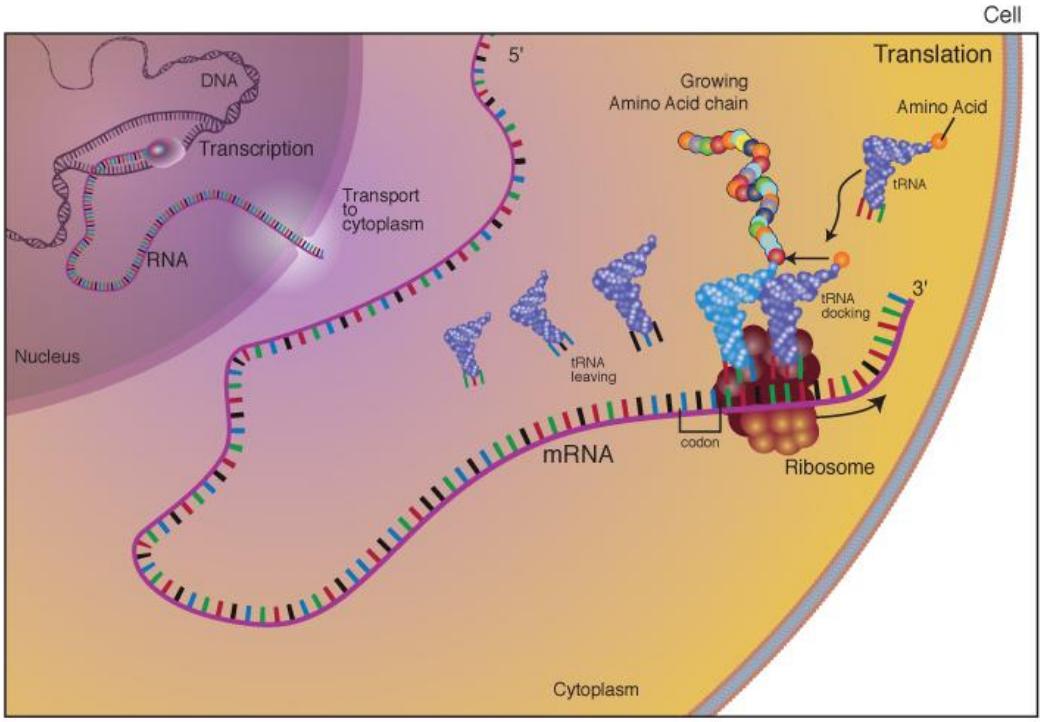

Figure 1-9: Translation

Taken from the National Human Genome Research Institute (www.genome.gov).

The mRNA sequence is "read" by a complex formed by ribosomal RNA (rRNA) and proteins, called ribosome. In eukaryotic cells, ribosomes are formed by a small subunit (40S), responsible for binding the mRNA molecule, and composed of an aminoacyl (A), peptidyl (P) and exit (E) sites, and a large (60S) subunit. The mRNA sequence is "read" by groups of three nucleotides, called codons, corresponding each of them to a complementary sequence (anticodon) contained in one end of the tRNA molecule. The anticodon sequence determines which amino acid must be added to the polypeptide chain. Translation begins at the start codon AUG, coding for methionine, and finishes at one of the three stop codons: UAG, UGA or UAA.

Translation is divided, as transcription, into three steps: initiation, elongation and termination. Initiation, in eukaryotes, is a complex multi-step process involving a large number of proteins called initiation factors (eIF). During elongation, aminoacyl tRNAs enter the

"free" A site on a ribosome already carrying the initiator Met-tRNAi in the P (peptidyl, because it is where the polypeptide chain is growing) site. If the correct tRNA is present, the ribosome catalyzes the formation of a peptide bond between the existing chain and the new amino acid. Then, tRNAs are translocated such that the next codon is moved into the A site, and the process is repeated. Termination takes place when a stop codon is encountered and the finished peptide is released from the ribosome. In a final stage, recycling, the ribosomal subunits are dissociated, releasing the mRNA and deacylated tRNA and setting the stage for another round of initiation, often on the same mRNA. As translation continues, the poly-A tail becomes shorter. Below a critical length, the mRNA loses its 5' cap, which protected against exonucleases, and it is degraded.

1.6 AIM OF THE PRESENT STUDY

Changes in synaptic structure and function are at the basis of learning and memory. This process of synaptic plasticity has been studied in detail with an almost exclusive focus on mechanisms that occur in neurons. Thus, the principal aim of this study is to investigate whether plasticity mechanisms are also engaged in neuron-glia metabolic coupling. Synaptic plasticity, learning and memory are processes which require the synthesis of new protein and consequently the induction of gene expression, including the activation of some immediate early genes (Stork and Welzl, 1999; Tischmeyer and Grimm, 1999; Bozon et al., 2003b; Miyashita et al., 2009). In consideration of the fact that regulation of gene expression reflects neural plasticity in the broadest sense, several studies have been conducted over the last few years, to determine the profile of gene expression associated with different conditions and experimental paradigms such as spatial learning (Cavallaro et al., 2002), cognitive impairment in aging animals (Rowe et al., 2007), memory loss in Alzheimer's disease (Dickey et al., 2003), the sleep/wake cycle (Cirelli and Tononi, 2004; Harbison et al., 2009), to give a few examples.

In order to test the possibility that expression genes involved in neuron-glia metabolic coupling could be modulated by learning, we have subjected mice to a 9 days spatial learning paradigm, the eight-arm radial maze. Regional brain metabolic activity was determined in several brain structures by (^{14}C) 2-deoxyglucose (2DG) autoradiography. Two of the brain regions showing the most important metabolic activations were microdissected by laser capture microscopy. Genes related to neuron-glia metabolic coupling, to glucose metabolism

and to synaptic plasticity were analyzed by quantitative RT-PCR.2DG and gene expression changes were analyzed at three different times: just after, 45 minutes and 6 hours after the spatial learning paradigm. These results indicate that plasticity of neuron-glia metabolic coupling is a concomitant of synaptic plasticity underlying learning and memory.

II

MATERIALS AND METHODS

2 MATERIALS AND METHODS

2.1 ANIMALS

C57BL/6 male mice (R. Janvier, France) aged of 3 months were used in this project. They were housed in groups of four on a 12h light-12h dark cycle (lights on from 7h to 19h). To minimize stress they were handled daily during ~2 weeks before the behavioral tests. Two days before starting the training protocol animals were food-deprived overnight and maintained at 90% of their initial body weight. All procedures described in "Material and Methods" were conducted in conformity with the Swiss national institutional guidelines on animal experimentation, and approved by the local committee for animal care.

2.2 APPARATUS (RAM)

The eight-arm radial maze (RAM) was the behavioral task we have chosen to assess spatial learning. It consists in a circular central platform of 16.5 cm diameter, from which radiate eight transparent arms made of Plexiglas (6 x 6 x 50 cm). Two wooden barriers (1.5 x 1 x 6 cm) are placed in each arm at 0 and 20 cm from the entry to prevent the animal to see the bait at the end of the arm and to increase the motivation for a visit. Arms were baited with ~10 µl of condensed milk diluted 1:1 with water. Arm access can be blocked with automated doors to prevent the reentry in an already visited arm (working memory errors). It was a home-made apparatus (Department of Physiology from the University of Lausanne), the same as described by Jacqueline Ros (Ros et al., 2006). The RAM was located in a room in which temperature was at 21-22°C and humidity conditions were between 40%-50%. Extra-maze cues as geometric shapes were fixed to the walls of the room. In figure 2-1 we can see a picture of our device.

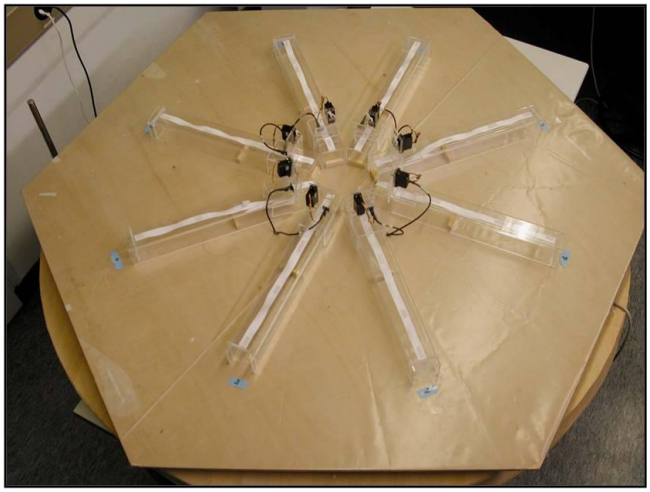

Figure 2-1: Behavioral paradigm, the eight-arm radial maze (RAM)

2.3 LEARNING PROTOCOL

Two days before starting the learning protocol some pre-training sessions were done, in order to familiarize animals with the new context and to minimize stress as much as possible. The first day of pre-training animals were allowed to go into the Radial Maze for exploration during 10 minutes. All arms were open and there was no food. The second day of pre-training was similar; with the only difference that there was food in all arms. The training protocol lasted 9 days and animals performed 6 trials/day. A set of 3 baited arms was assigned for each experimental group with sequential angles of 135°-90°-135° in order to test the reference memory. Each trial started by placing the mouse on the central platform, covering it by a transparent lid and opening all the doors. After an arm has been visited, the corresponding door was closed. One trial was over either if the animal found the 3 arms baited or 5 minutes after the beginning. The rest period between trials was one minute. Spatial learning was assessed by calculating the percentage of entries in correct arms out of the total number of entries.

Three experimental conditions were defined as follows: OLP (On-line Processing), PP (Post-Processing) and PPd (Post-Processing delayed) to map the different brain regions activated not only during the formation of a spatial memory trace (OLP) but also during memory consolidation at a short (45 minutes; PP) and a long time (6 hours, PPd) . All of these conditions were studied at Day 1 and Day 9 of the training protocol. Two different control groups were added to the experiment to ensure that the brain metabolic activation observed

was caused by the spatial learning process. The first one was the Quiet Control (QC), animals that never go to the RAM. And the second one was the Active Control (AC), animals that were allowed to explore the maze during the same time as trained animals (1 or 9 days, 6 trials/day) but with all eight arms baited with food, so no spatial strategy was developed.

2.4 TIME COURSE EXPERIMENT

At Day 1 or Day 9 of the training protocol, mice were injected intraperitoneally with ^{14}C-2DG either immediately before (OLP group), or immediately after (PP group) or 6 hours after (PPd group) the behavioral task. In all cases, they were sacrificed 45 minutes after the ^{14}C-2DG injection and their brains immediately frozen with carbon dioxide ice. Then brains were processed for 2DG autoradiography and laser microdissection. This period of time of 45 minutes in inherent to the kinetics properties of the 2DG to ensure homogeneous distribution and sufficient tracer signal in the brain (Sokoloff et al., 1977). Based on these different 2DG injection times we have defined 3 experimental groups that are represented in figure 2-2.

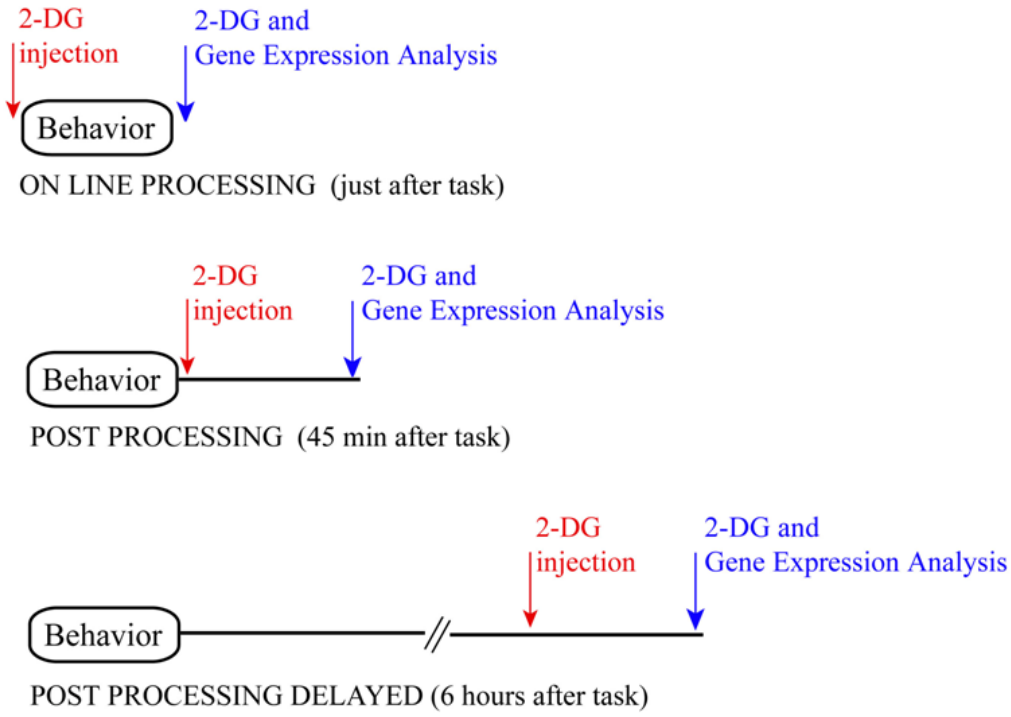

Figure 2-2: Experiment time course

The figure summarizes the sequence of events in time for the three experimental conditions. In the On-Line Processing (OLP) group, the 2DG injection made before the task allows us the identification of brain regions activated during learning. These activated regions were then microdissected and a gene expression analysis was performed by RT-PCR. For the Post-Processing (PP) and the Post-Processing delayed (PPd) group, 2DG and gene expression analysis took place 45 minutes and 6 hours after the learning task, respectively.

As we can see in the figure 2-2, in the On-Line Processing (OLP) group the 2DG injection occurs before the task and animals are sacrificed just at the end of the behavioral test. The 2DG mapping of this group represent the cerebral activity during the learning process. The Post-Processing (PP) group has been defined with the aim to answer the question of what happens in the brain when the animal has finished the training session. To assess that animals are injected immediately after the end of the training session and sacrificed 45 minutes later. A third experimental group was included in the project because of some in vitro results obtained in our lab, indicating that changes in the level of expression of certain genes involved in energy metabolism (such as glycogen synthase and protein targeting to glycogen) are observed within time-windows ranging between 3 and 9 hours after noradrenaline stimulation (Allaman et al., 2000; Allaman et al., 2003; Allaman et al., 2004). So, we were interested in study how energy metabolism can be affected by learning after a longer delay of time and we established this experimental time at 6 hours after the learning task. This is the Post-Processing delayed (PPd) group, in which mice are injected 315 minutes after training and sacrificed 45 minutes later, meaning 6 hours after performing the Radial Maze.

2.5 ^{14}C-2-DEOXYGLUCOSE TECHNIQUE (2DG)

Animals sacrified at day 1 or day 9 received an injection of ^{14}C-2-deoxyglucose intraperitoneally (0.165 mCi/kg, Sokoloff et al. 1977) either just before (OLP group), just after (PP group) or 6 hours after (PPd group) the training session. Control animals were injected and either left in their homecages (quiet controls) or released on the radial maze with all arms baited (active controls, no spatial memory required). 2DG was purchased from Hartmann Analytic. All animals were sacrificed (under pentobarbital anesthesia; 150 mg/kg) 45 minutes after injection of the tracer, the brains were rapidly frozen in dry ice and stored at -80°C until cutting at the cryostat. Coronal sections of 20 µm were collected either for autoradiography or laser microdissection. Every 2 slides for autoradiography, one slide for laser capture microdissection was taken.

The brain sectioning has changed three times during the experiment because of a new software we have developed in the lab (see next section in the Materials and Methods chapter). In the first one, 4 consecutives coronal sections (20 µm) were collected every 200 µm. For the 2nd protocol, 2 consecutives coronal sections were taken every 120 µm. And in the third one, a single section was collected every 60 µm. Brain sections were put on glass

slides and dries on a hotplate at 60°C for some minutes. Then, they were exposed on AGFA Mamoray HDR films (Röntgen Bender AG) with a ^{14}C-calibrated microscale (Amersham Bioscience) during 15 days. Films were developed and brain sections stained with cresyl violet. Images of stained brain sections and their corresponding autoradiograms were taken using an image densitometry system (MCID, Imaging Research). The regional cerebral 2DG uptake was assessed by optical densitometry (OD) of selected brain regions of interest (ROI) on the autoradiograms. The OD of ROI was then normalized to the optical density of the corpus callosum, see figure 2-3.

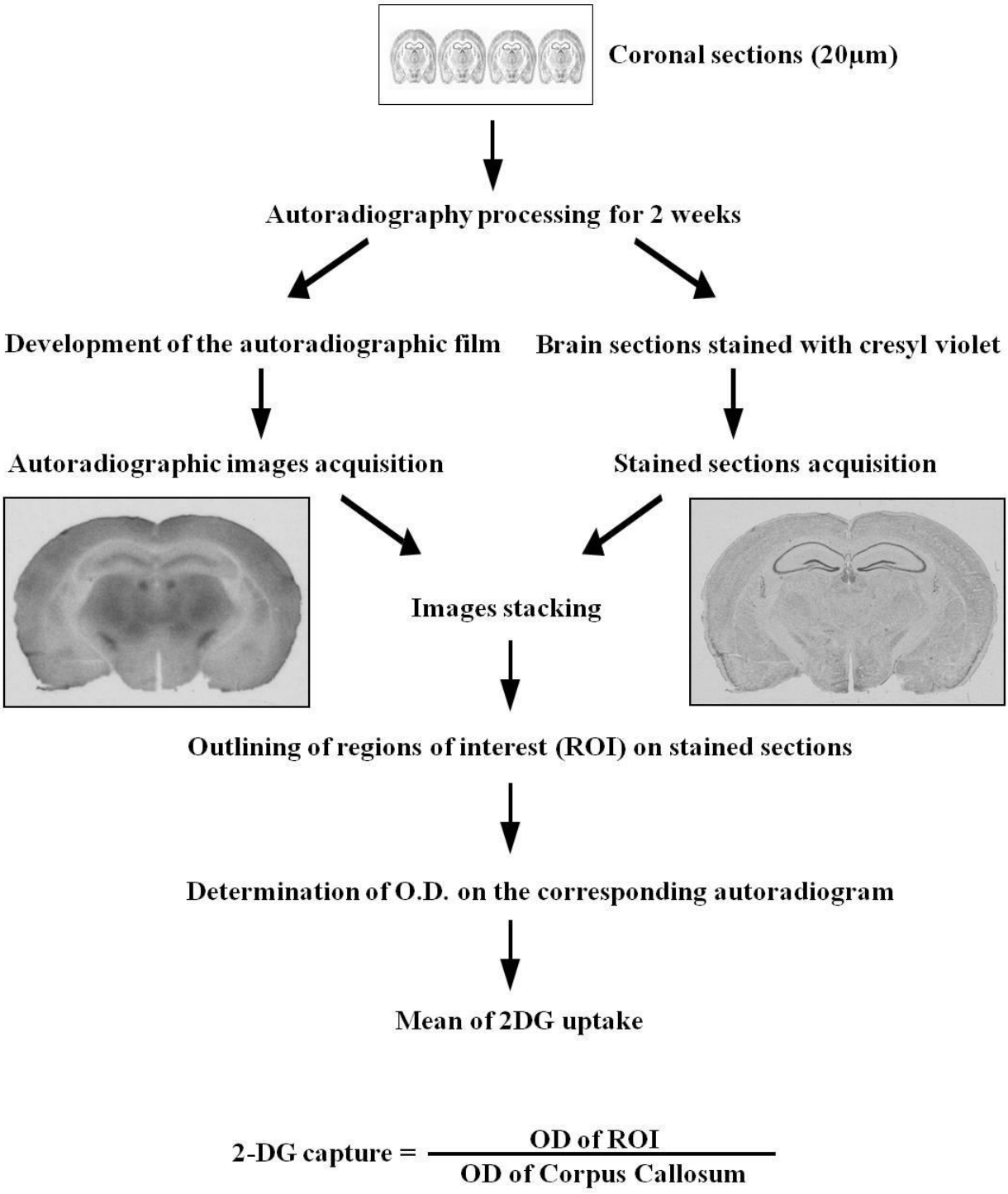

Figure 2-3: Procedure for quantitative analysis of metabolic activity in distinct brain regions

2.6 DEVELOPING A NEW SOFTWARE FOR AUTORADIOGRAMS ANALYSIS

The 2DG technique has its advantages (as the individual brain analysis for each animal allowing us to study the correlation between good or bad individual performance and a given pattern of brain metabolic activation), but one inconvenient is the biased analysis we can do and the subsequent (possible) omission of some, maybe, important activated regions. We also must consider that this type of analysis is time-consuming. To improve that, an alternative approach, based on merging and warping of autoradiograms of mice belonging to the same group, and aimed at the unbiased identification of regions of interest, has been developed in collaboration with the group of Jean-Philippe Thiran at the Signal Processing Institute at EPFL. This software has been called JULIDE and it is described below, in the chapter "Results".

2.7 LASER CAPTURE MICRODISSECTION (LCM)

As indicated above, every two slides for autoradiography, one slide for laser capture microdissection was taken. Four coronal sections were collected on a special membrane-covered slide (P.A.L.M Microlaser Technologies GmbH; Carl Zeiss) at -20°C (cryostat) and left at room temperature for ~5 seconds to allow sections well fixed to the membrane. Each brain section was covered (~50 µl) with RNA later-ICE (Ambion) to preserve the RNA quality for a long time at the freezer (-20°C). Just before LCM, sections were stained with HistoGene (Arcturus Bioscience), a specific dye for microdissection. Slides were removed from the freezer and allowed to thaw for approximately 30 seconds. Then, they were immersed in a 75% ethanol bath (30 seconds) followed by a distilled water bath (30 seconds). 100 µl of HistoGene staining solution was applied directly onto the glass slide covering all the brain sections (20 seconds). Slides were rinsed in a distilled water-75%-95%-100% ethanol bath for 30 seconds each and then immersed in a xylene bath for 5 minutes. They were allowed to dry in the hood for 5 minutes and placed in a slide box containing fresh desiccant.

The PALM MicroLaser System (Carl Zeiss) based on the LMPC (Laser Microdissection and Pressure Catapulting) technology was used in this part of the experiment. Microdissection was performed in 2 steps; the region of interest was cut by a first laser pulse

and then it was catapulted into a collection tube by a second laser pulse (see figure 2-4). This is a non-contact and therefore contaminant-free sample collection technology.

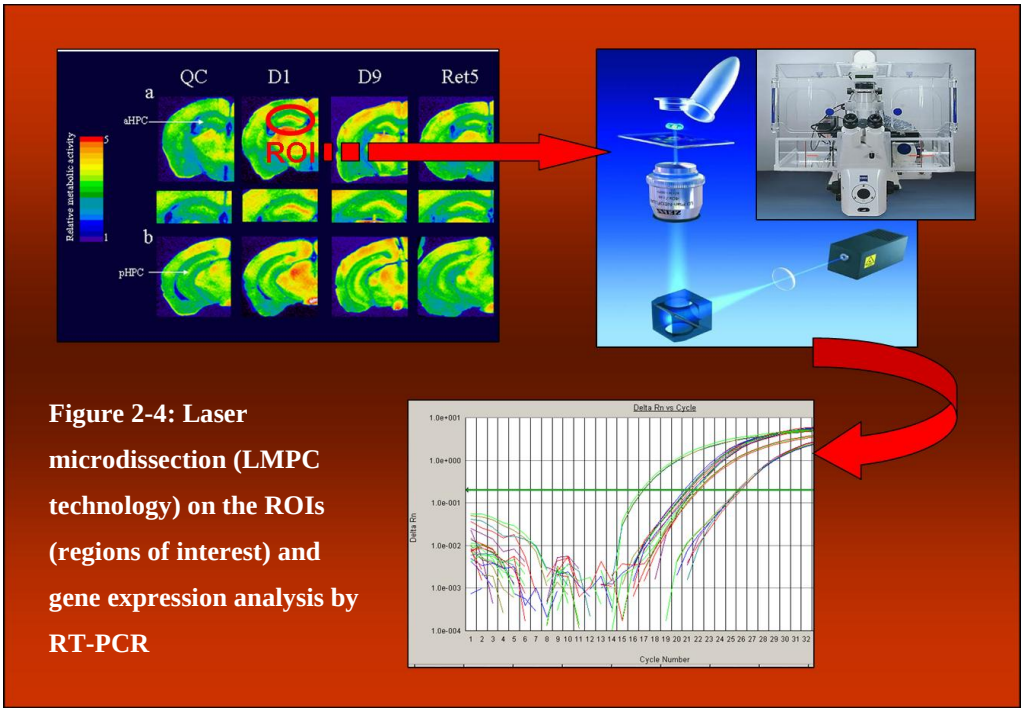

Figure 2-4: Laser microdissection (LMPC technology) on the ROIs (regions of interest) and gene expression analysis by RT-PCR

The hippocampus and the retrosplenial cortex were collected in this way in microtubes and then a cell lysate was generated using CellsDirect (resuspension buffer and lysis enhancer) from Invitrogen. Reverse transcription (SuperScript VILO cDNA Synthesis; Invitrogen) was performed immediately following the protocol provided with the kit. A total final volume of 20 µl per reaction was prepared, by mixing the reagents delivered with the kit with our RNA sample, and then incubated at 25°C for 10 minutes, at 42°C for 60 minutes and at 85°C for 5 minutes. Due to the low quantity of material, a preamplification step (Taqman Gene Expresion Assays and PreAmp Master Mix Kit from Applied Biosystems) was necessary before performing PCR. First, a pool of Taqman assays was done by combining 10 µl of each 20X assay (32 assays in total, one per gene of interest, see table 2) and diluting it with 1X TE buffer, so that the final pool concentration was at 0.2X. Then, a 50 µl reaction was prepared by combining the Taqman PreAmp Master Mix, the pooled assay mix and our cDNA sample. Preamplification reactions were run in a thermocycler at 95°C for 10 minutes and then at 95°C (15 seconds)-60°C (4 minutes) during 14 cycles. The product of this preamplification process was diluted 1:20 using 1X TE buffer. All these preamplification steps were performed according to the protocol provided with the kit.

Glycolysis			
Symbol	**Name**	**Public RefSeq**	**Assay ID**
Hk1	Hexokinase 1	NM_010438.2	Mm00439344_m1
Hk2	Hexokinase 2	NM_013820.3	Mm00443385_m1
Pfkl	Phosphofructokinase, liver	NM_008826.4	Mm00435587_m1
Pfkp	Phosphofructokinase, platelet	NM_019703.3	Mm00444792_m1
Aldoa	Aldolase 1, A isoform	NM_007438.3	Mm00833172_g1
Gapdh	Glyceraldehyde-3-phosphate dehydrogenase	NM_008084.2	Mm99999915_g1
Eno2	Enolase 2, gamma neuronal	NM_013509.2	Mm00469062_m1
Pyruvate metabolism			
Symbol	**Name**	**Public RefSeq**	**Assay ID**
Pcx	Pyruvate carboxylase	NM_008797.2	Mm00500992_m1
Pdk1	Pyruvate dehydrogenase kinase, isoenzyme 1	NM_172665.3	Mm00554306_m1
Pdk2	Pyruvate dehydrogenase kinase, isoenzyme 2	NM_133667.1	Mm00446681_m1
Pdk4	Pyruvate dehydrogenase kinase, isoenzyme 4	NM_013743.2	Mm00443325_m1
Pentose phosphate pathway			
Symbol	**Name**	**Public RefSeq**	**Assay ID**
G6pdx	Glucose-6-phosphate dehydrogenase, X-linked	NM_008062.2	Mm00656735_g1
Taldo1	Transaldolase 1	NM_011528.3	Mm00807080_g1
Tkt	Transketolase	NM_009388.5	Mm00447559_m1
Glycogenregulation			
Symbol	**Name**	**Public RefSeq**	**Assay ID**
Gyg1	Glycogenin	NM_013755.2	Mm00516516_m1
Gys1	Glycogen synthase 1, muscle	NM_030678.3	Mm00472712_m1
Ppp1r3c, PTG	Protein phosphatase 1, regulatory subunit 3C	NM_016854.2	Mm01204084_m1
Pygb	Brain glycogen phosphorylase	NM_153781.1	Mm00464080_m1
Pygm	Muscle glycogen phosphorylase	NM_011224.1	Mm00478582_m1
Lactate shuttle			
Symbol	**Name**	**Public RefSeq**	**Assay ID**
Ldha	Lactate dehydrogenase A	NM_010699.1	Mm00495282_g1
Ldhb	Lactate dehydrogenase B	NM_008492.2	Mm00493146_m1
Slc16a1, MCT1	Solute carrier family 16, member 1	NM_009196.3	Mm00436566_m1
Slc16a7, MCT2	Solute carrier family 16, member 7	NM_011391.1	Mm00441442_m1
Slc2a1, GLUT1	Solute carrier family 2, member 1	NM_011400.2	Mm00441473_m1
Slc2a3, GLUT3	Solute carrier family 2, member 3	NM_011401.3	Mm00441483_m1
Atp1a2	Na^+/K^+ ATPase, alpha 2 unit	NM_178405.3	Mm00617899_m1
Plasticity genes			

Symbol	Name	Public RefSeq	Assay ID
Arc	Activity regulated cytoskeletal-associated protein	NM_018790.2	Mm00479619_g1
Gap43	Growth associated protein 43	NM_008083.2	Mm00500404_m1
Dlg4, PSD95	Discs, large homolog 4 (Drosophila)	NM_007864.3	Mm00492193_m1
Egr1, Zif268	Early growth response 1	NM_007913.5	Mm00656724_m1

Table 2: Genes analyzed by RT-PCR using LDA cards

A list of studied genes showing the gene symbol, the gene name, the reference number and the Applied Biosystems identification number.

To perform PCR amplification, 100 µl of the preamplified and diluted cDNA were mixed with 100 µl of Taqman Gene Expression PCR Master Mix and loaded in a Low Density Array (LDA) card. The LDA card is a 384-well micro fluidic card in which 32 pre-established probes were already pre-loaded into each well of the card, in triplicate. The LDA card was designed to analyze 4 samples at the same time (hippocampus and retrosplenial cortex at day 1 and day 9 of the training protocol). PCR amplification was carried out for 40 cycles in a 7900HT PCR instrument (Applied Biosystems). Results from LDA cards are comparable (or even better) to those obtained by conventional qRT-PCR, see (Goulter et al., 2006) and table 3.

	Day 1 HP LDA (Ct)	Day 1 HP Conv. (Ct)
Actin	19.3	19.9
Arc	21.9	22.9
Cycloph.	17.5	17.9
MCT2	26.2	26.2
Pcx	24	24.6
PSD95	22.4	22.9
Zif268	29.9	29.8

Table 3: Comparison between LDA cards and conventional qRT-PCR

The results are expressed as the cycle threshold (Ct), i. e. the cycle number at which the PCR product crosses the threshold of detection. A comparison has been done between LDA cards and conventional qRT-PCR on a day 1-HP (hippocampus) sample. LDA cards are even more sensitive than the conventional technique.

2.8 PREPARATION OF RIBOPROBES AND IN SITU HYBRIDIZATION

cDNA fragments for Na^+/K^+ ATPase alpha2 subunit (400 bp) and actin (519 bp) were obtained from C57BL/6 mouse RNA using the High Capacity RNA-to-cDNA kit (Applied Biosystems). Then, cDNA fragments (for Na^+/K^+ ATPase: forward primer: 1430-1447 5'-TCTCGGATCGCTGGTCTC-3'; reverse primer: 1830-1809 5'-AGAAGCCCAGCACTCGTTCCC-3' and for actin: forward primer: 91-110 5'-TATCGCTGCGCTGGTCGTCG-3'; reverse primer: 610-591 5'-ACGCAGGATGGCGTGAGGGA-3') were cloned into the pGEM-T Easy vector (Promega). Plasmids were linearized to make accessible the DNA template for transcription, using appropriate restriction enzymes (SpeI for Na^+/K^+ ATPase and NcoI for actin), and paying attention to create 5' overhangs to avoid transcription of undesirables fragments. After restriction digest, DNA was purified via phenol-chloroform extraction and subsequent ethanol precipitation. RNA complementary probes (anti-sense) or anti-complementary probes (sens) to our mRNA of interest were obtained by in-vitro transcription using T7 or SP6 polymerases, labeling at the same time the RNA by incorporation of DIG-UTP (digoxigenin-uridine triphosphate) during the transcription process (DIG RNA Labeling Kit (SP6/T7); Roche Applied Science). The Na^+/K^+ ATPase antisense probe was synthesized by T7 polymerase while the actin antisense probe was synthesized by SP6 polymerase. After transcription, the DIG labeling efficiency was determined via the spot test according to the protocol provided with the kit. In situ hybridization was performed on the automated Discovery XT system from Ventana Medical Systems, Inc., at the Histology Core Facility at EPFL. Tissue sections were hybridized with 50 ng of probe for 6 hours at 65°C (for actin) and at 70°C (for Na^+/K^+ ATPase). ISH signal quantification was done by using the Metamorph software at the BIOP (Bioimaging and Optics Platform) at EPFL. ISH signal was measured as optical densities in our regions of interest (hippocampus and retrosplenial cortex).

2.9 DATA ANALYSIS

Comparison of learning performance was made using paired t-test between day1 and day9. Significant level was established at $p<0.05$. Optical densities of ROI were measured on all consecutive brain sections where the given region of interest was present: from Bregma -1.30 mm to -3.30 mm for the hippocampus and the retrosplenial cortex, from Bregma -0.70 mm to -1.60 mm for the laterodorsal nucleus of the thalamus, from Bregma -2.10 mm to -2.70

mm for the parietal cortex, from Bregma -2.50 mm to -3.00 mm for the mammillary bodies, from Bregma 0.5 mm to -1.10 mm for the anterior cingulate cortex and from Bregma 1.4 mm to -1.10 mm for the dorsal striatum (Hof et al., 2000). Regions of interest were drawn on Nissl images and optical densities determined on the corresponding autoradiograms, since both type of images were aligned. Optical densities were converted to ^{14}C concentration in nCi/g (2DG uptake) based on a ^{14}C-calibrated microscale. 2DG uptake of regions of interest was normalized to the mean 2DG uptake of the corpus callosum. Comparison between experimental groups (Day 1-Day 9 trained animals, AC and QC) for each analyzed region of interest was performed using unpaired t-test, except for the laterodorsal nucleus of the thalamus where an ANOVA followed by a Tukey-Kramer multiple comparison test was applied. Gene expression data were analyzed using an excel macro from Frontiers in Genetics (RT-PCR analysis-macro version 1.1) in which all LDA cards were put together. The average quantity for each triplicate was calculated and then all samples were normalized to a normalization factor obtained by calculating the geometric mean of the most stable reference genes (Vandesompele et al., 2002), being actin and cyclophilin the reference genes in our study. A threshold correction has also been done for each gene to allow comparison between different samples.

III

RESULTS

3 RESULTS

3.1 LEARNING PERFORMANCE

A total number of 43 animals were trained in the eight-arm radial maze (n= 7 for day 1-OLP; n= 7 for day 9-OLP; n= 5 for day 1-PP; n= 7 for day 9-PP; n= 8 for day 1-PPd and n= 9 for day 9-PPd). Trained mice have learned the spatial task with a level of performance at day 9 of 85% (see figures 3-1 and 3-2). During the first day of training (paired t-test, $p<0.0001$), mice make approximately 45% of correct choices, a value close to the expected percentage for finding the baited arm by chance. This percent correct choice at Day 1 was in fact higher than chance level (38%) possibly because it represents the average of 6 trials per daily session. Percentage of correct choice was calculated as the number of entries in correct arms out of the total number of entries during the session and is expressed as the mean ± the standard error of the mean (s.e.m). A mean of correct choice for all mice at each day of training is represented in figure 3-1. The graph of learning performance shows clearly that the learning performance is rapid and linear up to Day 6, leveling off until Day 9.

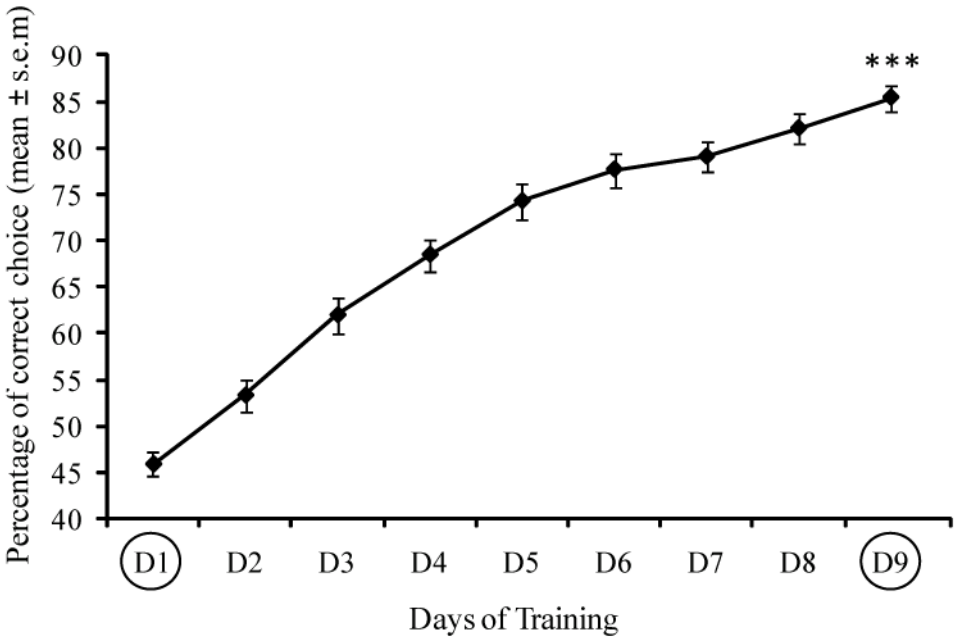

Figure 3-1: Learning performance graph

It shows the mean of correct choice per day of training. The two circled days (D1 and D9) represent the days of training where 2DG and gene analysis studies were performed. At day 9 mice reach an 85% of good choice.***p-value < 0.001 compared toDay 1.

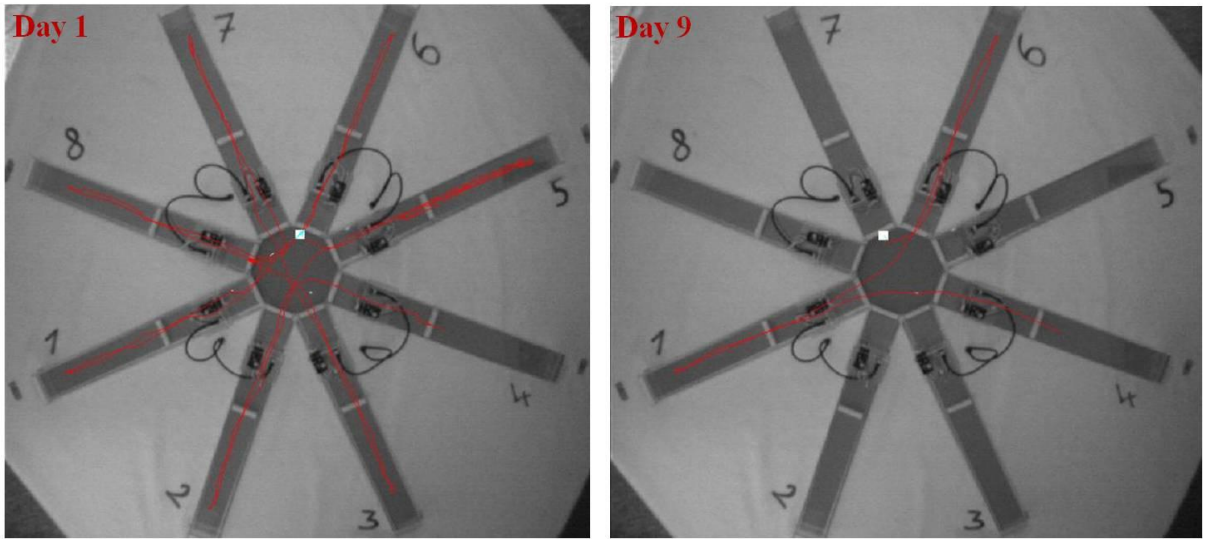

Figure 3-2: Training performance at Day 1 and Day 9

Trials start on the central platform of the RAM (white square). We can see that animals go everywhere the first day of training (no learning), whereas at Day 9 (learning has occurred) they go directly into the 3 arms baited (numbers 1-4-6 in this example).

3.2 METABOLIC MAPPING

Brain metabolic activity was assessed by two different softwares: MCID, a "conventional" image densitometry system, and JULIDE (Ribes et al., 2010), a new software developed during this thesis work in collaboration with Jean Philippe Thiran's lab, as described in "Materials and Methods". First, I am going to present the MCID results and then the JULIDE software framework followed by JULIDE results.

Brain MCID metabolic mapping revealed increases in energy consumption in several regions during the behavioral task, as measured by 2DG uptake (optical density of a given region of interest normalized to the optical density of the corpus callosum). The figure 3-3 represents 2DG uptake in the two regions showing the highest increases at day 1 or day 9 of the training protocol: the hippocampus and the retrosplenial cortex (n= 7 for both days), respectively. The 2DG uptake levels were normalized to the active control animal group (n= 8 for active control day 1; n= 7 for active control day 9). This "active control" group represented animals that had been placed in the radial maze with all 8 arms baited. The 2DG uptake comparison between day 1 and day 9 reveal that glucose utilization is high in the hippocampus the first day of training and decreased by 77 % at day 9 to reach 5 nCi/g

(unpaired t-test, p= 0.001, for the hippocampus day 1 versus day 9). In contrast, in the retrosplenial cortex, 2DG uptake is low at day 1 and increases by 79% at day 9 to reach 24 nCi/g (unpaired t-test, p= 0.032 for the retrosplenial cortex day 1 versus day 9). Color images were taken from the MCID analysis software and illustrate an autoradiographic image in which the color scale represents different concentrations of radioactivity, red corresponding to the highest radioactivity.

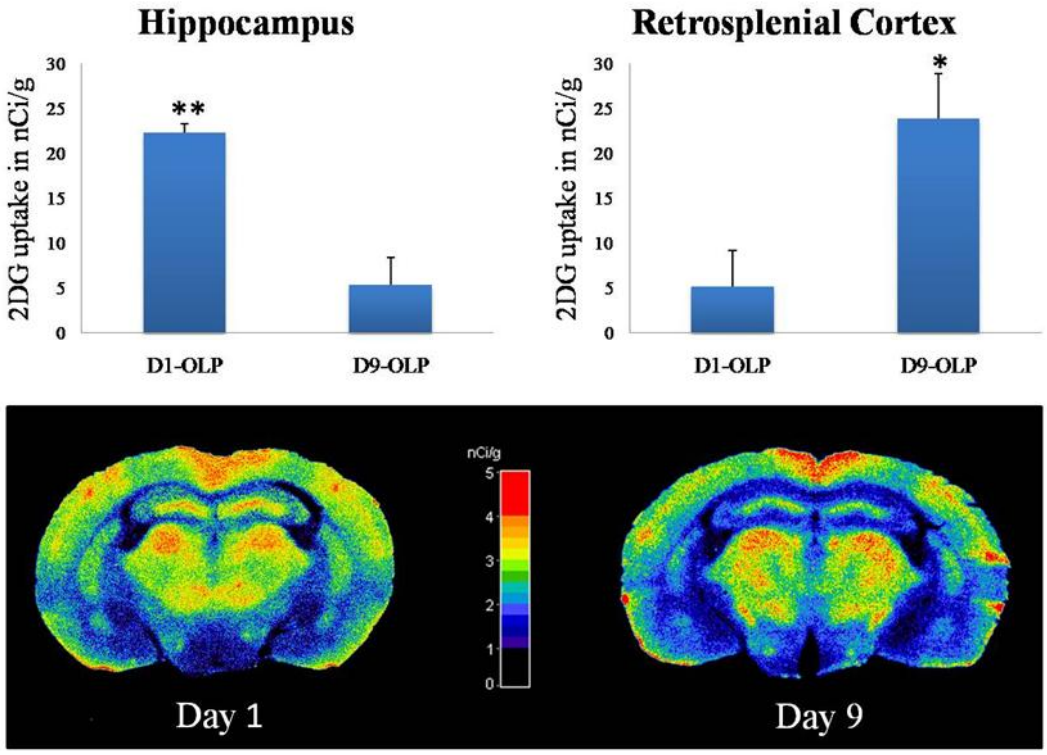

Figure 3-3: MCID results for the hippocampus (HP) and the retrosplenial cortex (RS)

Histograms representing the glucose consumption during the learning task (OLP) in the hippocampus and the restrosplenial cortex, the two most modulated regions in our paradigm as revealed by the 2DG metabolic mapping. The y axis represents the increase in 2DG uptake (nCi/g) compared to the active control 2DG level and is expressed as the mean + s.e.m. **p-value < 0.01 for the hippocampus, day 1 compared to day 9. *p-value < 0.05 for the retrosplenial cortex, day1 compared to day 9. Color images illustrate an autoradiogram of a coronal brain section from mice trained one and nine days. The color panel symbolizes different radioactivity concentrations: 1 = 50-200 nCi/g; 2 = 200-300 nCi/g; 3 = 300-400 nCi/g; 4 = 400-450 nCi/g; 5 = 450-600 nCi/g.

Other brain regions, moreover the hippocampus, were found to be activated at Day 1. These regions are: the laterodorsal nucleus of the thalamus, the fornix, the parietal cortex and the mamillary bodies.

In figure 3-4 we can see an activation of the laterodorsal nucleus of the thalamus the first day of training (Day 1) for the OLP condition (n= 7) compared to the quiet control (QC; n= 8). Glucose utilization increases at Day 1 about 18% compared to the 2DG level of the quiet control animals, which should represent the "basal" glucose consumption levels since these animals do not go to the RAM, neither for training nor for exploration. However, animals exploring the behavioral paradigm for one day but without spatial learning (AC, n= 8) present almost the same levels of glucose utilization as animals trained one day, suggesting that maybe this brain region is not spatial learning-specific but rather associated to the procedural aspect of the radial maze. This point will be discussed in detail later.

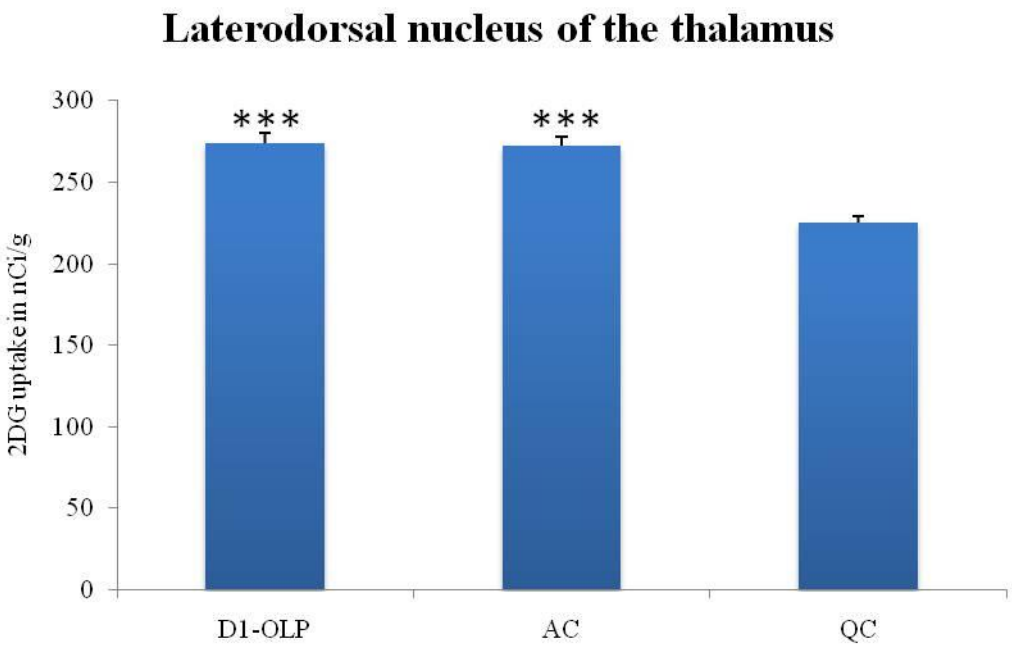

Figure 3-4: MCID results for the thalamic laterodorsal nucleus (LD)

Significant activation, measured as 2DG uptake, of the LD the first day of training (Day 1) compared to the Quiet Control (QC). Animals going to the RAM for one day but without spatial learning (AC) also present high levels of glucose utilization, comparable to those of one-day trained mice. Analysis of variance (ANOVA) followed by a Tukey-Kramer multiple comparison test. ***p-value< 0.001 for D1-OLP vs QC and AC vs QC.

At Day 1 also the parietal associative cortex was found to be activated in trained animals (see figure 3-5). This region is involved in spatial navigation since it is responsible for the integration of different sensory stimuli, including visual, tactile and auditory stimulus. An increase in glucose consumption (about 10% more) was found in the parietal cortex of

animals trained one day (n= 7) when compared to the Active Control-Day 1 (AC; n= 8) group.

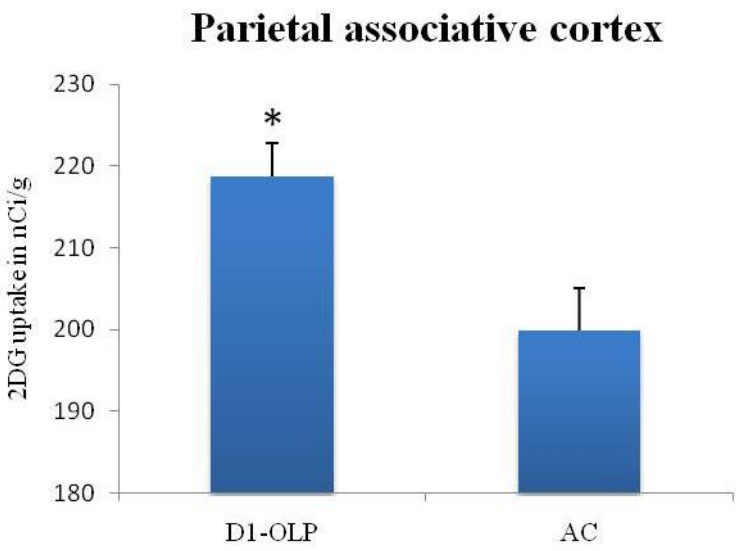

Figure 3-5: MCID results for the parietal associative cortex (PTL)

Increase in glucose consumption, measured as 2DG uptake, in the parietal cortex (PTL) the first day of training for the OLP condition. t-test comparison between Day 1-OLP trained mice (n= 7) and Active Control-Day 1 (AC; n= 8).*p-value = 0.015.

Moreover the Day 1-activation of the hippocampus, the laterodorsal nucleus of the thalamus and the parietal cortex during the learning task (OLP group), only one brain region was found activated the first day of training but 45 minutes after the end of the RAM, corresponding to the Post-Processing (PP) condition: the mammillary bodies (see figure 3-6). Results obtained from the MCID software concerning this brain region show an increase in 2DG uptake (about 27%) at Day 1 (n= 5) compared to Quiet Control (QC; n= 8). Even if this difference in glucose utilization between Day 1-PP and QC seems to be quite clear, it was not significant, due to the low number of animals forming the Day 1-PP group. Several inconvenient during the behavioral training, brain freezing and cryostat sectioning process have brought us to this low number of individuals in this experimental group.

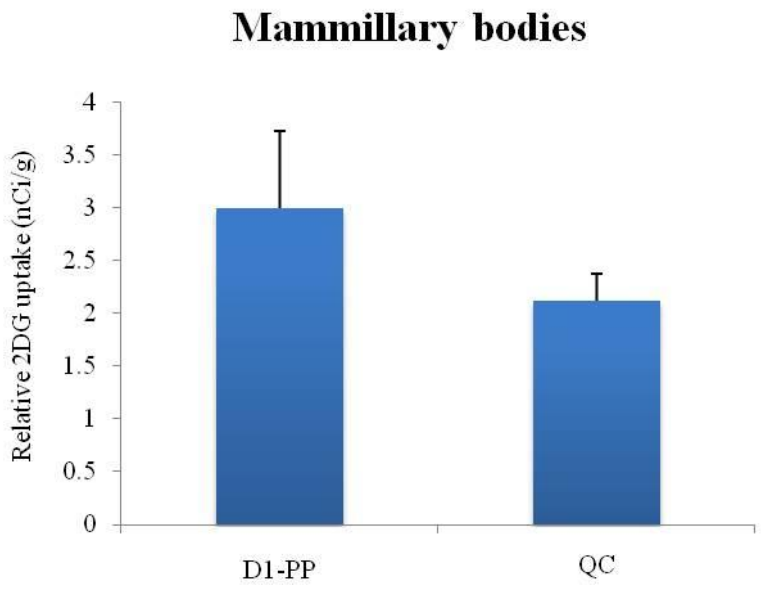

Figure 3-6: MCID results for the mammillary bodies (MB)

Increase in glucose utilization in the mammillary bodies the first day of training for the PP condition (45 minutes after the end of the training task). t-test comparison between Day 1-PP trained mice (n= 5) and Quiet Control (QC; n= 8). This difference in 2DG uptake was not found significant. MCID analysis done by Monika Saxena for this region.

In the same way as for Day 1, some other regions, moreover the retrosplenial cortex, were found activated the last day of training (Day 9). These regions were the cingulated cortex and the dorsal striatum.

Glucose consumption in the anterior cingulated cortex (ACC), measured by the MCID software, is represented in figure 3-7. A very significant activation (p-value < 0.001) was found in ACC the last day of training (Day 9, n= 7) when compared to Day 1 (n=7). The increase in 2DG uptake at Day 9 is about 37% more than at Day 1.

2DG results concerning the dorsal striatum, a region known to be implicated in skills and habits, show an increase in glucose utilization (about 13%) the last day of training (Day 9; n= 7) when compared to the corresponding active control (animals going to the RAM for 9 days; n= 7). See figure 3-8.

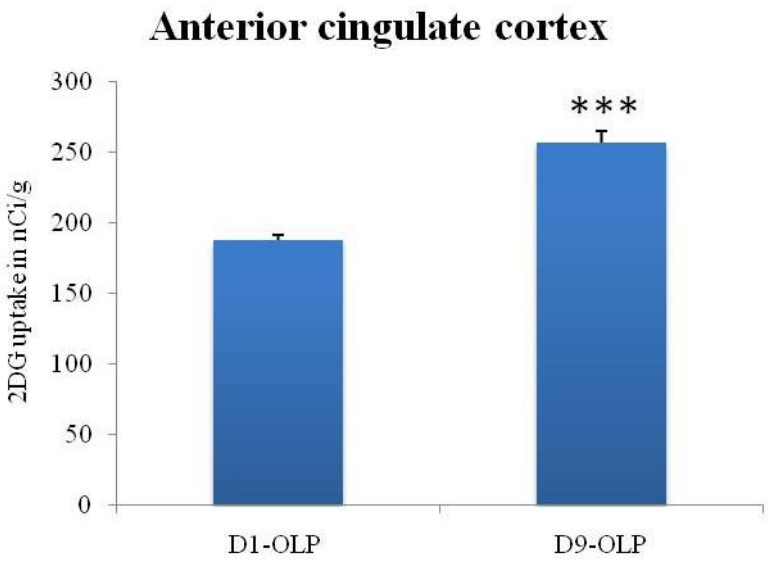

Figure 3-7: MCID results for the anterior cingulate cortex (ACC)

Glucose consumption, measured as 2DG uptake, in the ACC during the first (Day 1) and the last (Day 9) day of training. t-test comparison between Day 9 (n= 7) and Day 1 (n= 7) trained mice. ***p-value < 0.001. MCID analysis done by Monika Saxena for this region.

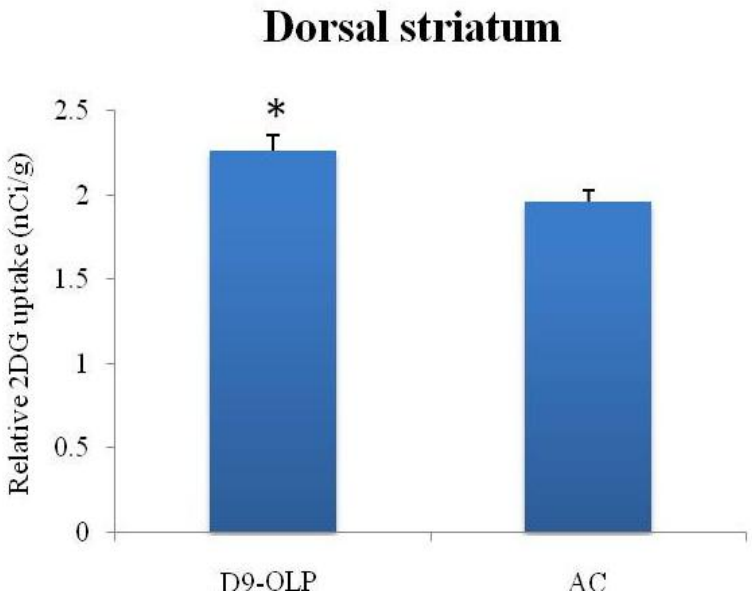

Figure 3-8: MCID results for dorsal striatum

Increase in glucose consumption at Day 9 when compared to the corresponding AC (active control animals going to the RAM for 9 days). T-test comparison between Day 9 (n= 7) and AC (n= 7). *p-value < 0.05. MCID analysis done by Monika Saxena for this region.

3.3 JULIDE: A NEW SOFTWARE FOR THE UNBIASED ANALYSIS AND 3D RECONSTRUCTION OF BRAIN AUTORADIOGRAMS.

JULIDE was born from a collaboration between Julia Parafita from the group of Pierre Magistretti at the LNDC (neuroenergetics and cellular dynamics laboratory) and Delphine Ribes from the group of Jean-Philippe Thiran at the LTS (signal processing laboratory), both groups at the EPFL. The software's name comes from JULIa and DElphine.

JULIDE is a software that allows users to detect activated areas in the brain by performing a voxel-based statistical analysis. This software give results in an unbiased manner as no specific brain regions need to be defined prior to the analysis. The software code is fully written in ITK (National Library of Medicine Insight Segmentation and Registration Toolkit (Ibanez and Schroeder, 2005)) and presents a user-friendly interface. JULIDE is based on a four-step approach which includes: (1) an automated pre-processing to select the desired section, (2) a 3D reconstruction of autoradiographic volumes, (3) a spatial normalization to compensate all the differences in position, orientation and shape and finally (4) a 3D voxel-based statistical analysis based on t-test. Outputs of JULIDE are 3D activation maps allowing to identify the significant differences in CMRGlu between two conditions. The comparison of CMRGlu between two groups is represented by color-coded statistical maps of p values defined by the user (figures 3-9 & 3-10).

JULIDE is free-available and can be downloaded at http://julide.epfl.ch

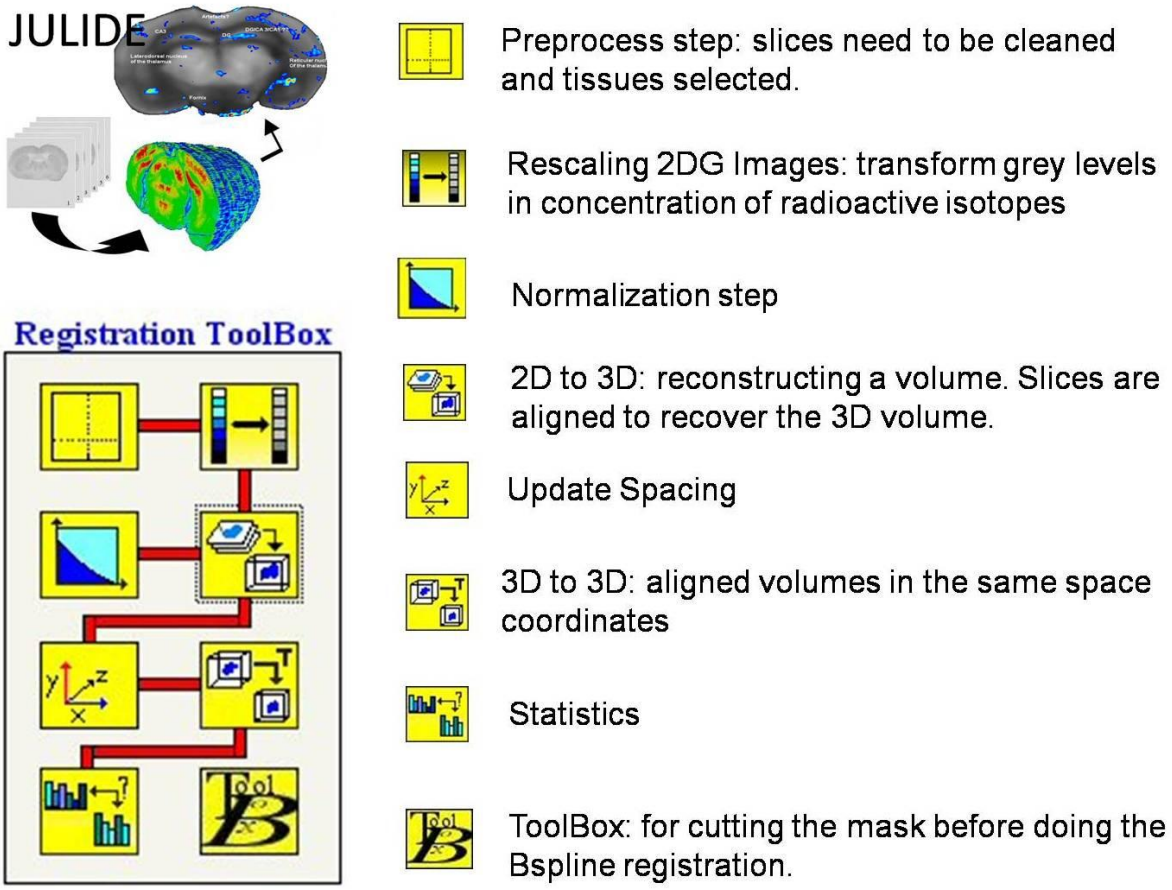

Figure 3-9: JULIDE software presentation

Summary of all main and complementary steps we can perform with our "home-made" program.

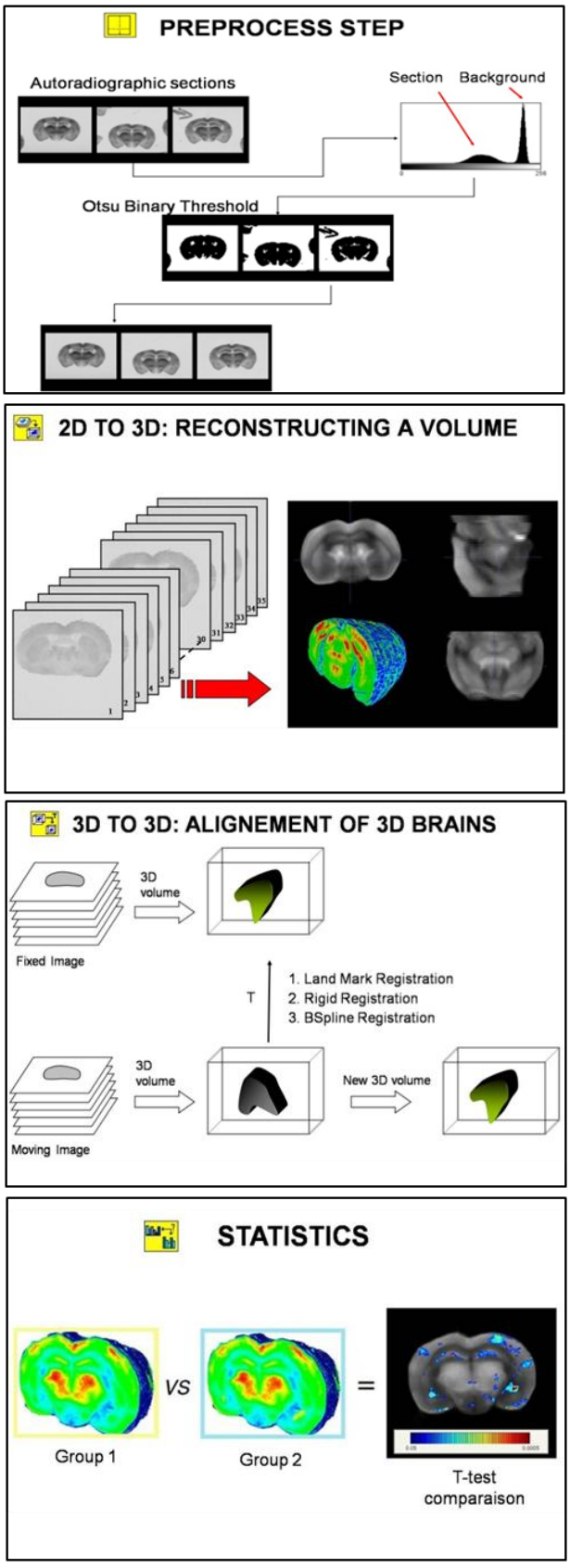

(1) The program can differentiate the pixels corresponding to the desired image and the pixels corresponding to the background and "clean" all the rest, as the arrow and the adjacent sections we can see on the autoradiographic sections on the left top of the figure.

(2) All autoradiographic sections are aligned and a 3D brain volume is reconstructed. We can visualize it in a coronal, sagittal and horizontal view. At the end of this step, we have a 3D volume for each animal.

(3) We need now to align 3D brains in the same space coordinate to be able to compare them statistically. Different transformations were applied to the "moving image": the volume we want to align to a reference one (fixed image). **Rigid reg.**: transformation in orientation and position. **Bspline reg.**: free-form deformation, to register sections by matching two images at increasing levels of detail.

(4) A mean 3D brain for each experimental group is created. Then, 3D volumes are compared two by two by performing a t-test. Results obtained are color-coded statistical maps allowing us the identification of significant differences in CMRGlu between 2 conditions.

Figure 3-10: The four main steps to process images with JULIDE

(1) Preprocessing, (2) reconstruction of a 3D volume, (3) alignment of 3D brains and (4) statistical analysis.

Moreover these four main steps, some others steps are necessary to achieve a good 3D brain reconstruction and analysis: (a) rescaling, (b) normalization, (c) update spacing and (d) toolbox. A rescaling step (a) is used to give a correspondence between gray level and 2DG concentration. A normalization step (b) is necessary if brain sections have different gray intensities due to film exposure, images acquisition procedures or different 2DG diffusion between animals. To do that a reference region, i.e. the corpus callosum, must be drawn on each brain section before aligning them to reconstruct a 3D volume. The number of slices per animal was not the same throughout the experiment and the cutting protocol was changed 3 times to improve this software, because we found that the less space we have between sections the better 3D virtual brain we get. To align all 3D brains to a reference one in the same space coordinate, the program needs to know how much distance there is between autoradiograms for each brain and this is done in the (c) update spacing step. Sometimes a tissue fragment is missing from one or more sections of a brain due to the cryostat sectioning procedure. The (d) tool box is a work tool allowing us to identify holes or fissures in the brain sections, like that the program will not deform the brain image during the Bspline registration explained above to compensate this missing tissue.

We have applied this mapping approach to the study of the regional variations in CMRGlu in mice undergoing a spatial learning task. Significant differences in the areas engaged during the behavioral task at day 1 (when animals are confronted for the first time to the maze) and at day 9 (when animals are highly performing) have been identified. These areas include the hippocampus, the fornix, the thalamic laterodorsal nucleus, the parietal cortex and the mamillary bodies at Day 1; and the anterior cingulate, the retrosplenial cortex and the dorsal striatum at Day 9.

In figure 3-11 we can see the first results we obtained with JULIDE which was in the first phase of development: comparison of two experimental conditions by subtraction of grey levels between different sections. So we get results in 2D, the 3D reconstruction not being implemented yet. In figure 3-11, a comparison has been done between animals trained one day (Day 1-OLP) versus the Quiet Control (QC) and activation was found in the hippocampus (HP), the laterodorsal nucleus of the thalamus (LD) and the fornix (fx). While confirming the findings, concerning the hippocampus (represented in figure 3-3), of the densitometrical analysis made by the MCID software, JULIDE points out differences in other brain regions, like LD and the fornix (fx). After having obtained these results, the thalamic laterodorsal

nucleus (LD) was analyzed by MCID and the same results were found: a Day 1-OLP activation compared to the QC (see figure 3-4 in the preceding section).

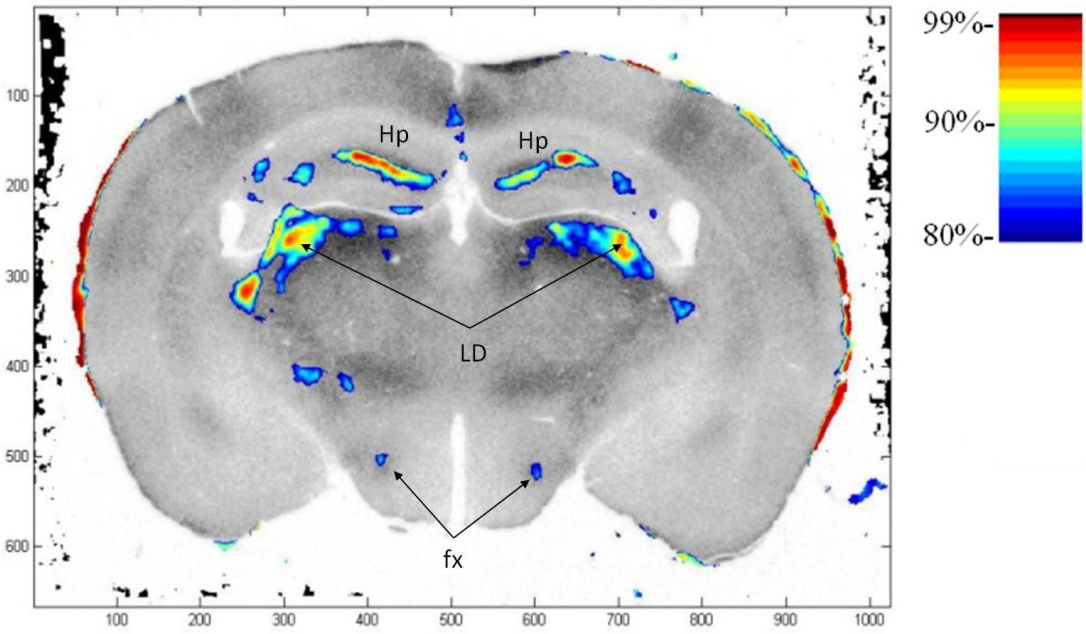

Figure 3-11: First JULIDE results when the software performed analysis only in 2D

Subtraction of grey levels between Day 1-OLP and Quiet Control showing an activation of the hippocampus (Hp), the laterodorsal nucleus of the thalamus (LD) and the fornix (fx). The color scale represents the significance level (80% in bleu, 90% in green and 99% in red). This image corresponds to early stages of the software's development.

Figure 3-12 shows a color-coded map in which the hippocampus, an area which is well-known to be implicated in spatial memory, is activated during the learning task the first day of training. The other activated region we can see on this figure is the parietal associative cortex that integrates sensory information from different modalities as vision, touch and audition, being involved in spatial navigation and visual processing. The t-test comparison was done between trained mice for one day and Active Control.

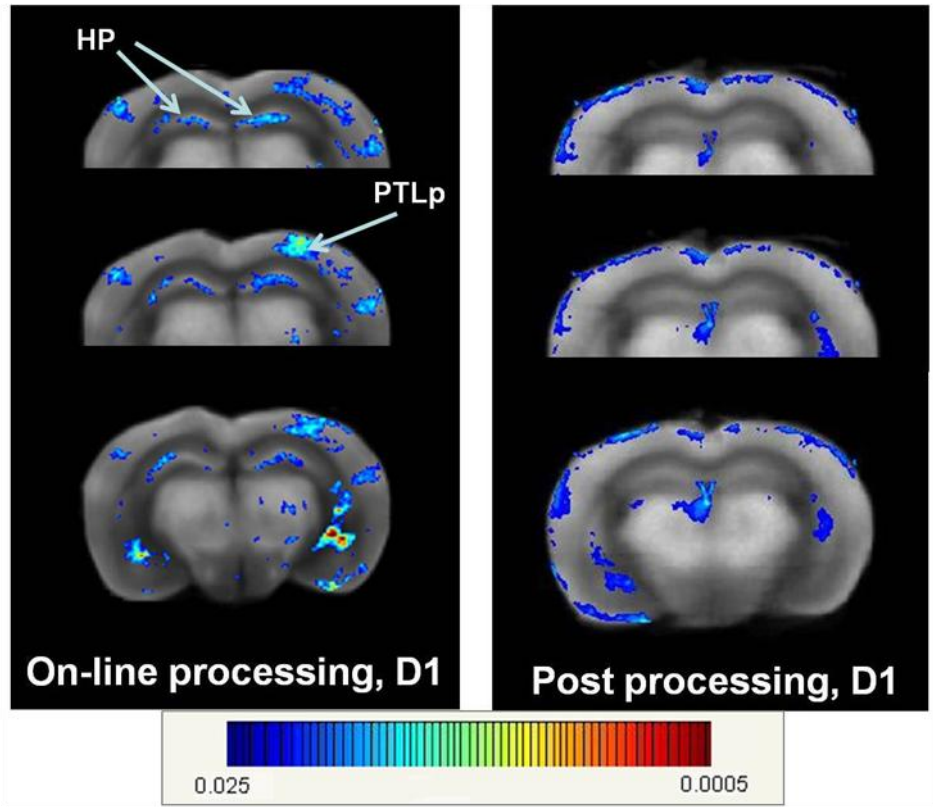

Figure 3-12: JULIDE results for the On-Line condition at Day 1

At Day 1, the hippocampus (HP) and the posterior parietal associative cortex (PTLp) are the most activated regions for the OLP condition (during learning), whereas 45 minutes later (Post-processing) the hippocampus is no more activated. The parietal associative cortex integrates sensory information from different modalities as vision, touch and audition. It is involved in spatial navigation and visual processing. t-test comparison between Day 1 and Active Control (AC). P-value = 0.02.

At day 9, the last day of training, the hippocampus is no longer activated but a high signal is detected in the anterior cingulate and the retrosplenial cortex (see figure 3-13), meaning that the 2DG recruitment has moved, over the nine days of training, from the regions that were activated at day 1 to these cortical areas, which is consistent with theories of memory consolidation (Alberini, 2005; Frankland and Bontempi, 2005). The t-test comparison was done between animals trained one and nine days.

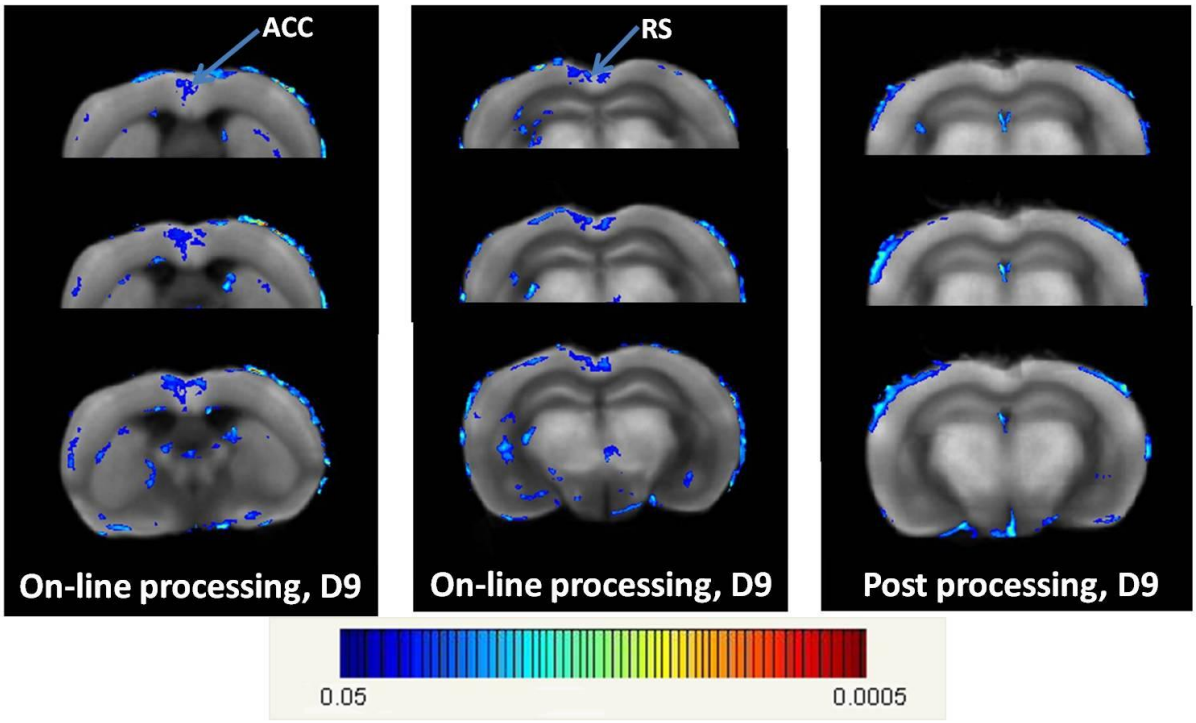

Figure 3-13: JULIDE results for the On-Line condition at Day 9 (ACC & RS)

Activation of the anterior cingulated (ACC) and the retrosplenial cortex (RS) during the last day of training, Day 9. Interestingly there is not at all activation of the hippocampal formation, meaning that the recruitment of 2DG has moved, in time, from the hippocampus to the cortex. Images of the post-processing condition are also included in the picture to show that no activation was found 45 minutes after the end of the task. T-test comparison between Day 9 and Day 1. P-value = 0.05.

At Day 9, the striatum (brain region implicated in skills and habits, besides being one of the major input relay station of the basal ganglia) was found activated the last day of training, Day 9, which is maybe consistent with some kind of habituation throughout the nine days of training. The t-test comparison was done between animals, belonging to the On-line condition, trained nine days (Day 9-OLP) and animals going to the RAM without developing a spatial strategy (AC), see figure 3-14.

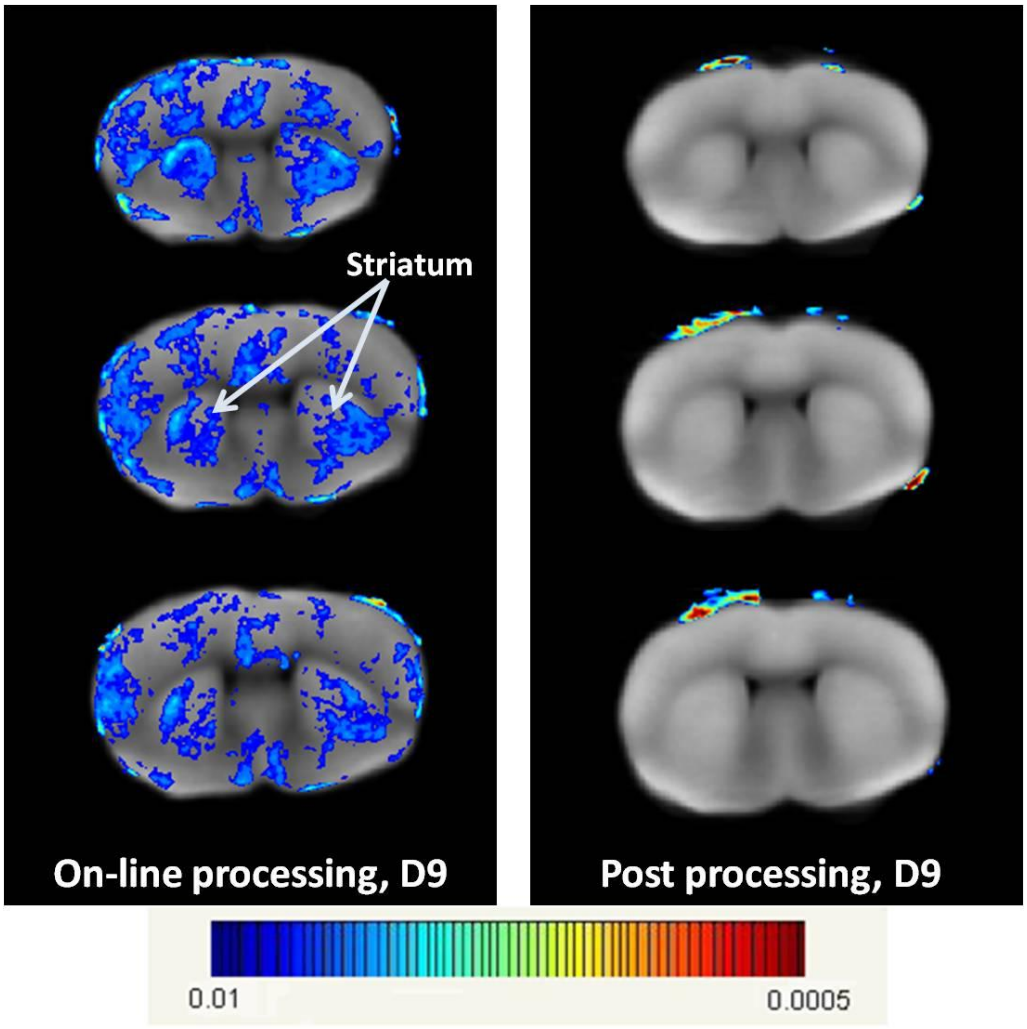

Figure 3-14: JULIDE results for the On-Line condition at Day 9 (Striatum)

The striatum, which anatomically corresponds to the caudate and the putamen nuclei of the basal ganglia, is found activated the last day of training when compared to the Active Control. T-test comparison between Day 9 and AC. P-value = 0.01. No activation was found when the comparison was made between Day 9-Post-Processing and AC.

We also looked at brain glucose consumption once the learning task was finished to see if the cerebral activity related to spatial learning continues for a while or if it is stopped at the same time as the learning task is over. In this case, the mammillary bodies were found activated the first day of training (see figure 3-15, t-test comparison was done between Day 1 trained mice and Quiet Control). Mammillary bodies are part of the Papez circuit, which is involved in storing memories, and receive inputs from the hippocampus via the fornix which is also a region we found activated during the learning task the first day of training (see figure 3-11, for fornix activation)

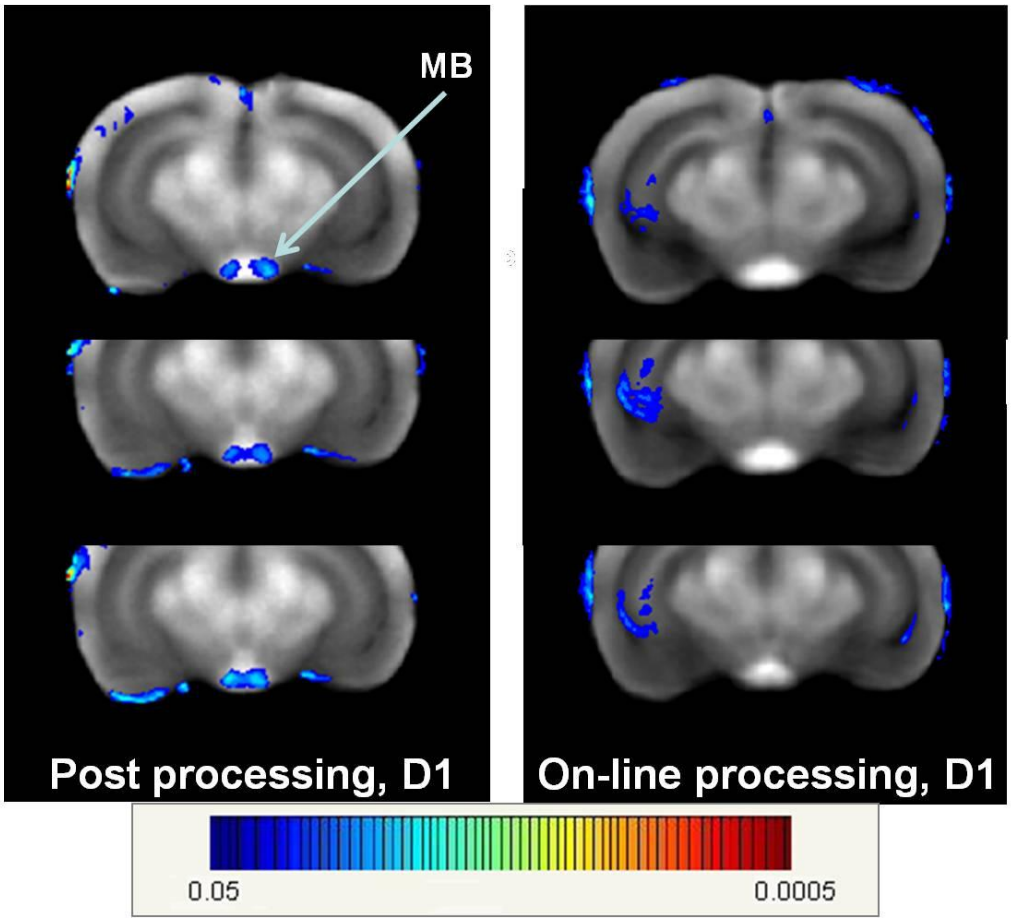

Figure 3-15: JULIDE results for the Post-Processing condition at Day 1

Mammillary bodies (MB) are the only brain region we found activated in the Post-Processing condition (45 minutes after the learning task). t-test comparison between Day 1-PP and Quiet Control (QC). p-value = 0.05. A group of three consecutive images belonging to Day 1-OLP was also included in the picture to show no activation of MB immediately after the end of the learning task.

Thus we have now a rather complete picture of the patterns of regional activations which are differentially engaged at Day 1 and Day 9 (see table 4). Results obtained with JULIDE are comparable to those obtained manually by optical densitometry of pre-selected ROI as indicated by figures 3-3 and 3-12 for the hippocampus, figures 3-3 and 3-13 for the retrosplenial cortex, figures 3-4 and 3-11 for the laterodorsal nucleus of the thalamus, figures3-5 and 3-12 for the parietal cortex, figures 3-6 and 3-15 for the mammillary bodies, figures3-7 and 3-13 for the anterior cingulated and figures 3-8 and 3-14 for the dorsal striatum.

Activated region	In (exp. group)	Compared to	Analyzed by MCID	Analyzed by JULIDE
Hippocampus	D1-OLP	D9-OLP/AC/QC	√	√
LD	D1-OLP	QC	√	√
Fornix	D1-OLP	QC	----	√
Parietal Cortex	D1-OLP	AC	√	√
Anterior cingulate	D9-OLP	D1-OLP	√	√
Retrosplenial cortex	D9-OLP	D1-OLP	√	√
Striatum	D9-OLP	AC	√	√
Mammillary bodies	D1-PP	AC/QC	√	√

Table 4: Summary of MCID and JULIDE results

3.4 GENE EXPRESSION RESULTS

As with the 2DG technique we measured glucose consumption, for the gene expression analysis we have chosen genes related to glucose metabolism. In table 2 (Materials and Methods), we can see a list of the studied genes with the gene symbol, the gene name, the reference number and the Applied Biosystems identification number. Genes are grouped by pathway, representing the glycolysis, the pyruvate metabolism, the pentose phosphate pathway, the glycogen regulation and the lactate shuttle. We have also studied some genes for synaptic plasticity. Moreover these 30 genes, 3 reference genes were also analyzed: 18S, actin and cyclophilin.

All these genes are represented in figure 3-16, in which two different compartments symbolizing a neuronal and an astrocytic cell have been drawn. Metabolic pathways are represented by different colors and, to simplify, only the first and the last metabolite for each pathway are indicated along with the selected enzymes. Genes with a darkest color in the same pathway represent astrocyte-specific genes (eg HK2 in glycolysis and GLUT1, LDHA, MCT1 and ATP1a2 in the lactate shuttle).

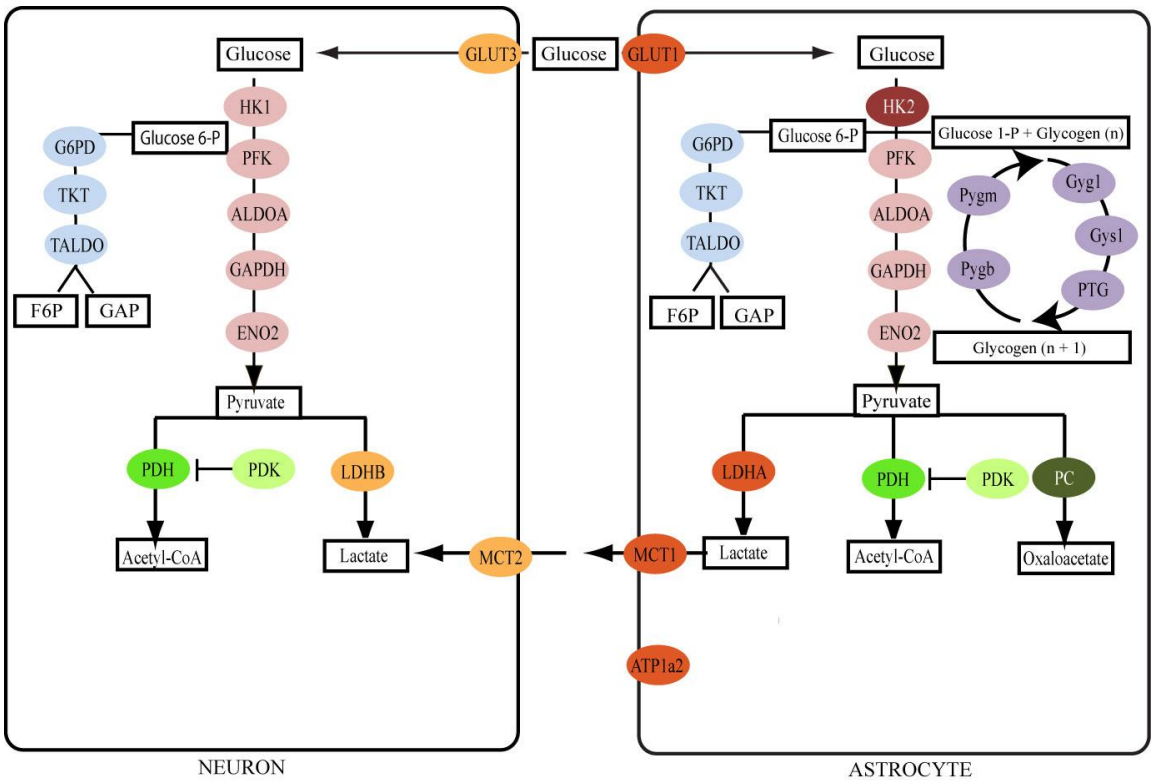

Figure 3-16: Representation of studied genes in astrocytes and neurons

The results of gene expression analysis for all 30 genes and 12 experimental conditions are presented in table 5:

	GLYCOLYSIS							PYRUVATE METABOLISM				PENTOSE P. P.			GLYCOGEN REGULATION			
	HK1	HK2	Pfkl	Pfkp	Aldoa	Gapdh	Eno2	Pcx	Pdk1	Pdk2	Pdk4	G6pdx	Taldo1	Tkt	Gyg1	Gys1	PTG	Pygb	Pygm
D10LP HP	0.504	0.796	0.833	0.059	0.524	2.736	0.011	0.610	1.063	0.167	1.362	0.468	0.021	0.005	0.333	1.471	0.059	0.257	0.274
D1PP HP	0.979	1.012	1.310	1.170	0.039	1.320	1.154	1.207	0.320	1.196	0.474	0.299	1.258	1.293	0.945	1.023	0.992	1.208	0.110
D1PPd HP	0.022		0.021	0.014	0.017	2.757	0.009	0.008	0.014	0.058	0.033	0.076	0.003	0.004	0.052	0.002	0.016	0.030	0.012
D90LP HP	0.410	0.565	0.662	0.106	0.540	2.272	0.031	0.586	1.006	0.722	2.452	0.632	0.023	0.284	1.103	1.495	0.156	0.355	0.242
D9PP HP	0.029		0.038	0.013	0.007	2.754	0.054	0.133		0.021	0.086	0.131	0.006	0.049	0.026		0.070	0.041	0.030
D9PPd HP	0.111	2.269	1.092	0.364	0.213	0.001	2.447	0.896	0.336	0.458	0.891	0.829	0.211	0.791	0.637	0.213	0.248	1.173	0.053
D10LP RS	0.652	0.867	0.505	0.086	0.876	2.537	0.005	1.354	3.227	0.135	1.336	1.749	0.004	0.004	1.145	2.527	0.009	0.125	3.298
D1PP RS	1.164	0.888	0.008	0.183	1.547	1.749	0.010	0.023	0.007	0.447	0.017	1.751	0.010	0.046	0.078	0.060	0.226	0.105	0.014
D1PPd RS	0.003			0.008		2.602	0.003		0.009	0.026	0.059				0.014	0.037	0.102	0.004	
D90LP RS	0.596	0.496	0.387	0.072	0.859	2.528	0.013	1.182	2.350	0.303	2.147	1.175	0.015	0.030	0.599	2.183	0.028	0.070	1.404
D9PP RS	0.388	0.121	0.435	1.317	0.340	1.893	3.607	1.139	0.630	0.463	3.277	2.938	0.148	1.261	1.479	2.404	1.053	3.123	2.055
D9PPd RS	0.164		0.046	0.555	0.072	2.737	0.891	1.898	0.324	0.451	2.625	0.666	0.084	0.372	1.920	1.032	0.181	1.421	0.829

	LACTATE SHUTTLE							PLASTICITY GENES			
	Ldha	Ldhb	MCT1	MCT2	GLUT1	GLUT3	ATP1a2	Arc	Gap43	PSD95	Zif268
D10LP HP	1.088	2.214	1.541	0.815	1.235	2.353	0.066	0.998	0.008	0.021	0.969
D1PP HP	0.923	1.302	0.996	1.003	1.261	0.969	1.280	1.243	1.321	1.300	0.026
D1PPd HP	1.762	2.331	0.138	0.117	0.021	0.063	0.008	0.980	0.039	0.007	
D90LP HP	1.064	2.065	1.638	0.851	0.913	2.982	0.490	0.680	0.157	0.345	0.498
D9PP HP	0.973	2.274	0.212	0.002	0.045	0.136	0.526	0.316	0.119	0.111	0.015
D9PPd HP	3.737	1.708	0.181	1.464	0.477	2.438	2.033	0.348	0.530	1.039	0.237
D10LP RS	1.832	1.970	1.290	1.258	1.809	3.311	0.024	0.933	0.020	0.002	2.649
D1PP RS	1.626	1.450	1.494	0.892	0.006	0.005	0.058	1.239	0.105	0.119	1.025
D1PPd RS	2.292	1.842		0.160		0.058	0.018	0.978	0.031		
D90LP RS	0.979	1.989	1.623	1.271	1.251	4.129	0.115	0.873	0.133	0.021	2.105
D9PP RS	0.762	2.094	1.035	1.337	1.242	4.461	10.785	1.068	3.833	0.625	1.631
D9PPd RS	1.288	1.799	1.200	0.914	0.419	3.272	5.118	0.549	1.454	0.258	0.354

Table 5: Gene expression primary data

Gene quantities were calculated for each gene from PCR cycle number comparison and normalized to a normalization factor obtained from the values of actin and cyclophilin. Missing values correspond to samples with results above 2 standard deviation. We decided to not include these results to avoid bias in the expression levels of studied genes.

Table 6 illustrates which are the most induced genes at Day 1 and Day 9 in the hippocampus and the retrosplenial cortex at 45 minutes (PP) and 6 hours (PPd) after the learning task. Induced genes were divided in 2-10 fold increase and more than 10 fold increase for each time point.

A Genes induced at Day 1 in the hippocampus

45 min.		6h	
2-10 fold	> 10 fold	2-10 fold	> 10 fold
Hk1	Pfkp	Ldha	
Pfkl	Eno2	Gap43	
Pcx	Taldo		
Pdk2	Tkt		
Gyg	PTG		
Pygb	ATP1a2		
	Gap43		
	PSD95		

B Genes induced at Day 9 in the hippocampus

45 min.		6h	
2-10 fold	> 10 fold	2-10 fold	> 10 fold
Eno2		Hk2	Eno2
		Pfkl	
		Pfkp	
		Pcx	
		Taldo	
		Tkt	
		PTG	
		Pygb	
		Ldha	
		MCT2	
		ATP1a2	
		Gap43	
		PSD95	

C Genes induced at Day 1 in the retrosplenial cortex

45 min.		6h	
2-10 fold	> 10 fold	2-10 fold	> 10 fold
Hk1	PTG	Gap43	PTG
Pfkp	PSD95		
Aldoa			
Eno2			
Pdk2			
Taldo			
Tkt			
ATP1a2			
Gap43			

D Genes induced at Day 9 in the retrosplenial cortex

45 min.		6h	
2-10 fold	> 10 fold	2-10 fold	> 10 fold
Pdk2	Pfkp	Pfkp	Eno2
Pdk4	Eno2	Pcx	Tkt
G6pdx	Tkt	Taldo	Pygb
Taldo	PTG	Gyg	ATP1a2
Gyg	Pygb	PTG	Gap43
	ATP1a2		PSD95
	Gap43		
	PSD95		

Table 6: Gene expression kinetics

Genes induced at Day 1 and Day 9 of the training protocol in the hippocampus and the retrosplenial cortex at 45 minutes and 6 hours after the learning task. The OLP condition was taken as baseline. Gene induction was classified in two categories: 2-10 fold increase and more than 10 fold increase.

Table 6-A: genes induced at Day 1 in the hippocampus

The majority of genes whose expression was increased at Day 1 in the hippocampus belong to the PP condition (gene expression analysis performed 45 minutes after the learning task). These genes are: hexokinase 1 (Hk1), phosphofructokinase (Pfkl and Pfkp) and Enolase (Eno2) for glycolysis; pyruvate carboxylase (Pcx) and pyruvate dehydrogenase kinase 2 (Pdk2) for pyruvate metabolism; transaldolase (Taldo) and transketolase (Tkt) for the pentose phosphate pathway; glycogenin (Gyg), protein targeting to glycogen (PTG) and brain glycogen phosphorylase (Pygb) for glycogen regulation; Na^+/K^+-ATPase (ATP1a2) for the lactate shuttle and Gap43 and PSD95 as plasticity genes.

Table 6-B: genes induced at Day 9 in the hippocampus

Increased gene expression in the hippocampus at Day 9 was mostly detected 6 hours after task (PPd condition). Thus genes whose expression is increased include : hexokinase 2 (Hk2), phosphofructokinase (Pfkl and Pfkp) and Enolase (Eno2) for glycolysis; pyruvate carboxylase (Pcx) for pyruvate metabolism; transaldolase (Taldo) and transketolase (Tkt) for the pentose phosphate pathway; protein targeting to glycogen (PTG) and brain glycogen phosphorylase (Pygb) for glycogen regulation; lactate dehydrogenase A (Ldha), monocarboxylate transporter 2 (MCT2) and Na^+/K^+-ATPase (ATP1a2) for the lactate shuttle and, as genes for plasticity, Gap43 and PSD95.

Table 6-C: genes induced at Day 1 in the retrosplenial cortex

Most of genes induced in the retrosplenial cortex during the first day of training were induced 45 minutes after the task. These genes included the hexokinase 1 (Hk1), phosphofructokinase (Pfkp), aldolase (Aldoa) and Enolase (Eno2) for glycolysis; pyruvate dehydrogenase kinase 2 (Pdk2) for pyruvate metabolism; transaldolase (Taldo) and transketolase (Tkt) for the pentose phosphate pathway; protein targeting to glycogen (PTG) for glycogen regulation; Na^+/K^+-ATPase (ATP1a2) for the lactate shuttle and, as genes for plasticity, Gap43 and PSD95.

Table 6-D: genes induced at Day 9 in the retrosplenial cortex

At Day 9, gene expression was augmented in the retrosplenial cortex at both times, 45 minutes and 6 hours. Increased expression 45 minutes after the task was observed for the following genes: phosphofructokinase (Pfkp) and Enolase (Eno2) for glycolysis; pyruvate dehydrogenase kinase 2 and 4 (Pdk2 and Pdk4) for pyruvate metabolism; glucose-6-

phosphate dehydrogenase (G6pdx), transaldolase (Taldo) and transketolase (Tkt) for the pentose phosphate pathway; glycogenin (Gyg), protein targeting to glycogen (PTG) and brain glycogen phosphorylase (Pygb) for glycogen regulation; Na^+/K^+-ATPase (ATP1a2) for the lactate shuttle and Gap43 and PSD95 for plasticity genes. A similar profile of gene expression was observed 6 hours after the task, except for pyruvate metabolism: pyruvate carboxylase (Pcx) was induced but no induction was observed for pyruvate dehydrogenase kinase 2 and 4 (Pdk2 and Pdk4).

In order to provide an overall view of the gene expression profiles, a graphic representation of the mean level of gene expression for a given pathway was calculated at days 1 and 9 in the hippocampus and retrosplenial cortex, using the expression in the OLP condition as baseline. Geometric means of the levels of expression of the genes in a given pathway were displayed as blue horizontal bars (see figure 3-17), the shortest bar representing the lowest geometric mean.

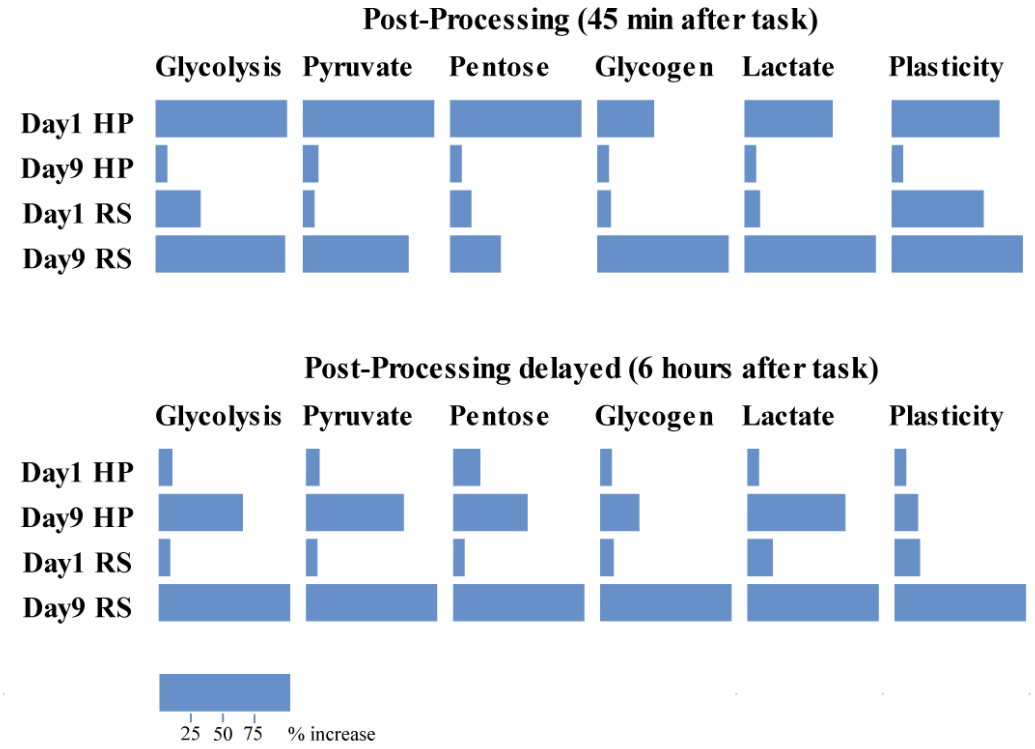

Figure 3-17: Metabolic pathway profile at 45 minutes and 6 hours after the learning task

The OLP condition was taken as baseline. The metabolic pathway score represented in colored bars is the geometric mean of all genes studied for this pathway. The different lengths of colored bars represent different increase percentages compared to the geometric mean of the same pathway for the OLP condition.

As illustrated in figure3-17, in the PP condition (post processing corresponding to 45 minutes after end of the task) expression of genes for glucose metabolism and synaptic plasticity was increased in the hippocampus at Day 1 compared to Day 9, whereas in the retrosplenial cortex gene expression was more important at Day 9 compared to Day 1. However, 6 hours after training (Post-Processing delayed, PPd) the level of gene expression was higher at Day 9 in both regions.

In order to reveal the effect of learning on gene expression, a subtraction between Day 9 and Day 1 was done for both regions of interest, the hippocampus and the retrosplenial cortex, and for the 3 experimental times; OLP, PP and PPd (see figure 3-18). Relative normalized gene expression data are represented by horizontal histograms. Negative values mean that the level of gene expression was higher at Day 1. Positive values mean that the level of gene expression was higher at Day 9. The most induced genes at Day 9 in the retrosplenial cortex – the time and region corresponding to learning, from the behavioral point of view, in association with a metabolic activation as revealed by increased glucose utilization - are phosphofructokinase (Pfkp) and enolase (Eno2) for glycolysis, pyruvate carboxylase (Pcx) and pyruvate dehydrogenase kinase 4 (Pdk4) for pyruvate metabolism, all genes tested involved with glycogen regulation (Gyg1, Gys1, PTG, Pygb and Pygm), glucose transporter GLUT3 and the Na^+/K^+-ATPase for the lactate shuttle.

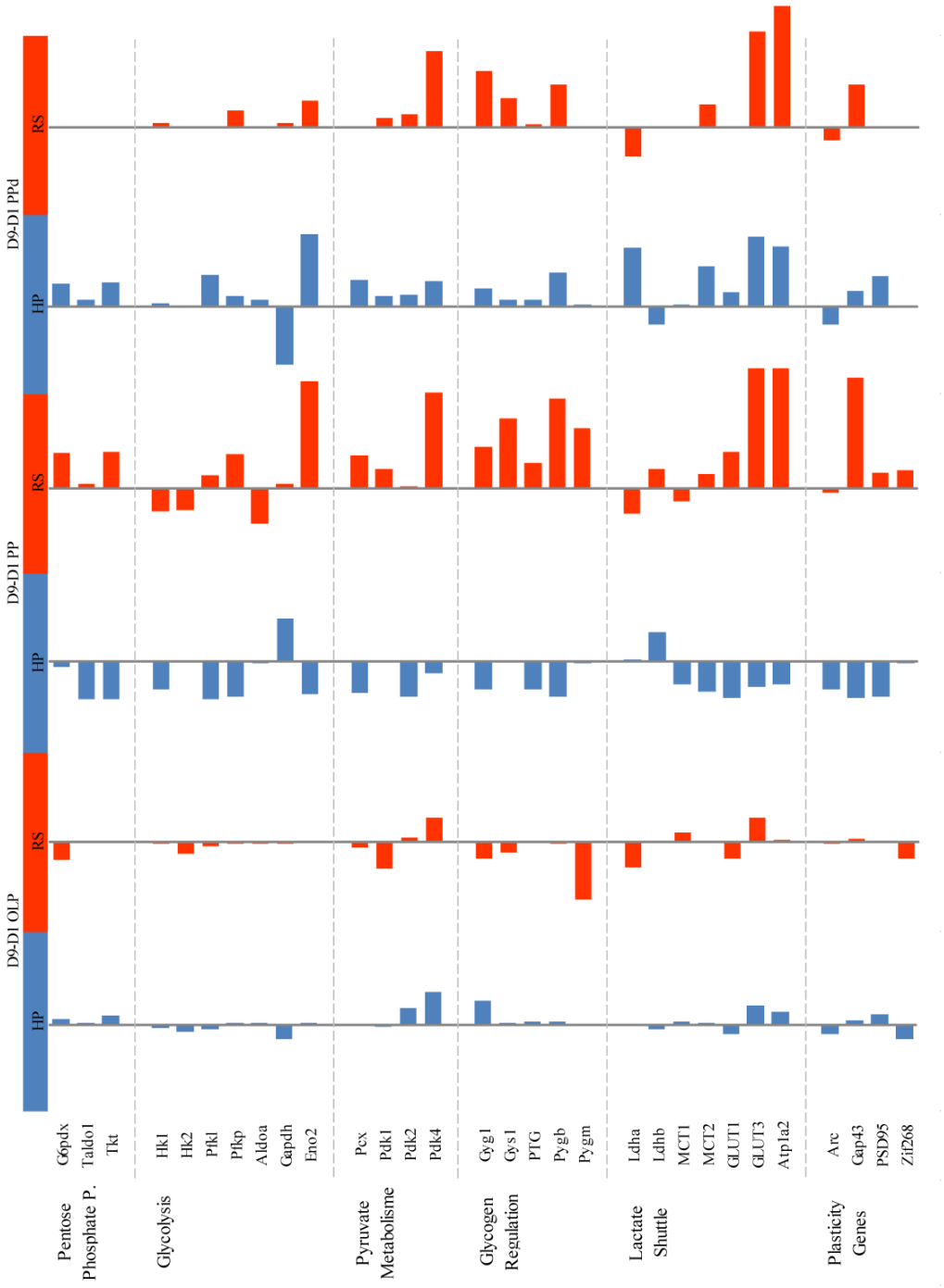

Figure 3-18: Subtraction of gene expression levels between Day 9 and Day 1

Results are represented in horizontal histograms for the 3 different times OLP, PP and PPd. In blue, the results for the hippocampus; in red, the results for the retrosplenial cortex. Negative values mean that the level of gene expression is higher at Day 1. Positive values mean that the level of gene expression is higher at Day 9.

The schematic representations in figure 3-19 show the effect of learning on gene expression for each pathway. This has been done by calculating the average resulting from the

subtraction of expression levels at Day 9 minus Day 1 at all three experimental times OLP, PP and PPd, thus providing the main tendency of the metabolic pathway in the two regions at both experimental days. This schematic representation is aimed at providing at a glance how each metabolic pathway related to glucose (glycolysis, pyruvate metabolism, pentose phosphate pathway, glycogen metabolism and lactate shuttle) is modulated by learning. To do so, two different radial cycles are represented, one for each region of interest. Each radial cycle is formed by 5 big "balls" illustrating each of the 5 pathways related to glucose metabolism. Inside each big ball, the 3 different learning times are represented in the form of little "balls": OLP in blue, PP in red and PPd in green.

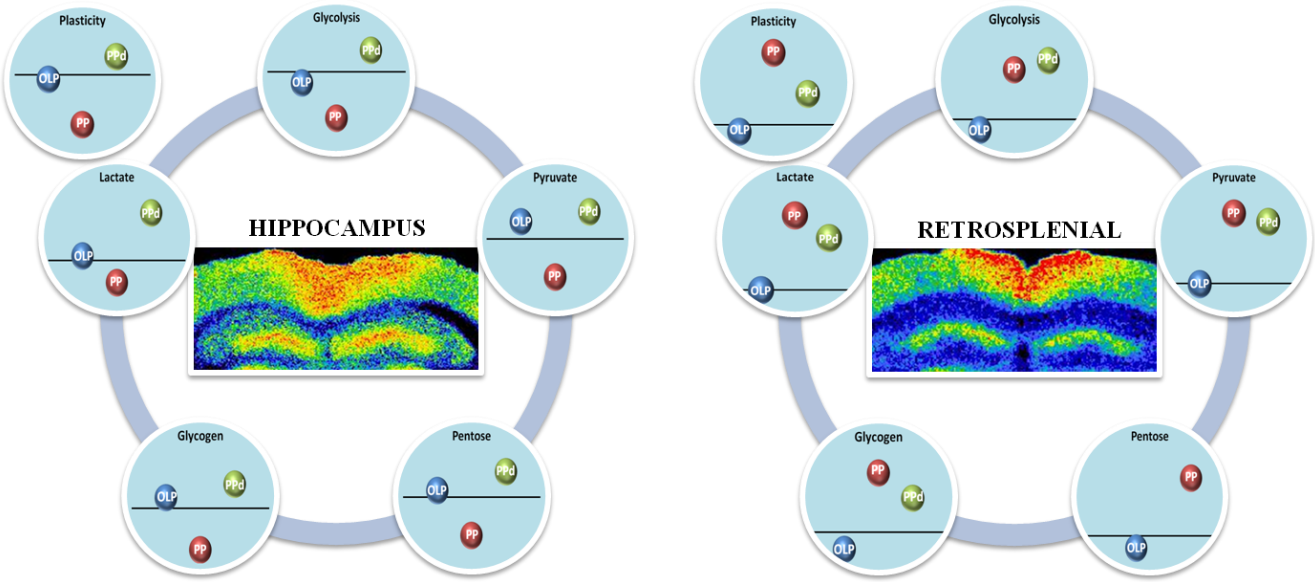

Figure 3-19: Effect of learning on gene expression per pathway

The score was calculated as the mean of gene expression of all genes for a given pathway at Day 9, minus the mean of gene expression of the same genes at Day 1. The blue, red and green balls illustrate the OLP, PP and PPd times, respectively. Moreover the five pathways related to glucose metabolism, the same transcriptional score was calculated for plasticity genes and represented in a similar graph for each brain region.

In the hippocampus, the same expression pattern was found for all three experimental conditions OLP, PP and PPd. There was no change for OLP, remaining close to zero for all metabolic pathways, whereas PP expression was lower in all cases meaning that there is a higher gene expression at Day 1 for this experimental time. In contrast, PPd was augmented compared to OLP and PP, meaning that the levels of gene expression for this condition were

higher at Day 9. In the retrosplenial cortex, we found the same results as observed in the hippocampus for OLP, staying close to the baseline in all pathways. However, and contrary to what we found in the hippocampus, PP expression was increased in all pathways at Day 9, as did PPd.

3.5 IN SITU HYBRIDIZATION (ISH)

In order to confirm the results obtained by RT-PCR, we performed some in situ hybridization experiments to demonstrate a difference between Day 1 and Day 9 in the level of expression of the Na^+/K^+-ATPase alpha2 subunit, since this gene seemed to be strongly modulated by the learning task.

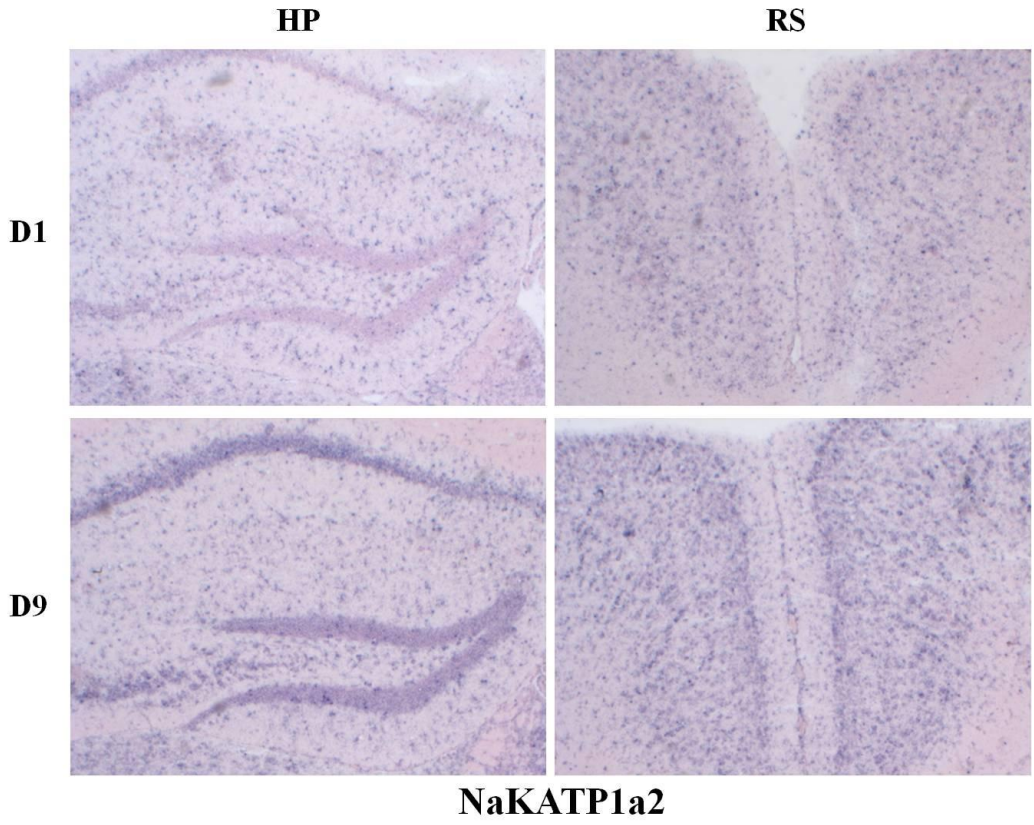

Figure 3-20: ISH results for the Na^+/K^+-ATPase alpha2 subunit

In figure 3-20, we can see the results of the ISH experiments for the Na^+/K^+-ATPase alpha2 subunit, in both regions were laser microdissection and RT-PCR were performed (hippocampus and retrosplenial cortex) and at both days (Day 1 and Day 9). ISH was performed on brain sections corresponding to the Post-Processing group (45 minutes after the end of the learning task). By eye, it seems that there is a slightly higher signal in the

retrosplenial cortex at Day 9, compared to Day 1, which would be consistent with the gene expression results. However, concerning the hippocampus, a high ISH signal is also detected at Day 9 and this is not consistent with RT-PCR results, since the highest gene expression for ATP1a2 mRNA was found the first day of training (see figure 3-18). Moreover, after doing a quantification of the ISH signal (optical density measurement) no significant difference was found between Day 1 and Day 9, neither for the hippocampus nor for the retrosplenial cortex.

IV

DISCUSSION

4 DISCUSSION

The eight-arm radial maze (RAM) has been widely used to study spatial learning in rodents (Masuda et al., 1994; Bontempi et al., 1996; Smith et al., 1998; Winocur and Gagnon, 1998; Bontempi et al., 1999; Routtenberg et al., 2000; Pothuizen et al., 2004; Yoshihara and Ichitani, 2004; Ros et al., 2006); however the training protocol has not been always the same. I took the same training schedule as used by Jacqueline Ros (Ros et al., 2006) who replicated the one described by Bruno Bontempi (Bontempi et al., 1999), a procedure consisting in 9 daily training sessions composed of 6 consecutive trials separated by a 1 minute interval (as explained in Materials and Methods). It has been published, several years ago, that a RAM-spatial protocol lasting 5 days is sufficient to demonstrate a significant progress in learning performance over time (Roullet, 1995), which is consistent with our behavioral results (figure 3-1) as animals present a 74% of correct choice at Day 5, which is highly significant ($p<0.001$; t-student test) when compared to the 45% obtained at Day 1. Nevertheless, we kept our 9-days training protocol since we were interested in a very complex and intensive training task to have more opportunities to detect post-learning (PP and PPd) changes at the level of 2DG and gene expression.

Roullet established the important role of the inter-session delay to get good performances on a spatial task. On a spatial learning paradigm like the radial arm maze, animals should visit each arm only once, so they need to remember which arms they already explored during the session. If the delay between two successive training sessions is very short, a kind of interference can occur and mice will be confused about those arms already visited and those that were not. Roullet has shown that with an inter-session delay inferior to 2 hours animals are bad learners, while with a 2-hours, 8-hours and, the most frequently used (as in our case), 24-hours delay mice reach very good performances (Roullet, 1995). Contrary, an intra-session delay (between the different trials performed on the same day) longer than 2 hours disturbed spatial, mainly working, memory in rats (Yoshihara and Ichitani, 2004). In this kind of delayed-RAM, the delay period is normally interposed after the four first choices, establishing a pre-delay and a post-delay training. All arms are baited and after the delay-period animals must find the four arms there were not visited before (Chrobak and Napier, 2002).

The 2DG results for the hippocampus and the retrosplenial cortex corroborate the theoretical model of memory consolidation published by Frankland and Bontempi (Frankland and Bontempi, 2005), according to which the hippocampus is engaged in the early stages of learning, gradually establishing reciprocal connections with the neocortex. The daily reactivation of this hippocampal-cortical circuit, as in the protocol used in this study by re-exposing mice to the radial maze once they have learned, leads to the strengthening of this network, mainly in the neocortex. Reinforcement of cortico-cortical connections allows new memories to be stabilized and integrated with other pre-existing cortical memories and becoming, over time, independent of the hippocampus (figure 4-1).

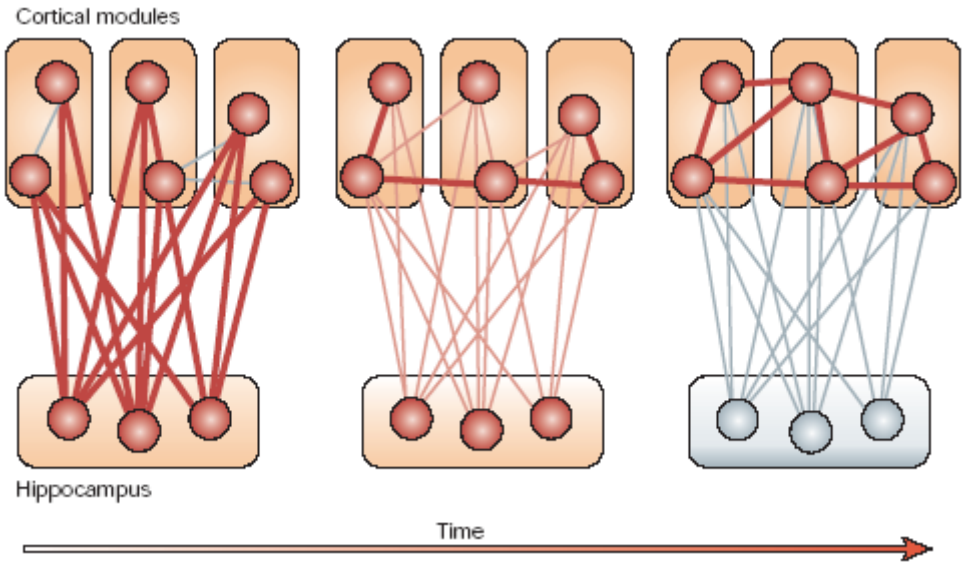

Figure 4-1: Standard consolidation model

Evolution of memory consolidation over time. During early stages of learning, information remains in a hippocampal-cortical circuitry. Synaptic activity leads to the strengthening of synapses in the neocortex either by reinforcement of already existing connections or by establishing new ones. Gradually, information is integrated in cortico-cortical circuits becoming independent of the hippocampus. Taken from Frankland and Bontempi, 2005.

This is consistent with the important reduction in 2DG uptake in the hippocampus observed at day 9 of learning when compared to day 1, showing that this brain structure is particularly engaged during early stages of learning. Interestingly, the opposite modulation is observed in the retrosplenial cortex where a significant increase in glucose consumption occurs at day 9, consistent with the notion that memory traces are transferred, over the nine days of training, from the hippocampal formation to this region of the neocortex. In both cases, the increase of 2DG uptake is linked to an increase in energy need. As we compare groups of mice with or without learning, we can conclude that this additional energy demand

is related to memory formation/storage of information. In agreement with this concept, Squire and Alvarez have observed that changes in connections between the hippocampus and cortical regions are rapid and transient, whereas changes in cortico-cortical connections are slow and long-lasting (Squire and Alvarez, 1995). A more recent paper (Tse et al., 2007) points to the capacity of the neocortex for rapid consolidation when newly acquired information is compatible with previously acquired knowledge, forming an associative "schema" in which new traces are quickly assimilated.

When an already stored information is recalled, the traces encoding it become labile and sensitive to disruption (Taubenfeld et al., 2001; Alberini, 2005) requiring another round of consolidation (reconsolidation), which involves de novo protein synthesis to preserve it (Nader et al., 2000; Debiec et al., 2002). In a certain way, each daily training session of the spatial learning paradigm used in this study can be considered as a reactivation of a cortical integrated memory that engages again in a hippocampal-cortical circuitry. The fact that 2DG levels in the hippocampus of trained animals at day 9, while considerably lower that at day 1, still remain higher than levels observed in the hippocampus of animals that visit the radial maze without developing a spatial learning strategy because all arms were baited (active controls) is consistent with this view. This observation suggests that the process of reconsolidation requires energy. Thus, the hippocampus would be again mobilized even on the last day of training, when the radial maze task causes a retrieval of acquired information, but considerably less so than on day 1. Interestingly, the 2DG results are in excellent agreement with gene expression data to be discussed below.

A hippocampal, retrosplenial and prefrontal hypoactivity, determined as c-fos expression levels after an eight-arm radial maze task, has been shown in a model of diencephalic amnesia (lesions of the mammillothalamic tract) pointing at a subcortical-cortical memory circuit subserving episodic learning (Vann and Albasser, 2009). Along the same lines, lesions of the hippocampal formation but not of the entorhinal cortex decrease c-fos and Zif268 expression levels in the retrosplenial cortex, further stressing the interconnection of these two cerebral regions (Albasser et al., 2007).

If there is no doubt about the implication of the hippocampus in the formation of a declarative episodic memory, there is no really a consensus on the role of different

subregions/parts of the hippocampus in this kind of memory. Moser and Moser, after performing rat hippocampal lesions studies, have showed that a large dorsal hippocampal region (70%) is involved in spatial learning, either encoding or retrieval, while the small ventral part is not essential for navigation in a water maze task (Moser and Moser, 1998b). In the same year, other authors, using human PET studies, published that the anterior hippocampus is activated by encoding and the posterior hippocampus by retrieval (Lepage et al., 1998). Based on human fMRI studies, other researchers said that there is no anatomical difference in hippocampal activation between encoding and retrieval, even though the middle and posterior hippocampus is more strongly activated than the anterior part (Greicius et al., 2003). Pothuizen and collaborators (rat hippocampal lesions studies) state that dorsal lesions led to significant impairments in spatial reference and working memory, and that extending lesions to the entire hippocampus did not change the behavioral results, suggesting that addition of ventral damage did not aggravate the memory deficits observed after dorsal lesions alone (Pothuizen et al., 2004). Essentially, Moser & Moser and Pothuizen present the same results i.e. the ventral part of the hippocampus seems to be not necessary for episodic memory and only the dorsal hippocampus is important. This is maybe due to the kind of experiment performed to study this issue, since both groups did rat hippocampal lesions, highlighting the importance of being careful when comparing results from different techniques (animal lesions, PET and fMRI). In our project, 2DG uptake in the hippocampus was assessed in the entire region; if differences exist between the dorsal and the ventral parts of this brain region this must be "masked" by our analysis procedure.

The hippocampal formation and the retrosplenial cortex are also reciprocally connected to the anterior thalamic nuclei (ATN) (Shibata, 1993; Aggleton et al., 2010), formed by the anterodorsal (AD), the anteroventral (AV) and the anteromedial (AM) nucleus. They are anatomically close to the laterodorsal thalamic nucleus (LD). Lesions of both regions (ATN and LD) cause spatial learning and memory deficits in a water maze task, even though the degree of impairment is dependent on the extent of the injury: if the lesion is restricted to LD, animals are mildly impaired and can finally learn the task if the training period is prolonged, whereas if the lesion affects LD and also the anterior thalamic nuclei they are not able to learn, even after a prolonged exposition to the water maze (van Groen et al., 2002). Another study shows that the anterior thalamic nuclei are involved in acquisition and recent memory (tested 5 days after training on a water maze task) while the intralaminar thalamic nuclei, together with the adjacent LD, contribute to remote spatial memory (25 days

after initial acquisition) (Lopez et al., 2009). In our study, LD seems to be implicated in the formation of a spatial memory trace since this region is activated, as the hippocampus, the first day of training in the On-Line Processing group (Day 1-OLP), when compared to QC (figure 3-4). However, animals going to the RAM but without developing a spatial strategy (active control, AC) present the same high metabolic activity (about 270 nCi/g) as one-day trained animals, suggesting that the LD activation could be rather associated to the procedural aspect of the radial maze (just visit the arms to get food) than the spatial learning process per se.

If we assumed that even in a spatial task there is a procedural learning component (Morris, 1984; Morris et al., 2003; Rossato et al., 2006), the learning deficits observed by van Groen et al. in LD-lesioned mice could be explained by the loss of the procedural aspect of the water maze (to swim to escape) that contributes to the final declarative spatial memory system. That could also help to explain why these LD-lesioned animals can finally learn the task with a double training period (5 days of water maze training-7 days' rest-5 days of water maze training) since one additional training week could compensate the loss of inputs from LD to the limbic system and reinforce the collective role in spatial learning and memory of each of the anterior thalamic nuclei, that were not affected by this lesion.

Maviel et al have found that the anterior cingulate cortex was essential for storage and retrieval of remote spatial memories, 30 days after training in a "one baited arm in a five-arm maze" task (Maviel et al., 2004). In another learning context (fear memories), ACC was also identified as a key structure for processing remote memory (Frankland et al., 2004). A spatio-temporal evolution in 2DG consumption from subcortical to cortical regions (including the frontal, parietal and anterior cingulate cortex) was identified after a spatial discrimination task performed in an eight-arm radial maze (Bontempi et al., 1996). In agreement with these papers, and also with our results concerning the retrosplenial cortex, ACC is activated in the Day 9-OLP group when compared to Day 1 (figures 3-7 and 3-13), supporting the role of this region in storage and consolidation of a spatial memory trace.

Two major memory systems have been recognized over the years: the declarative (explicit) memory system, under the control of the hippocampus and related temporal regions (in green, figure 4-2), and the non-declarative (implicit) or procedural or habit formation

memory system, under the control of the striatum (in blue, figure 4-2) and its connections (Squire, 1987).

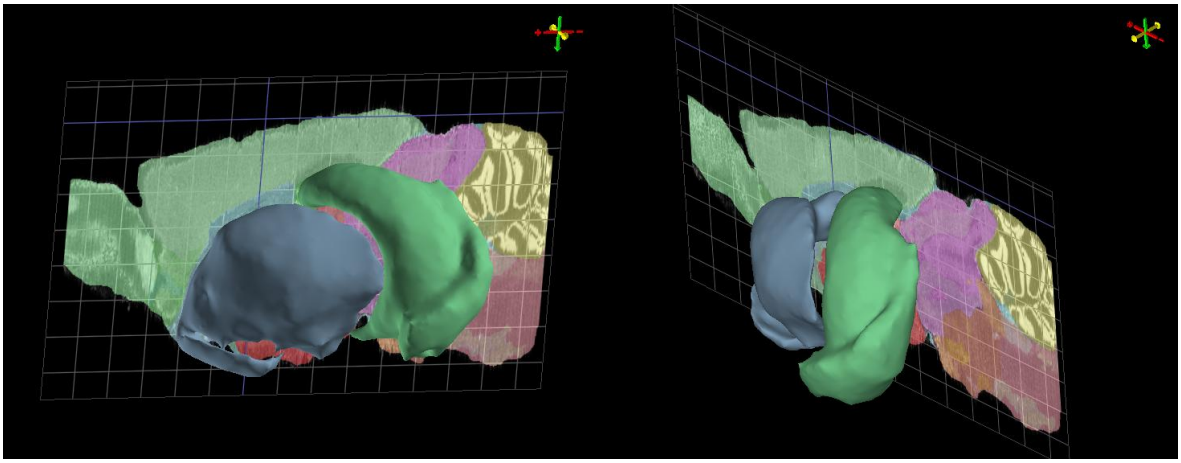

Figure 4-2: Hippocampal and striatal memory systems

Sagittal views of a 3D reconstruction of the hippocampus (in green) and the striatum (in blue). Taken from the Allen Brain Atlas (www.brain-map.org).

Learning tasks in animals imply the performance of some form of movement in response to visual or other cues. When they become well learned by repetition, memories of these tasks may be viewed as habits (Rossato et al., 2006). Several evidences coming from brain lesions methodology indicate that hippocampus and dorsal striatum mediate different types of memory. Lesions of the hippocampal formation, but not the dorsal striatum, impair spatial learning acquisition in a Morris water maze task. Conversely, lesions of the dorsal striatum, but not the hippocampus, impair acquisition of stimulus-response "habit" learning in another version of the Morris water maze task (Packard and McGaugh, 1992; McDonald and White, 1994). Using a water maze task with a visible or not visible platform, a double dissociation of the mnemonic functions of hippocampus and dorsal striatum has been established by (Teather et al., 2005) by studying the expression of immediate early genes products (c-Jun and Fos-like proteins) in these two regions. Training in a spatial (i.e., hidden escape platform) water maze task produced a marked increase in both (c-Jun and Fos-like) protein expression levels in the dorsal hippocampus. In contrast, training in a non-spatial (i.e., visible escape platform) water maze task increased c-Jun levels in the dorsal striatum (Teather et al., 2005). The fact that in our training protocol, a high 2DG signal was found in the dorsal striatum the last day of training (Day 9-OLP) indicate that going to the RAM becomes a habit over the nine days of training. However, since we are talking about a procedural learning-related region, we could expect the same high metabolic glucose rate in active control (AC)

animals going to the maze for 9 days, and this was not the case. This could be due to the fact that learning which are the three baited arms, by repetition from day to day, engage the striatal region in a large manner than the "only" exploratory activity of AC mice.

It was proposed, several years ago, that a common feature of anterograde amnesia (where new memories are affected) is damage to part of an "extended hippocampal system", comprising the hippocampus, the fornix, the mammillary bodies and the anterior thalamic nuclei (Aggleton and Saunders, 1997). Two of these regions (hippocampus and anterior thalamic nuclei) were already discussed above, now it is time to focus on the fornix and mammillay bodies which were also activated by our spatial learning paradigm. The fornix is the major fiber tract connecting the two brain systems that are most consistently associated with anterograde amnesia, the medial temporal lobe and the medial diencephalon (Tsivilis et al., 2008). Thus, as explained in the introduction (learning and memory-related brain regions), the fornix acts as a relay station of many inputs coming from the medial temporal lobe (hippocampus, entorhinal and perirhinal cortex) to diencephalic structures as different thalamic nuclei (ATN, LD, MD) and the mammillary bodies (MB).

All these interactions reflect an interdependent and complex system that can become even more complicated if we consider the different subdivisions in some of these brain regions. It appears that separate cell populations in the hippocampal formation innervate ATN and MB; the deepest subicular neurons projecting to ATN while the more superficial cells project to MB (Wright et al., 2010). Also the MB structure should be divided in two different systems (lateral mammillary nucleus and medial mammillary nucleus) instead of being considered as a unique region with a unique function (Vann and Aggleton, 2004). Even if both nuclei contribute, basically, to the same kind of learning, some differences in terms of connectivity and function were identified supporting the idea of treating them as different parts of the same related system: the lateral mammillary nucleus projects to the anterodorsal thalamic nucleus (AD), while the medial mammillary nucleus projects to the anteromedial (AM) and anteroventral (AV) thalamic nucleus. One more evidence is the discovery of head direction cells in the lateral, but not the medial, mammillary nuclei of the rat (Vann and Aggleton, 2004). A diagram illustrating this intricate "extended hippocampal system" was recently published (Aggleton et al., 2010). Atrophy of mammillary bodies was almost always associated to the Korsakoff's syndrome characterized by anterograde amnesia, even though retrograde amnesia was often also observed (Yoneoka et al., 2004; Beracochea, 2005;

Radyushkin et al., 2005; Kopelman et al., 2009). Furthermore, rodents with lesions of the mammillary bodies are impaired on spatial memory tasks as T-maze, radial-arm maze and water maze (Saravis et al., 1990; Sziklas and Petrides, 2000; Vann and Aggleton, 2003; Radyushkin et al., 2005). Results from this study (figures 3-6, 3-11 and 3-15) support the fornix and the mammillary bodies as a part of a complex brain network involved in spatial learning since both regions were found activated the first day of training, with the particularity that MB are activated with a little delay (45 minutes) compared to the fornix.

The parietal lobe is not traditionally thought to support declarative memory. Some studies provide evidences of its role in memory processes, even for simple recognition tasks as words, pictures or sounds in human fMRI studies (Shannon and Buckner, 2004; Wagner et al., 2005). In a different way, it was published that posterior parietal areas were not essential for recognition memory, being the activations found in others fMRI studies the result of a widespread brain attentional network, suggesting that the parietal region is associated with, but not necessary for, the memory process (Rossi et al., 2006). Furthermore, patients with damage in parietal areas were not impaired in recognition tasks (Haramati et al., 2008). We should be cautious in the interpretation of Haramati's results since their subjects were CVA (cerebro-vascular accident) patients, meaning that brain damages were not restricted to only parietal regions.

Based, again, on human fMRI studies it was established that the parietal lobe was responsible for encoding associations (for example, linking an object to a certain location) and the subsequent recognition of spatial locations (Sommer et al., 2005). Since associative memory is a crucial aspect of episodic memory, this paper insists on the role of parietal regions in declarative memory. In the same way, Rogers and Kesner state that the hippocampus and the parietal cortex process spatial information, but in a different context frame. The hippocampus is responsible for allocentric (spatial learning based on visual cues distributed in the walls of the behavioral room) maze acquisition and the parietal cortex for egocentric (spatial learning based on the own body movements for orientation) maze acquisition, since hippocampal and parietal lesioned-animals were impaired for allocentric and egocentric, respectively, versions of the water maze (Rogers and Kesner, 2006). From our results we can infer that the parietal cortex should be responsible, at least in part, for spatial information processing, since this region is significantly activated in Day 1-OLP animals when compared to the active controls. This could be due to the integration of different sensory

stimuli, especially visual stimulus, while performing the spatial learning task. Thus, parietal cortex ought to be involved in some kind of associative memory (encoding associations between a radial (baited) arm/food and a given spatial cue-given wall-given location in the room), in agreement with Sommer's paper. Our RAM is an allocentric task, even though we cannot be completely sure about an egocentric component in the final spatial learning process.

Keeping in mind all these results, we can say that spatial learning and memory are a phenomenon involving several brain regions, each of them playing a role in a complex and intricate memory network. A diagram, summarizing all these results and also some data from other works about the interconnections between different brain regions, is presented in figure 4-3.

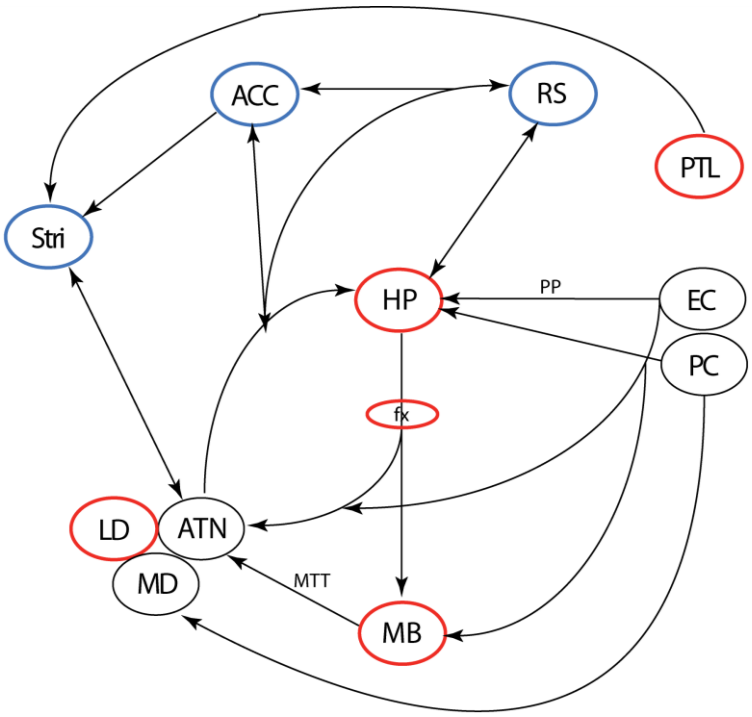

Figure 4-3: Brain circuitry of spatial learning and memory

This diagram is based on the results obtained in this study and the work of (Shibata, 1993; Aggleton and Saunders, 1997; Haber, 2003; Aggleton et al., 2010). In red, the brain regions activated at Day 1; in blue, the brain regions activated at Day 9. ACC: anterior cingulated cortex; ATN: anterior thalamic nuclei; EC: entorhinal cortex; fx: fornix; HP: hippocampus; LD: laterodorsal thalamic nucleus; MB: mammillary bodies; MD: mediosorsal thalamic nucleus; MTT: mammillothalamic tract;PC: perirhinal cortex; PP: perforant pathway; PTL: parietal cortex; RS: retrosplenial cortex; Stri: striatum.

Some of the major events represented in this figure are:

- HP projects to MB and ATN via the fx.
- HP projects to LD but not all efferents passed through the fx.
- MB projects to ATN via MTT.
- MB projects indirectly to HP via ATN.
- ATN projects directly to HP, ACC and RS.
- HP projects reciprocally to RS.
- RS projects reciprocally to ACC.
- ACC projects reciprocally to ATN.
- EC and PC project to HP.
- EC projects to ATN, LD, MD and MB.
- PC projects to MD.
- PTL, ACC, ATN and MD project to the Striatum.
- Striatum projects to ATN which, in turn, projects to the cortex.

Communication across all these regions and circuits is essential in order to help the learning process and to elaborate a complex response, going from processing visuospatial information, establishing a spatial strategy and coordinating a motor action, to achieve a goal-directed behavior (find the three arms baited = get food).

The ^{14}C-2 Deoxy-D-Glucose (2DG) autoradiographic technique affords a valuable means to assess in laboratory animals the engagement of brain regions and circuits in a given behavioral task or following a pharmacological intervention, by indirectly determining glucose utilization (CMRGlu) associated with neuronal activity. One of the drawbacks of the technique is that it implies an a priori definition of regions of interest (ROI); in addition 3D reconstructions of the whole brain with unbiased identification of activated (or deactivated) regions would be highly desirable, as currently achieved in human functional imaging studies. Recent attempts in this direction have been proposed (Lee et al., 2005; Dubois et al., 2007; Dubois et al., 2008). With JULIDE, we have developed a novel approach to achieve such goals, based on merging and warping of brain autoradiograms prepared from mice belonging to the same experimental group, and aimed at the unbiased identification of regions of interest combined with 3D reconstruction. Softwares such as JULIDE and other recently proposed (Lee et al., 2005; Dubois et al., 2007; Dubois et al., 2008) are likely to provide useful tools to

exploit to its full extent the use of 2DG autoradiography to complement behavioral and pharmacological studies in laboratory animals.

In the process of learning and memory, synaptic plasticity represents a fundamental mechanism, supporting the idea that the brain is plastic and can undergo adaptations following an experience. These adaptations are related to changes in synaptic strength as illustrated by the well characterized process of long-term potentiation (LTP), in the weakening of synaptic strength: long-term depression (LTD), in synaptogenesis and remodeling of synapses, and in neurogenesis (Bruel-Jungerman et al., 2007). All these forms of brain plasticity are dependent as LTP promote the proliferation and survival of new generated neurons in adult rat hippocampus and neurogenesis would facilitate LTP (Bruel-Jungerman et al., 2006; Trouche et al., 2009). Studies aimed at unraveling the molecular mechanisms of learning and memory have focused almost exclusively on genes involved in neuronal function such as brain-derived neurotrophic factor (BDNF), Ca^{2+}/calmodulin-dependent protein kinase II (CaMKII), N-methyl-D-aspartate (NMDA) receptor, mitogen-activated protein kinase (MAPK) (Giovannini et al., 2001; Wang et al., 2003; Vaynman et al., 2006) as well as transcription factors like cAMP-response-element-binding (CREB) and CCAAT-enhancer-binding protein (C/EBP) (Alberini, 2009) and immediate early genes like c-fos, Zif268 and Homer 1a (Bozon et al., 2003a; Davis et al., 2003; Frankland et al., 2004; Maviel et al., 2004; Duncan et al., 2005).

Activation of plasticity genes appears to be induced with specific time courses. Thus, for example NMDA is induced during memory acquisition; CaMKII, amino-3-hydroxy-5-methyl-4-isoxazolepropionic acid (AMPA) receptor, protein kinase C (PKC) and post-synaptic density 95 (PSD95) during the early phases of memory establishment; protein kinase A (PKA), MAPK, CREB and C/EBP during long-term memory (Micheau and Riedel, 1999; Dunning and During, 2003). These proteins contribute to complex intracellular signalling networks leading eventually, at least for most of them, to protein synthesis necessary for long-term memory.

In the molecular part of this study we have taken another angle to study the molecular mechanisms of long-term memory, by focusing our attention on genes involved in energy metabolism, with a particular focus on neuron-glia metabolic coupling. The underlying hypothesis that we were interested to test was whether the plastic changes that have been

revealed for the synaptic machinery are accompanied by parallel changes in the expression of genes involved in energy metabolism. This angle seemed particularly justified considering the high energy demands of the brain, which are largely related to synaptic (mainly glutamatergic) signaling (Sibson et al., 1998; Hyder et al., 2006; Magistretti, 2006).

Gene expression results reported here clearly indicate that there is indeed a marked plasticity in the expression of energy metabolism genes. Indeed, out of 30 genes studied, the level of expression of 20 genes was modified at one point or another of the learning paradigm (see table 6). A set of genes appears to be particularly upregulated by learning (figure 3-18) and deserves some discussion:

Glycolysis: increased levels of expression for phosphofructokinase (Pfkl and Pfkp) and enolase (Eno2) mRNAs.

Phosphofructokinase (Pfk) is a rate-limiting glycolytic enzyme that catalyzes the conversion of fructose-6-phosphate to fructose-1,6-bisphosphate.Pfkis modulated by the energy status of the cell, being activated by AMP, ADP and inorganic phosphate and inhibited by ATP, citrate and fatty acids. High ATP levels indicate sufficient energy availability and no need of glycolytic pathway activity; so the ATP-dependent inhibition of phosphofructokinase can stop the glycolysis at this point. Induction of Pfk gene expression as observed during the spatial learning paradigm is consistent with increased energy demands. Consistent with this, it has been shown that contracting rat skeletal muscle cells present increased glycolytic activity as indicated by augmented glucose uptake, hexokinase and Pfk activities, and lactate production (Pinheiro et al., 2010). Also Pfkm, which is the muscle-specific form of phosphofructokinase, is up-regulated at the mRNA level by exercise in skeletal muscle of wild-type mice (Mason et al., 2004). Both Pfk analyzed genes in our study are induced, namely Pfkl, the liver isozyme form and Pfkp, the platelet one.

Enolase2 (Eno2) is a neuronal-specific enzyme which catalyzes the conversion of 2-phosphoglycerate to phosphoenolpyruvate, corresponding to the penultimate step of glycolysis. This reaction can be reversible depending on the substrates concentration. Moreover the glycolytic implication, enolase seems to be related to ischemia, hypoxia and Alzheimer's disease (Butterfield and Lange, 2009).

Pyruvate metabolism: increased levels of expression for pyruvate carboxylase (Pcx) and pyruvate dehydrogenase kinase 4 (Pdk4) mRNAs.

Pyruvate carboxylase (Pcx), an astrocytic-specific enzyme, catalyzes the conversion of pyruvate (final product of glycolysis) to oxaloacetate. The importance of this metabolic reaction is to replenish the TCA cycle in carbons, in a process known as the anaplerotic (meaning replenishing) cycle. Pyruvate can of course also be converted to Acetyl-CoA which will also enter the TCA cycle. This conversion is catalyzed by the pyruvate dehydrogenase complex and takes place in the mithocondria. Pyruvate dehydrogenase kinase (Pdk) inhibits pyruvate dehydrogenase complex by phosphorylating it. This is reversed by the pyruvate dehydrogenase phosphatase that removes the phosphate from the pyruvate dehydrogenase, a process that renders it active. Increased levels of pyruvate dehydrogenase kinase, as it is the case in our study, would favor a decrease in pyruvate oxidation favoring lactate production. Interestingly, the muscle form of Pdk is strongly induced by exercise (Nordsborg et al., 2003; Pilegaard and Neufer, 2004).

Pentose phosphate pathway: increased levels of expression for transaldolase (Taldo) and transketolase (Tkt) mRNAs.

The pentose phosphate pathway is divided in two phases: oxidative and non-oxidative. The oxidative phase leads to the production of NADPH and pentoses. During the non-oxidative phase, several reactions implicating the transfer of carbon units between molecules lead to the formation of fructose-6-phosphate (F6P) and glyceraldehyde-3-phosphate (GAP) from the pentose molecules generated during the oxidative part. These interconversions are catalyzed by transketolase (Tkt), which is responsible for the transfer of 2 carbon atoms, and transaldolase (Taldo), which is responsible for the transfer of 3 carbon atoms. These two enzymes represent the link between the pentose phosphate pathway and glycolysis, since both products (F6P and GAP) are intermediate metabolites of the glycolytic pathway. Induction of Tkt and Taldo is consistent with a switch of the pentose phosphate pathway to a more non-oxidative profile aimed at providing additional substrates to glycolysis and energy production.

Glycogen regulation: increased levels of expression for glycogenin (Gyg), protein targeting to glycogen (PTG) and brain glycogen phosphorylase (Pygb) mRNAs.

Glycogen is the major energy reserve of the brain and it is localized almost exclusively in astrocytes (Magistretti, 2008). The enzyme responsible for its synthesis, the glycogen synthase (Gys), is an elongation enzyme that catalyzes the progressive extension of a

glycogen chain by adding successive glucose molecules. That means that glycogen synthase is not able to start the synthesis of glycogen by itself; it needs a "primer", an already existing glycogen chain of, at least, 4 glucose residues. Glycogenin (Gyg) is the enzyme responsible for the initiation of glycogen synthesis, starting it by adding a glucose molecule to one of its own tyrosine residues. In this way, a short linear glucose polymer is produced by glycogenin (Smythe and Cohen, 1991; Lomako et al., 2004).

Protein targeting to glycogen (PTG) is implicated in glycogen synthesis since it promotes the activity of the phosphatase protein 1 (PP1). Activation of PP1 causes the dephosphorylation of glycogen synthase resulting in its activation. Thus, glycogen production and storage is augmented in cells and tissues where high levels of PTG were found (Allaman et al., 2000; Greenberg et al., 2003).

Glycogen phosphorylase (Pygb) is responsible for glycogen degradation, breaking down the molecule of glycogen to release glucose subunits that can enter in the glycolytic pathway to produce energy. Glycogen synthesis and glycogen degradation are regulated in a reciprocal way. Both enzymes, glycogen synthase (glycogen anabolism) and glycogen phosphorylase (glycogen catabolism) are phosphorylated by the same protein kinase (PKA) and dephosphorylated by the same protein phosphatase (PP1). The phosphorylated state transforms glycogen synthase in an inactive form but activates glycogen phosphorylase. Dephosphorylation makes glycogen synthase active and transforms glycogen phosphorylase in an inactive enzyme.

The fact that, in our results, all studied genes for glycogen regulation, either for synthesis or for degradation, are augmented could be explained by the fact that laser microdisecction and the ensuing gene analysis were performed at the tissue (and not cellular) level. In our ROI, hippocampus and retrosplenial cortex, some cells could be synthesizing glycogen while some others cells could be degrading it. What it is clear is that our training paradigm profoundly affects glycogen turnover, supporting a role of glycogen metabolism in learning. Interestingly, recent data have shown that pharmacological inhibition of brain glycogen phosphorylase with the antidiabetic drug DAB, which results in impaired glycogen mobilization, strongly inhibits learning in chicks (Gibbs et al., 2006; Gibbs et al., 2007) and long term memory in an inhibitory avoidance task in rats (Suzuki et al., submitted).

One more aspect we must consider here is the effect of barbiturate anesthesia on glycogen metabolism. It has been published that an 85% increase in glycogen content was found in rat cerebral cortex after 6h of pentobarbital anesthesia (Swanson, 1992). I do not believe such an effect due to anesthesia is causing the increase in glycogen synthesis-related mRNAs expression (Gyg, Gys and PTG) since 5 minutes after the i.p. pentobarbital administration the brains were already frozen, having not enough time to modify glycogen metabolism. Swanson's study also showed no anesthesia effects on cortical astrocytes cultured without neurons, suggesting that the effect of barbiturate anesthesia on glial glycogen content *in vivo* may be secondary to depression of neuronal activity rather than a direct effect on glial metabolism.

Lactate shuttle: increased levels of expression for Na^+/K^+-ATPase alpha2 subunit (ATP1a2) mRNA.

Most of synapses in the brain are glutamatergic. Glutamate released during the synaptic transmission is removed predominantly by astrocytes from the synaptic cleft. The driving force for glutamate into astrocytes is provided by the electrochemical gradient of Na^+ with a stoichiometry of 3 Na^+ ions per glutamate co-transported resulting in an increase in intracellular Na^+concentration (Chatton et al., 2000). As is the case in any cell, Na^+ homeostasis is maintained by the activity of the Na^+/K^+-ATPase. In astrocytes glutamate uptake results in an acute mobilization of the alpha2 subunit (ATP1a2), an astrocytic-specific form of the enzyme (Pellerin and Magistretti, 1997). This sodium signal and the ensuing activation of the pump, causes ATP consumption and decreased levels (Magistretti and Chatton, 2005), which provides a trigger for glucose uptake and activation of glycolysis (Magistretti, 2006). Thus, Na^+/K^+-ATPase activity is central for the coupling of synaptic activity with glucose utilization (Magistretti and Pellerin, 1999).

Na^+/K^+-ATPase and its possible role in spatial learning and memory.

Na^+/K^+-ATPase is a membrane protein formed by α and β subunits and a regulatory FXYD protein. The α catalytic subunit is responsible for binding sodium and potassium ions and also for ATP hydrolysis. The β subunit is responsible for appropriate insertion of α in the membrane and for modulating substrate affinity. Four isoforms have been identified for the alpha subunit (α1, α2, α3 and α4) and another four for the beta subunit (β1, β2, β3 and β4) showing specific tissue and cell distribution (Kaplan, 2002; Shinoda et al., 2009). Three alpha

isoforms are found in the brain; the α1 is expressed in all cell types, the α2 is mainly expressed in astrocytes and the α3 is exclusively expressed in neurons.

Consistent with a possible implication of Na^+/K^+-ATPase in learning, Zhan and collaborators have shown that intraventricular administration of ouabain, which is an inhibitor of Na^+/K^+-ATPase, impairs spatial water maze learning in rats during the all period of treatment. However, after interruption of ouabain injection, spatial learning performance recovers to the same level of non-treated animals, suggesting that maybe Na^+/K^+-ATPase contributes to spatial learning (Zhan et al., 2004). To determine which α isoform is implicated in learning and memory processes, a research group has developed α1, α2 and α3 haploinsufficient mice. Haploinsufficiency is the absence of one of the two copies of each gene. Both α2 and α3 deficient mice showed learning and memory deficits when tested in the Morris water maze, further supporting the view that Na^+/K^+-ATPase is implicated in spatial learning (Lingrel et al., 2007; Moseley et al., 2007). Moreover, decreased levels of expression and activity of Na^+/K^+-ATPase have been demonstrated in an animal model of Alzheimer's disease with memory impairments (Dickey et al., 2004; Dickey et al., 2005).

Results presented here are consistent with the view that Na^+/K^+-ATPase may be implicated in the formation of a spatial memory trace, since it is one of the genes that presents the greatest induction in the retrosplenial cortex when gene expression levels are compared between day 9 and day 1 (i.e. corresponding behaviorally to learning), in agreement with the other papers described above. Interestingly, there is a large body of evidence indicating the induction of Na^+/K^+-ATPase alpha subunits in muscle after physical exercise (Nordsborg et al., 2003; Petersen et al., 2005; Murphy et al., 2006; Aughey et al., 2007; Murphy et al., 2007).

In addition to the well established role of Na^+/K^+-ATPase in maintaining electrochemical gradients, several other physiological processes seem to engage this protein such as signal transduction and modulation of dendritic growth (Desfrere et al., 2009) and protection against hypoxia/reoxygenation (Kasai et al., 2003). Dysfunctions of this protein have also been implicated in certain neuropsychiatric diseases such as familial migraine (De Fusco et al., 2003; Moskowitz et al., 2004; Gallanti et al., 2008; Tavraz et al., 2008), epilepsy (Grisar et al., 1992; Gallanti et al., 2008), rapid-onset dystonia parkinsonism (de Carvalho

Aguiar et al., 2004), depression (Goldstein et al., 2006) and Alzheimer's disease (Harris et al., 1996; Chauhan et al., 1997; Hattori et al., 1998; Dickey et al., 2005).

A modulation of expression of Zif268 gene and protein has been described in many behavioral paradigms, including spatial learning (Davis et al., 2003; Knapska and Kaczmarek, 2004). Due to the numerous events taking place after synaptic stimulation, it is not always possible to establish a direct or indirect engagement of this gene in neuronal plasticity. Indeed, the expression of Zif268 is controlled by a complex mechanism, and the interactions between this gene and other transcription factors are numerous. We found no changes (at least, not the great changes we expected) in the expression of Zif268 in our experiment. One possible explanation is that extensive training decreases in a general way the levels of Zif268 in many brain structures, including the hippocampus and the cingulate cortex (Hernandez et al., 2006). Or maybe, because it is an immediate-early gene, we are too late in time to detect important changes on its expression. A rapid increase in Arc, Zif268 and c-fos RNA levels has been demonstrated after a spatial water task showing a peak of expression at 30 minutes after training (Guzowski et al., 2001). Data obtained in this study confirm results obtained by other researchers (Skibinska et al., 2001; Rekart et al., 2005; Holahan et al., 2007; Holahan and Routtenberg, 2008; Hu et al., 2009) that neuronal plasticity and information storage processes are being engaged by the induction of Gap43 and PSD95 which, in our paradigm, were strongly modulated in all experimental conditions and in both regions, the hippocampus and the retrosplenial cortex.

In summary for this molecular part of the study, induction of genes in the retrosplenial cortex at day 9 may well represent a molecular concomitant of memory consolidation (Frankland and Bontempi, 2005; Suzuki, 2006) . Interestingly, with the exception of *GLUT3* which has an exclusively neuronal distribution, all genes related to glycogen metabolism are selectively expressed in astrocytes along with pyruvate carboxylase and the Na^+/K^+-ATPase alpha2 subunit. These results are consistent with a strong mobilization of energy-producing pathways in astrocytes as a concomitant of synaptic plasticity. In a very recent article it was shown that GLUT3 heterozygous mice presented deficiencies in spatial learning and working memory, both reliant on environmental cues, after training in a water maze and an eight-arm radial maze task, respectively (Zhao et al., 2010).

The results obtained with the transcriptomic approach in functionally-defined brain areas metabolically-activated by a spatial learning paradigm, indicate a remarkable modulation of gene expression, indicating the existence of adaptive mechanisms particularly in terms of energy metabolism and neuron-glia metabolic coupling. Gene expression levels do not change during the on-line processing time and immediately after the end of the task. Indeed, under these conditions, the time delay is too short to expect activation, except possibly for immediate-early genes. In contrast, under post-processing conditions in the hippocampus, i.e. 45 minutes after the end of the task, the expression level of a large number of genes analyzed is induced on the first day of the learning protocol. This is in contrast to what is observed in the retrosplenial cortex where gene induction is higher at day 9 when compared to day 1.

This profile of gene activation matches the spatial and temporal pattern of metabolic activation as monitored with the 2DG technique. This pattern is consistent with a transfer of activation and plasticity mechanisms from the hippocampus to the retrosplenial cortex as previously suggested (Frankland and Bontempi, 2005; Albasser et al., 2007), indicating a spatial as well as temporal shift in brain areas engaged in learning. This transfer is reflected both at the neuroenergetic (2DG) and molecular levels (genes expression), indicating a coincidence in gene induction and increased glucose utilization.

mRNAs levels in biological samples can be analyzed by different procedures as Northern blot, ribonuclease protection assay (RPA), in situ hybridization (ISH) and, more recently, the reverse transcription-polymerase chain reaction (RT-PCR). The last one is, maybe, the preferred technique of a large number of investigators due to its ability to detect mRNAs from samples containing small number of cells or small amount of tissue (Ceol et al., 2001). Several papers published in the last 15 years have emphasized the higher sensitivity of RT-PCR compared to ISH techniques (Komminoth et al., 1994; Bates et al., 1997; Biedermann et al., 2004). A well-illustrating example can be taken from the study of Wakamatsu about the detection of the Newcastle disease virus mRNA using different techniques: RT-PCR, ISH and immunohistochemistry (IHC). All 10 samples they analyzed from infected birds were found positive by RT-PCR while only 4 of 10 and 2 of 10 were found positive with IHC and ISH, respectively (Wakamatsu et al., 2007).

In our ISH experiments we had a very low number of animals per group (n=4 for Day 1 and n=4 for Day 9). This could, maybe, explain the lack of significant differences after optical density signal quantification. But it doesn't account for the high signal we can see on the hippocampus at Day 9 as shown in figure 3-20. The main reason that could explain the lack of ISH results certainly come from the low quantity of material we have and the difficulty to normalize the observed signal expression with references genes as we can do for the RT-PCR technique.

5 CONCLUSION AND FUTURE PERSPECTIVES

This study demonstrates that memory encoding is a phenomenon involving several brain regions. Nerve cells activated by the learning task need more energy to make synaptic transmission more efficient in order to store the "learned" information somewhere in the brain. Glutamate release during synaptic activity and glutamate removal from the synaptic cleft by both post-synaptic neurons and astrocytes triggers a cascade of molecular events leading to the strengthening of synapses. Our genetic analysis at different times after learning has shown that these molecular events evolve in time between the different brain regions implicated in learning and memory formation processes. The same pattern of flow of information was found at a cellular and a molecular level. Transcriptional modifications for glucose metabolism pathways and for plasticity genes occurred in the same brain regions where glucose is being consumed to support the cellular increase in energetic demands provoked by the learning activity. The identification of metabolic genes induced as a concomitant of learning, provides novel insights into molecular aspects of synaptic plasticity in particular by pointing at certain metabolic pathways that may be either disrupted in pathological conditions associated with memory impairment or become the targets for pharmacological interventions aimed at improving cognitive performance.

A more in-depth study about the possible role on learning and memory of some of the genes identified in this project, like Na^+/K^+-ATPase alpha2 subunit, Pdk4 and glycogen-related genes, could be done in the future. Gene silencing and posterior behavioral testing could assess the importance of these genes on information acquisition and storage.

REFERENCES

REFERENCES

Aggleton JP, Saunders RC (1997) The relationships between temporal lobe and diencephalic structures implicated in anterograde amnesia. Memory 5:49-71.

Aggleton JP, Desimone R, Mishkin M (1986) The origin, course, and termination of the hippocampothalamic projections in the macaque. J Comp Neurol 243:409-421.

Aggleton JP, O'Mara SM, Vann SD, Wright NF, Tsanov M, Erichsen JT (2010) Hippocampal-anterior thalamic pathways for memory: uncovering a network of direct and indirect actions. Eur J Neurosci 31:2292-2307.

Albasser MM, Poirier GL, Warburton EC, Aggleton JP (2007) Hippocampal lesions halve immediate-early gene protein counts in retrosplenial cortex: distal dysfunctions in a spatial memory system. Eur J Neurosci 26:1254-1266.

Alberini CM (2005) Mechanisms of memory stabilization: are consolidation and reconsolidation similar or distinct processes? Trends Neurosci 28:51-56.

Alberini CM (2009) Transcription factors in long-term memory and synaptic plasticity. Physiol Rev 89:121-145.

Alberts B, Bray D, Lewis J, Raff M, Roberts K, Watson JD (1994) Molecular biology of the cell, third Edition. New York: Garland publishing.

Allaman I, Pellerin L, Magistretti PJ (2000) Protein targeting to glycogen mRNA expression is stimulated by noradrenaline in mouse cortical astrocytes. Glia 30:382-391.

Allaman I, Pellerin L, Magistretti PJ (2004) Glucocorticoids modulate neurotransmitter-induced glycogen metabolism in cultured cortical astrocytes. J Neurochem 88:900-908.

Allaman I, Lengacher S, Magistretti PJ, Pellerin L (2003) A2B receptor activation promotes glycogen synthesis in astrocytes through modulation of gene expression. Am J Physiol Cell Physiol 284:C696-704.

Amaral D, Lavenex P (2006) Hippocampal neuroanatomy. In: The hippocampus book (Andersen P, Morris R, Amaral D, Bliss T, O'Keefe J, eds), pp 37-110. Oxford; Engalnd: Oxford University Press.

Aughey RJ, Murphy KT, Clark SA, Garnham AP, Snow RJ, Cameron-Smith D, Hawley JA, McKenna MJ (2007) Muscle Na+-K+-ATPase activity and isoform adaptations to intense interval exercise and training in well-trained athletes. J Appl Physiol 103:39-47.

Bates PJ, Sanderson G, Holgate ST, Johnston SL (1997) A comparison of RT-PCR, in-situ hybridisation and in-situ RT-PCR for the detection of rhinovirus infection in paraffin sections. J Virol Methods 67:153-160.

Beracochea D (2005) Interaction between emotion and memory: importance of mammillary bodies damage in a mouse model of the alcoholic Korsakoff syndrome. Neural Plast 12:275-287.

Biagiotti E, Guidi L, Del Grande P, Ninfali P (2003) Glucose-6-phosphate dehydrogenase expression associated with NADPH-dependent reactions in cerebellar neurons. Cerebellum 2:178-183.

Biedermann K, Dandachi N, Trattner M, Vogl G, Doppelmayr H, More E, Staudach A, Dietze O, Hauser-Kronberger C (2004) Comparison of real-time PCR signal-amplified in situ hybridization and conventional PCR for detection and quantification of human papillomavirus in archival cervical cancer tissue. J Clin Microbiol 42:3758-3765.

Bollen M, Keppens S, Stalmans W (1998) Specific features of glycogen metabolism in the liver. Biochem J 336 (Pt 1):19-31.

Bontempi B, Jaffard R, Destrade C (1996) Differential temporal evolution of post-training changes in regional brain glucose metabolism induced by repeated spatial discrimination training in mice: visualization of the memory consolidation process? Eur J Neurosci 8:2348-2360.

Bontempi B, Laurent-Demir C, Destrade C, Jaffard R (1999) Time-dependent reorganization of brain circuitry underlying long-term memory storage. Nature 400:671-675.

Bozon B, Davis S, Laroche S (2003a) A requirement for the immediate early gene zif268 in reconsolidation of recognition memory after retrieval. Neuron 40:695-701.

Bozon B, Kelly A, Josselyn SA, Silva AJ, Davis S, Laroche S (2003b) MAPK, CREB and zif268 are all required for the consolidation of recognition memory. Philos Trans R Soc Lond B Biol Sci 358:805-814.

Brett R, MacKenzie F, Pratt J (2001) Delta 9-tetrahydrocannabinol-induced alterations in limbic system glucose use in the rat. Neuroreport 12:3573-3577.

Brooks DJ (2003) PET studies on the function of dopamine in health and Parkinson's disease. Ann N Y Acad Sci 991:22-35.

Bruel-Jungerman E, Davis S, Laroche S (2007) Brain plasticity mechanisms and memory: a party of four. Neuroscientist 13:492-505.

Bruel-Jungerman E, Davis S, Rampon C, Laroche S (2006) Long-term potentiation enhances neurogenesis in the adult dentate gyrus. J Neurosci 26:5888-5893.

Butterfield DA, Lange ML (2009) Multifunctional roles of enolase in Alzheimer's disease brain: beyond altered glucose metabolism. J Neurochem 111:915-933.

Cavallaro S, D'Agata V, Manickam P, Dufour F, Alkon DL (2002) Memory-specific temporal profiles of gene expression in the hippocampus. Proc Natl Acad Sci U S A 99:16279-16284.

Ceol M, Forino M, Gambaro G, Sauer U, Schleicher ED, D'Angelo A, Anglani F (2001) Quantitation of TGF-beta1 mRNA in porcine mesangial cells by comparative kinetic RT/PCR: comparison with ribonuclease protection assay and in situ hybridization. J Clin Lab Anal 15:215-222.

Chatton JY, Marquet P, Magistretti PJ (2000) A quantitative analysis of L-glutamate-regulated Na+ dynamics in mouse cortical astrocytes: implications for cellular bioenergetics. Eur J Neurosci 12:3843-3853.

Chauhan NB, Lee JM, Siegel GJ (1997) Na,K-ATPase mRNA levels and plaque load in Alzheimer's disease. J Mol Neurosci 9:151-166.

Chrobak JJ, Napier TC (2002) Basal forebrain infusions impair delayed-non-match-to-sample radial arm maze performance. Pharmacol Biochem Behav 72:209-212.

Cirelli C, Tononi G (2004) Locus ceruleus control of state-dependent gene expression. J Neurosci 24:5410-5419.

Cole MR, Chappell-Stephenson R (2003) Exploring the limits of spatial memory in rats, using very large mazes. Learn Behav 31:349-368.

Conejo NM, Gonzalez-Pardo H, Vallejo G, Arias JL (2007) Changes in brain oxidative metabolism induced by water maze training. Neuroscience 145:403-412.

Crawley JN, Belknap JK, Collins A, Crabbe JC, Frankel W, Henderson N, Hitzemann RJ, Maxson SC, Miner LL, Silva AJ, Wehner JM, Wynshaw-Boris A, Paylor R (1997) Behavioral phenotypes of inbred mouse strains: implications and recommendations for molecular studies. Psychopharmacology (Berl) 132:107-124.

D'Hooge R, De Deyn PP (2001) Applications of the Morris water maze in the study of learning and memory. Brain Res Brain Res Rev 36:60-90.

Davis S, Bozon B, Laroche S (2003) How necessary is the activation of the immediate early gene zif268 in synaptic plasticity and learning? Behav Brain Res 142:17-30.

de Carvalho Aguiar P, Sweadner KJ, Penniston JT, Zaremba J, Liu L, Caton M, Linazasoro G, Borg M, Tijssen MA, Bressman SB, Dobyns WB, Brashear A, Ozelius LJ (2004) Mutations in the Na^+/K^+-ATPase alpha3 gene ATP1A3 are associated with rapid-onset dystonia parkinsonism. Neuron 43:169-175.

De Fusco M, Marconi R, Silvestri L, Atorino L, Rampoldi L, Morgante L, Ballabio A, Aridon P, Casari G (2003) Haploinsufficiency of ATP1A2 encoding the Na+/K+ pump alpha2 subunit associated with familial hemiplegic migraine type 2. Nat Genet 33:192-196.

Deacon RM, Rawlins JN (2006) T-maze alternation in the rodent. Nat Protoc 1:7-12.

Debiec J, LeDoux JE, Nader K (2002) Cellular and systems reconsolidation in the hippocampus. Neuron 36:527-538.

Desfrere L, Karlsson M, Hiyoshi H, Malmersjo S, Nanou E, Estrada M, Miyakawa A, Lagercrantz H, El Manira A, Lal M, Uhlen P (2009) Na,K-ATPase signal transduction triggers CREB activation and dendritic growth. Proc Natl Acad Sci U S A 106:2212-2217.

Dickey CA, Loring JF, Montgomery J, Gordon MN, Eastman PS, Morgan D (2003) Selectively reduced expression of synaptic plasticity-related genes in amyloid precursor protein + presenilin-1 transgenic mice. J Neurosci 23:5219-5226.

Dickey CA, Gordon MN, Wilcock DM, Herber DL, Freeman MJ, Morgan D (2005) Dysregulation of Na+/K+ ATPase by amyloid in APP+PS1 transgenic mice. BMC Neurosci 6:7.

Dickey CA, Gordon MN, Mason JE, Wilson NJ, Diamond DM, Guzowski JF, Morgan D (2004) Amyloid suppresses induction of genes critical for memory consolidation in APP + PS1 transgenic mice. J Neurochem 88:434-442.

Dodart JC, Mathis C, Bales KR, Paul SM, Ungerer A (1999) Early regional cerebral glucose hypometabolism in transgenic mice overexpressing the V717F beta-amyloid precursor protein. Neurosci Lett 277:49-52.

Dubois A, Dauguet J, Herard AS, Besret L, Duchesnay E, Frouin V, Hantraye P, Bonvento G, Delzescaux T (2007) Automated three-dimensional analysis of histological and autoradiographic rat brain sections: application to an activation study. J Cereb Blood Flow Metab 27:1742-1755.

Dubois A, Herard AS, Flandin G, Duchesnay E, Besret L, Frouin V, Hantraye P, Bonvento G, Delzescaux T (2008) Quantitative validation of voxel-wise statistical analyses of autoradiographic rat brain volumes: application to unilateral visual stimulation. Neuroimage 40:482-494.

Duncan RS, Hwang SY, Koulen P (2005) Effects of Vesl/Homer proteins on intracellular signaling. Exp Biol Med (Maywood) 230:527-535.

Dunning J, During MJ (2003) Molecular mechanisms of learning and memory. Expert Rev Mol Med 5:1-11.

Eichenbaum H (2000) A cortical-hippocampal system for declarative memory. Nat Rev Neurosci 1:41-50.

Elkashef AM, Doudet D, Bryant T, Cohen RM, Li SH, Wyatt RJ (2000) 6-(18)F-DOPA PET study in patients with schizophrenia. Positron emission tomography. Psychiatry Res 100:1-11.

Foreman N, Ermakova I (1998) The radial arm maze: twenty years on. In: A handbook of spatial research paradigms and methodologies (Foreman N, Gillett R, eds), pp 87-143. Hove: Psychology press Ltd.

Frankland PW, Bontempi B (2005) The organization of recent and remote memories. Nat Rev Neurosci 6:119-130.

Frankland PW, Bontempi B, Talton LE, Kaczmarek L, Silva AJ (2004) The involvement of the anterior cingulate cortex in remote contextual fear memory. Science 304:881-883.

Gallanti A, Tonelli A, Cardin V, Bussone G, Bresolin N, Bassi MT (2008) A novel de novo nonsense mutation in ATP1A2 associated with sporadic hemiplegic migraine and epileptic seizures. J Neurol Sci 273:123-126.

Galldiks N, Thiel A, Haense C, Fink GR, Hilker R (2008) 11C-flumazenil positron emission tomography demonstrates reduction of both global and local cerebral benzodiazepine receptor binding in a patient with Stiff Person Syndrome. J Neurol 255:1361-1364.

Gibbs ME, Anderson DG, Hertz L (2006) Inhibition of glycogenolysis in astrocytes interrupts memory consolidation in young chickens. Glia 54:214-222.

Gibbs ME, Lloyd HG, Santa T, Hertz L (2007) Glycogen is a preferred glutamate precursor during learning in 1-day-old chick: biochemical and behavioral evidence. J Neurosci Res 85:3326-3333.

Giovannini MG, Blitzer RD, Wong T, Asoma K, Tsokas P, Morrison JH, Iyengar R, Landau EM (2001) Mitogen-activated protein kinase regulates early phosphorylation and delayed expression of Ca2+/calmodulin-dependent protein kinase II in long-term potentiation. J Neurosci 21:7053-7062.

Goldstein I, Levy T, Galili D, Ovadia H, Yirmiya R, Rosen H, Lichtstein D (2006) Involvement of Na(+), K(+)-ATPase and endogenous digitalis-like compounds in depressive disorders. Biol Psychiatry 60:491-499.

Goulter AB, Harmer DW, Clark KL (2006) Evaluation of low density array technology for quantitative parallel measurement of multiple genes in human tissue. BMC Genomics 7:34.

Greenberg CC, Meredith KN, Yan L, Brady MJ (2003) Protein targeting to glycogen overexpression results in the specific enhancement of glycogen storage in 3T3-L1 adipocytes. J Biol Chem 278:30835-30842.

Greicius MD, Krasnow B, Boyett-Anderson JM, Eliez S, Schatzberg AF, Reiss AL, Menon V (2003) Regional analysis of hippocampal activation during memory encoding and retrieval: fMRI study. Hippocampus 13:164-174.

Grisar T, Guillaume D, Delgado-Escueta AV (1992) Contribution of Na+,K(+)-ATPase to focal epilepsy: a brief review. Epilepsy Res 12:141-149.

Guzowski JF, Setlow B, Wagner EK, McGaugh JL (2001) Experience-dependent gene expression in the rat hippocampus after spatial learning: a comparison of the immediate-early genes Arc, c-fos, and zif268. J Neurosci 21:5089-5098.

Haber SN (2003) The primate basal ganglia: parallel and integrative networks. J Chem Neuroanat 26:317-330.

Haber SN, Calzavara R (2009) The cortico-basal ganglia integrative network: the role of the thalamus. Brain Res Bull 78:69-74.

Haramati S, Soroker N, Dudai Y, Levy DA (2008) The posterior parietal cortex in recognition memory: a neuropsychological study. Neuropsychologia 46:1756-1766.

Harbison ST, Carbone MA, Ayroles JF, Stone EA, Lyman RF, Mackay TF (2009) Co-regulated transcriptional networks contribute to natural genetic variation in Drosophila sleep. Nat Genet 41:371-375.

Harris ME, Wang Y, Pedigo NW, Jr., Hensley K, Butterfield DA, Carney JM (1996) Amyloid beta peptide (25-35) inhibits Na+-dependent glutamate uptake in rat hippocampal astrocyte cultures. J Neurochem 67:277-286.

Hattori N, Kitagawa K, Higashida T, Yagyu K, Shimohama S, Wataya T, Perry G, Smith MA, Inagaki C (1998) CI-ATPase and Na+/K(+)-ATPase activities in Alzheimer's disease brains. Neurosci Lett 254:141-144.

Hernandez PJ, Schiltz CA, Kelley AE (2006) Dynamic shifts in corticostriatal expression patterns of the immediate early genes Homer 1a and Zif268 during early and late phases of instrumental training. Learn Mem 13:599-608.

Hof PR, Young WG, Bloom FE, Belichenko PV, Celio MR (2000) Comparative cytoarchitectonic atlas of the C57BL/6 and 129/Sv mouse brains. In. Amsterdam: Elsevier.

Holahan M, Routtenberg A (2008) The protein kinase C phosphorylation site on GAP-43 differentially regulates information storage. Hippocampus 18:1099-1102.

Holahan MR, Honegger KS, Tabatadze N, Routtenberg A (2007) GAP-43 gene expression regulates information storage. Learn Mem 14:407-415.

Hu S, Ying Z, Gomez-Pinilla F, Frautschy SA (2009) Exercise can increase small heat shock proteins (sHSP) and pre- and post-synaptic proteins in the hippocampus. Brain Res 1249:191-201.

Hyder F, Patel AB, Gjedde A, Rothman DL, Behar KL, Shulman RG (2006) Neuronal-glial glucose oxidation and glutamatergic-GABAergic function. J Cereb Blood Flow Metab 26:865-877.

Ibanez L, Schroeder W (2005) The ITK software guide 2.4. Kitware, Inc.

Jitrapakdee S, St Maurice M, Rayment I, Cleland WW, Wallace JC, Attwood PV (2008) Structure, mechanism and regulation of pyruvate carboxylase. Biochem J 413:369-387.

Kaplan JH (2002) Biochemistry of Na,K-ATPase. Annu Rev Biochem 71:511-535.

Kasai K, Yamashita T, Yamaguchi A, Yoshiya K, Kawakita A, Tanaka H, Sugimoto H, Tohyama M (2003) Induction of mRNAs and proteins for Na/K ATPase alpha1 and beta1 subunits following hypoxia/reoxygenation in astrocytes. Brain Res Mol Brain Res 110:38-44.

Kennedy SH, Evans KR, Kruger S, Mayberg HS, Meyer JH, McCann S, Arifuzzman AI, Houle S, Vaccarino FJ (2001) Changes in regional brain glucose metabolism measured with positron emission tomography after paroxetine treatment of major depression. Am J Psychiatry 158:899-905.

Kesner RP, Hopkins RO (2006) Mnemonic functions of the hippocampus: a comparison between animals and humans. Biol Psychol 73:3-18.

Kety SS (1967) Relationship between energy metabolism of the brain and functional activity. Res Publ Assoc Res Nerv Ment Dis 45:39-47.

Kirsch M, De Groot H (2001) NAD(P)H, a directly operating antioxidant? FASEB J 15:1569-1574.

Knapska E, Kaczmarek L (2004) A gene for neuronal plasticity in the mammalian brain: Zif268/Egr-1/NGFI-A/Krox-24/TIS8/ZENK? Prog Neurobiol 74:183-211.

Komminoth P, Adams V, Long AA, Roth J, Saremaslani P, Flury R, Schmid M, Heitz PU (1994) Evaluation of methods for hepatitis C virus detection in archival liver biopsies. Comparison of histology, immunohistochemistry, in-situ hybridization, reverse transcriptase polymerase chain reaction (RT-PCR) and in-situ RT-PCR. Pathol Res Pract 190:1017-1025.

Kopelman MD, Thomson AD, Guerrini I, Marshall EJ (2009) The Korsakoff syndrome: clinical aspects, psychology and treatment. Alcohol Alcohol 44:148-154.

Laughton JD, Charnay Y, Belloir B, Pellerin L, Magistretti PJ, Bouras C (2000) Differential messenger RNA distribution of lactate dehydrogenase LDH-1 and LDH-5 isoforms in the rat brain. Neuroscience 96:619-625.

Lee JS, Ahn SH, Lee DS, Oh SH, Kim CS, Jeong JM, Park KS, Chung JK, Lee MC (2005) Voxel-based statistical analysis of cerebral glucose metabolism in the rat cortical deafness model by 3D reconstruction of brain from autoradiographic images. Eur J Nucl Med Mol Imaging 32:696-701.

Lee TI, Young RA (2000) Transcription of eukaryotic protein-coding genes. Annu Rev Genet 34:77-137.

Lepage M, Habib R, Tulving E (1998) Hippocampal PET activations of memory encoding and retrieval: the HIPER model. Hippocampus 8:313-322.

Li AJ, Oomura Y, Sasaki K, Suzuki K, Tooyama I, Hanai K, Kimura H, Hori T (1998) A single pre-training glucose injection induces memory facilitation in rodents performing various tasks: contribution of acidic fibroblast growth factor. Neuroscience 85:785-794.

Lingrel JB, Williams MT, Vorhees CV, Moseley AE (2007) Na,K-ATPase and the role of alpha isoforms in behavior. J Bioenerg Biomembr 39:385-389.

Lodish H, Berk A, Matsudaira P, Kaiser CA, Krieger M, Scott MP, Zipursky L, Darnell J (2004) Molecular cell biology, fifth Edition. New York: W. H. Freeman & Co.

Lomako J, Lomako WM, Whelan WJ (2004) Glycogenin: the primer for mammalian and yeast glycogen synthesis. Biochim Biophys Acta 1673:45-55.

Lopez J, Wolff M, Lecourtier L, Cosquer B, Bontempi B, Dalrymple-Alford J, Cassel JC (2009) The intralaminar thalamic nuclei contribute to remote spatial memory. J Neurosci 29:3302-3306.

Magistretti PJ (2006) Neuron-glia metabolic coupling and plasticity. J Exp Biol 209:2304-2311.

Magistretti PJ (2008) Brain energy metabolism. In: Fundamental Neuroscience (Squire LR, Berg D, Bloom F, du Lac S, Ghosh A, eds), pp 271-292. Amsterdam: Elsevier.

Magistretti PJ (2009) Neuroscience. Low-cost travel in neurons. Science 325:1349-1351.

Magistretti PJ, Pellerin L (1999) Astrocytes Couple Synaptic Activity to Glucose Utilization in the Brain. News Physiol Sci 14:177-182.

Magistretti PJ, Chatton JY (2005) Relationship between L-glutamate-regulated intracellular Na+ dynamics and ATP hydrolysis in astrocytes. J Neural Transm 112:77-85.

Maguire EA, Valentine ER, Wilding JM, Kapur N (2003) Routes to remembering: the brains behind superior memory. Nat Neurosci 6:90-95.

Mason SD, Howlett RA, Kim MJ, Olfert IM, Hogan MC, McNulty W, Hickey RP, Wagner PD, Kahn CR, Giordano FJ, Johnson RS (2004) Loss of skeletal muscle HIF-1alpha results in altered exercise endurance. PLoS Biol 2:e288.

Masuda Y, Odashima J, Murai S, Saito H, Itoh M, Itoh T (1994) Radial arm maze behavior in mice when a return to the home cage serves as the reinforcer. Physiol Behav 56:785-788.

Maviel T, Durkin TP, Menzaghi F, Bontempi B (2004) Sites of neocortical reorganization critical for remote spatial memory. Science 305:96-99.

McDonald RJ, White NM (1994) Parallel information processing in the water maze: evidence for independent memory systems involving dorsal striatum and hippocampus. Behav Neural Biol 61:260-270.

McGaugh JL (2000) Memory--a century of consolidation. Science 287:248-251.

Michal G (1999) Biochemical pathways: an atlas of biochemistry and molecular biology. New York: Wiley.

Micheau J, Riedel G (1999) Protein kinases: which one is the memory molecule? Cell Mol Life Sci 55:534-548.

Miller PW, Long NJ, Vilar R, Gee AD (2008) Synthesis of 11C, 18F, 15O, and 13N radiolabels for positron emission tomography. Angew Chem Int Ed Engl 47:8998-9033.

Miyashita T, Kubik S, Haghighi N, Steward O, Guzowski JF (2009) Rapid activation of plasticity-associated gene transcription in hippocampal neurons provides a mechanism for encoding of one-trial experience. J Neurosci 29:898-906.

Mori S, Kato M, Fujishima M (1995) Impaired maze learning and cerebral glucose utilization in aged hypertensive rats. Hypertension 25:545-553.

Morris R (1981) Spatial localization does not require the presence of local cues. Learn Motiv 12:239-260.

Morris R (1984) Developments of a water-maze procedure for studying spatial learning in the rat. J Neurosci Methods 11:47-60.

Morris RG, Moser EI, Riedel G, Martin SJ, Sandin J, Day M, O'Carroll C (2003) Elements of a neurobiological theory of the hippocampus: the role of activity-dependent synaptic plasticity in memory. Philos Trans R Soc Lond B Biol Sci 358:773-786.

Moseley AE, Williams MT, Schaefer TL, Bohanan CS, Neumann JC, Behbehani MM, Vorhees CV, Lingrel JB (2007) Deficiency in Na,K-ATPase alpha isoform genes alters spatial learning, motor activity, and anxiety in mice. J Neurosci 27:616-626.

Moser MB, Moser EI (1998a) Functional differentiation in the hippocampus. Hippocampus 8:608-619.

Moser MB, Moser EI (1998b) Distributed encoding and retrieval of spatial memory in the hippocampus. J Neurosci 18:7535-7542.

Moskowitz MA, Bolay H, Dalkara T (2004) Deciphering migraine mechanisms: clues from familial hemiplegic migraine genotypes. Ann Neurol 55:276-280.

Murphy KT, Petersen AC, Goodman C, Gong X, Leppik JA, Garnham AP, Cameron-Smith D, Snow RJ, McKenna MJ (2006) Prolonged submaximal exercise induces isoform-

specific Na+-K+-ATPase mRNA and protein responses in human skeletal muscle. Am J Physiol Regul Integr Comp Physiol 290:R414-424.

Murphy KT, Aughey RJ, Petersen AC, Clark SA, Goodman C, Hawley JA, Cameron-Smith D, Snow RJ, McKenna MJ (2007) Effects of endurance training status and sex differences on Na+,K+-pump mRNA expression, content and maximal activity in human skeletal muscle. Acta Physiol (Oxf) 189:259-269.

Nader K, Schafe GE, Le Doux JE (2000) Fear memories require protein synthesis in the amygdala for reconsolidation after retrieval. Nature 406:722-726.

Nordsborg N, Bangsbo J, Pilegaard H (2003) Effect of high-intensity training on exercise-induced gene expression specific to ion homeostasis and metabolism. J Appl Physiol 95:1201-1206.

O'Keefe J, Nadel L (1978) The hippocampus as a cognitive map. Oxford; England: Oxford University press.

Olton DS, Samuelson RJ (1976) Remembrance of places passed: spatial memory in rats. J Exp Psychol Anim Behav Process 2:97-116.

Otonkoski T, Nanto-Salonen K, Seppanen M, Veijola R, Huopio H, Hussain K, Tapanainen P, Eskola O, Parkkola R, Ekstrom K, Guiot Y, Rahier J, Laakso M, Rintala R, Nuutila P, Minn H (2006) Noninvasive diagnosis of focal hyperinsulinism of infancy with [18F]-DOPA positron emission tomography. Diabetes 55:13-18.

Packard MG, McGaugh JL (1992) Double dissociation of fornix and caudate nucleus lesions on acquisition of two water maze tasks: further evidence for multiple memory systems. Behav Neurosci 106:439-446.

Paul CM, Magda G, Abel S (2009) Spatial memory: Theoretical basis and comparative review on experimental methods in rodents. Behav Brain Res 203:151-164.

Pellerin L, Magistretti PJ (1994) Glutamate uptake into astrocytes stimulates aerobic glycolysis: a mechanism coupling neuronal activity to glucose utilization. Proc Natl Acad Sci U S A 91:10625-10629.

Pellerin L, Magistretti PJ (1997) Glutamate uptake stimulates Na+,K+-ATPase activity in astrocytes via activation of a distinct subunit highly sensitive to ouabain. J Neurochem 69:2132-2137.

Pellerin L, Magistretti PJ (2004) Neuroenergetics: calling upon astrocytes to satisfy hungry neurons. Neuroscientist 10:53-62.

Petersen AC, Murphy KT, Snow RJ, Leppik JA, Aughey RJ, Garnham AP, Cameron-Smith D, McKenna MJ (2005) Depressed Na+-K+-ATPase activity in skeletal muscle at fatigue is correlated with increased Na+-K+-ATPase mRNA expression following intense exercise. Am J Physiol Regul Integr Comp Physiol 289:R266-274.

Pick CG, Yanai J (1983) Eight arm maze for mice. Int J Neurosci 21:63-66.

Pilegaard H, Neufer PD (2004) Transcriptional regulation of pyruvate dehydrogenase kinase 4 in skeletal muscle during and after exercise. Proc Nutr Soc 63:221-226.

Pinheiro CH, Silveira LR, Nachbar RT, Vitzel KF, Curi R (2010) Regulation of glycolysis and expression of glucose metabolism-related genes by reactive oxygen species in contracting skeletal muscle cells. Free Radic Biol Med 48:953-960.

Poeppel TD, Krause BJ (2008) Functional imaging of memory processes in humans: positron emission tomography and functional magnetic resonance imaging. Methods 44:315-328.

Pothuizen HH, Zhang WN, Jongen-Relo AL, Feldon J, Yee BK (2004) Dissociation of function between the dorsal and the ventral hippocampus in spatial learning abilities of the rat: a within-subject, within-task comparison of reference and working spatial memory. Eur J Neurosci 19:705-712.

Radyushkin K, Anokhin K, Meyer BI, Jiang Q, Alvarez-Bolado G, Gruss P (2005) Genetic ablation of the mammillary bodies in the Foxb1 mutant mouse leads to selective deficit of spatial working memory. Eur J Neurosci 21:219-229.

Rekart JL, Meiri K, Routtenberg A (2005) Hippocampal-dependent memory is impaired in heterozygous GAP-43 knockout mice. Hippocampus 15:1-7.

Remondes M, Schuman EM (2004) Role for a cortical input to hippocampal area CA1 in the consolidation of a long-term memory. Nature 431:699-703.

Ribes D, Parafita J, Charrier R, Magara F, Magistretti PJ, Thiran JP (2010) JULIDE: a software tool for 3D reconstruction and statistical analysis of autoradiographic mouse brain sections. PLoS One 5:e14094.

Rice O, Saintvictor S, Michaelides M, Thanos P, Gatley SJ (2006) MicroPET investigation of chronic long-term neurotoxicity from heavy ion irradiation. AAPS J 8:E508-514.

Rogers JL, Kesner RP (2006) Lesions of the dorsal hippocampus or parietal cortex differentially affect spatial information processing. Behav Neurosci 120:852-860.

Ros J, Pellerin L, Magara F, Dauguet J, Schenk F, Magistretti PJ (2006) Metabolic activation pattern of distinct hippocampal subregions during spatial learning and memory retrieval. J Cereb Blood Flow Metab 26:468-477.

Rossato JI, Zinn CG, Furini C, Bevilaqua LR, Medina JH, Cammarota M, Izquierdo I (2006) A link between the hippocampal and the striatal memory systems of the brain. An Acad Bras Cienc 78:515-523.

Rossi S, Pasqualetti P, Zito G, Vecchio F, Cappa SF, Miniussi C, Babiloni C, Rossini PM (2006) Prefrontal and parietal cortex in human episodic memory: an interference study by repetitive transcranial magnetic stimulation. Eur J Neurosci 23:793-800.

Roullet P (1995) Inter-session delay and its effects on performance and retention of spatial learning on a radial maze with mice. Neurobiol Learn Mem 64:4-9.

Routtenberg A, Cantallops I, Zaffuto S, Serrano P, Namgung U (2000) Enhanced learning after genetic overexpression of a brain growth protein. Proc Natl Acad Sci U S A 97:7657-7662.

Rowe WB, Blalock EM, Chen KC, Kadish I, Wang D, Barrett JE, Thibault O, Porter NM, Rose GM, Landfield PW (2007) Hippocampal expression analyses reveal selective

association of immediate-early, neuroenergetic, and myelinogenic pathways with cognitive impairment in aged rats. J Neurosci 27:3098-3110.

Salmi E, Aalto S, Hirvonen J, Langsjo JW, Maksimow AT, Oikonen V, Metsahonkala L, Virkkala J, Nagren K, Scheinin H (2008) Measurement of GABAA receptor binding in vivo with [11C]flumazenil: a test-retest study in healthy subjects. Neuroimage 41:260-269.

Saravis S, Sziklas V, Petrides M (1990) Memory for Places and the Region of the Mamillary Bodies in Rats. Eur J Neurosci 2:556-564.

Shank RP, Leo GC, Zielke HR (1993) Cerebral metabolic compartmentation as revealed by nuclear magnetic resonance analysis of D-[1-13C]glucose metabolism. J Neurochem 61:315-323.

Shank RP, Bennett GS, Freytag SO, Campbell GL (1985) Pyruvate carboxylase: an astrocyte-specific enzyme implicated in the replenishment of amino acid neurotransmitter pools. Brain Res 329:364-367.

Shannon BJ, Buckner RL (2004) Functional-anatomic correlates of memory retrieval that suggest nontraditional processing roles for multiple distinct regions within posterior parietal cortex. J Neurosci 24:10084-10092.

Shibata H (1993) Efferent projections from the anterior thalamic nuclei to the cingulate cortex in the rat. J Comp Neurol 330:533-542.

Shilatifard A, Conaway RC, Conaway JW (2003) The RNA polymerase II elongation complex. Annu Rev Biochem 72:693-715.

Shinoda T, Ogawa H, Cornelius F, Toyoshima C (2009) Crystal structure of the sodium-potassium pump at 2.4 A resolution. Nature 459:446-450.

Sibson NR, Dhankhar A, Mason GF, Rothman DL, Behar KL, Shulman RG (1998) Stoichiometric coupling of brain glucose metabolism and glutamatergic neuronal activity. Proc Natl Acad Sci U S A 95:316-321.

Skibinska A, Lech M, Kossut M (2001) PSD95 protein level rises in murine somatosensory cortex after sensory training. Neuroreport 12:2907-2910.

Smith CT, Conway JM, Rose GM (1998) Brief paradoxical sleep deprivation impairs reference, but not working, memory in the radial arm maze task. Neurobiol Learn Mem 69:211-217.

Smythe C, Cohen P (1991) The discovery of glycogenin and the priming mechanism for glycogen biogenesis. Eur J Biochem 200:625-631.

Sokoloff L (2008) The physiological and biochemical bases of functional brain imaging. Cogn Neurodyn 2:1-5.

Sokoloff L, Reivich M, Kennedy C, Des Rosiers MH, Patlak CS, Pettigrew KD, Sakurada O, Shinohara M (1977) The [14C]deoxyglucose method for the measurement of local cerebral glucose utilization: theory, procedure, and normal values in the conscious and anesthetized albino rat. J Neurochem 28:897-916.

Sommer T, Rose M, Weiller C, Buchel C (2005) Contributions of occipital, parietal and parahippocampal cortex to encoding of object-location associations. Neuropsychologia 43:732-743.

Sorg O, Magistretti PJ (1991) Characterization of the glycogenolysis elicited by vasoactive intestinal peptide, noradrenaline and adenosine in primary cultures of mouse cerebral cortical astrocytes. Brain Res 563:227-233.

Sorg O, Magistretti PJ (1992) Vasoactive intestinal peptide and noradrenaline exert long-term control on glycogen levels in astrocytes: blockade by protein synthesis inhibition. J Neurosci 12:4923-4931.

Squire LR (1987) Memory and Brain, first Edition. New York: Oxford University Press.

Squire LR (2004) Memory systems of the brain: a brief history and current perspective. Neurobiol Learn Mem 82:171-177.

Squire LR, Alvarez P (1995) Retrograde amnesia and memory consolidation: a neurobiological perspective. Curr Opin Neurobiol 5:169-177.

Squire LR, Knowlton B, Musen G (1993) The structure and organization of memory. Annu Rev Psychol 44:453-495.

Squire LR, Stark CE, Clark RE (2004) The medial temporal lobe. Annu Rev Neurosci 27:279-306.

Steeves TD, Miyasaki J, Zurowski M, Lang AE, Pellecchia G, Van Eimeren T, Rusjan P, Houle S, Strafella AP (2009) Increased striatal dopamine release in Parkinsonian patients with pathological gambling: a [11C] raclopride PET study. Brain 132:1376-1385.

Stork O, Welzl H (1999) Memory formation and the regulation of gene expression. Cell Mol Life Sci 55:575-592.

Suzuki WA (2006) Encoding new episodes and making them stick. Neuron 50:19-21.

Swanson RA (1992) Physiologic coupling of glial glycogen metabolism to neuronal activity in brain. Can J Physiol Pharmacol 70 Suppl:S138-144.

Sziklas V, Petrides M (2000) Selectivity of the spatial learning deficit after lesions of the mammillary region in rats. Hippocampus 10:325-328.

Taubenfeld SM, Milekic MH, Monti B, Alberini CM (2001) The consolidation of new but not reactivated memory requires hippocampal C/EBPbeta. Nat Neurosci 4:813-818.

Tavraz NN, Friedrich T, Durr KL, Koenderink JB, Bamberg E, Freilinger T, Dichgans M (2008) Diverse functional consequences of mutations in the Na+/K+-ATPase alpha2-subunit causing familial hemiplegic migraine type 2. J Biol Chem 283:31097-31106.

Teather LA, Packard MG, Smith DE, Ellis-Behnke RG, Bazan NG (2005) Differential induction of c-Jun and Fos-like proteins in rat hippocampus and dorsal striatum after training in two water maze tasks. Neurobiol Learn Mem 84:75-84.

Teixeira AP, Santos SS, Carinhas N, Oliveira R, Alves PM (2008) Combining metabolic flux analysis tools and 13C NMR to estimate intracellular fluxes of cultured astrocytes. Neurochem Int 52:478-486.

Thobois S, Fraix V, Savasta M, Costes N, Pollak P, Mertens P, Koudsie A, Le Bars D, Benabid AL, Broussolle E (2003) Chronic subthalamic nucleus stimulation and striatal D2 dopamine receptors in Parkinson's disease--A [(11)C]-raclopride PET study. J Neurol 250:1219-1223.

Tischmeyer W, Grimm R (1999) Activation of immediate early genes and memory formation. Cell Mol Life Sci 55:564-574.

Trouche S, Bontempi B, Roullet P, Rampon C (2009) Recruitment of adult-generated neurons into functional hippocampal networks contributes to updating and strengthening of spatial memory. Proc Natl Acad Sci U S A 106:5919-5924.

Tse D, Langston RF, Kakeyama M, Bethus I, Spooner PA, Wood ER, Witter MP, Morris RG (2007) Schemas and memory consolidation. Science 316:76-82.

Tsivilis D, Vann SD, Denby C, Roberts N, Mayes AR, Montaldi D, Aggleton JP (2008) A disproportionate role for the fornix and mammillary bodies in recall versus recognition memory. Nat Neurosci 11:834-842.

van Groen T, Kadish I, Wyss JM (2002) The role of the laterodorsal nucleus of the thalamus in spatial learning and memory in the rat. Behav Brain Res 136:329-337.

Vandesompele J, De Preter K, Pattyn F, Poppe B, Van Roy N, De Paepe A, Speleman F (2002) Accurate normalization of real-time quantitative RT-PCR data by geometric averaging of multiple internal control genes. Genome Biol 3:RESEARCH0034.

Vann SD, Aggleton JP (2003) Evidence of a spatial encoding deficit in rats with lesions of the mammillary bodies or mammillothalamic tract. J Neurosci 23:3506-3514.

Vann SD, Aggleton JP (2004) The mammillary bodies: two memory systems in one? Nat Rev Neurosci 5:35-44.

Vann SD, Albasser MM (2009) Hippocampal, retrosplenial, and prefrontal hypoactivity in a model of diencephalic amnesia: Evidence towards an interdependent subcortical-cortical memory network. Hippocampus 19:1090-1102.

Vaynman S, Ying Z, Wu A, Gomez-Pinilla F (2006) Coupling energy metabolism with a mechanism to support brain-derived neurotrophic factor-mediated synaptic plasticity. Neuroscience 139:1221-1234.

Wagner AD, Shannon BJ, Kahn I, Buckner RL (2005) Parietal lobe contributions to episodic memory retrieval. Trends Cogn Sci 9:445-453.

Wakamatsu N, King DJ, Seal BS, Brown CC (2007) Detection of Newcastle disease virus RNA by reverse transcription-polymerase chain reaction using formalin-fixed, paraffin-embedded tissue and comparison with immunohistochemistry and in situ hybridization. J Vet Diagn Invest 19:396-400.

Wang H, Shimizu E, Tang YP, Cho M, Kyin M, Zuo W, Robinson DA, Alaimo PJ, Zhang C, Morimoto H, Zhuo M, Feng R, Shokat KM, Tsien JZ (2003) Inducible protein knockout reveals temporal requirement of CaMKII reactivation for memory consolidation in the brain. Proc Natl Acad Sci U S A 100:4287-4292.

Wilson JE (2003) Isozymes of mammalian hexokinase: structure, subcellular localization and metabolic function. J Exp Biol 206:2049-2057.

Winocur G, Gagnon S (1998) Glucose treatment attenuates spatial learning and memory deficits of aged rats on tests of hippocampal function. Neurobiol Aging 19:233-241.

Wright NF, Erichsen JT, Vann SD, O'Mara SM, Aggleton JP (2010) Parallel but separate inputs from limbic cortices to the mammillary bodies and anterior thalamic nuclei in the rat. J Comp Neurol 518:2334-2354.

Yoneoka Y, Takeda N, Inoue A, Ibuchi Y, Kumagai T, Sugai T, Takeda K, Ueda K (2004) Acute Korsakoff syndrome following mammillothalamic tract infarction. AJNR Am J Neuroradiol 25:964-968.

Yoshihara T, Ichitani Y (2004) Hippocampal N-methyl-D-aspartate receptor-mediated encoding and retrieval processes in spatial working memory: delay-interposed radial maze performance in rats. Neuroscience 129:1-10.

Zhan H, Tada T, Nakazato F, Tanaka Y, Hongo K (2004) Spatial learning transiently disturbed by intraventricular administration of ouabain. Neurol Res 26:35-40.

Zhao Y, Fung C, Shin D, Shin BC, Thamotharan S, Sankar R, Ehninger D, Silva A, Devaskar SU (2010) Neuronal glucose transporter isoform 3 deficient mice demonstrate features of autism spectrum disorders. Mol Psychiatry 15:286-299.

Zola-Morgan S, Squire LR (1993) Neuroanatomy of memory. Annu Rev Neurosci 16:547-563.